

AN EXPERIMENTAL ANALYSIS OF BENDING STRESSES  
INDUCED IN FLOOR GRIDS SUBJECTED TO  
LOADS FROM BEEF CATTLE

By

BERHANE BERHE

Bachelor of Science

College of Agriculture

Haile Selassie I University

Alemaya, Ethiopia

1962




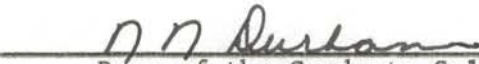
Submitted to the Faculty of the Graduate College  
of the Oklahoma State University  
in partial fulfillment of the requirements  
for the degree of  
MASTER OF SCIENCE  
May, 1967

OKLAHOMA  
STATE UNIVERSITY  
LIBRARY

JAN 9 1968

AN EXPERIMENTAL ANALYSIS OF BENDING STRESSES  
INDUCED IN FLOOR GRIDS SUBJECTED TO  
LOADS FROM BEEF CATTLE

Thesis Approved:

  
\_\_\_\_\_ Thesis Adviser  
  
\_\_\_\_\_  
  
\_\_\_\_\_  
  
\_\_\_\_\_  
Dean of the Graduate College

658331

## ACKNOWLEDGMENTS

The experimental investigations of this study were conducted with the financial support of the Oklahoma Agricultural Experiment Station Project 1208 and the research facilities of the Department of Agricultural Engineering.

My gratitude goes to the United States Agency For International Development through whose financial aid my program of study was possible.

I am deeply grateful to Dr. G. L. Nelson, my major adviser, who capably guided me throughout my program of study with great patience. He has been a great source of knowledge, inspiration, and confidence. His constructive criticisms, suggestions and ideas have been very helpful in the development and outcome of the study.

I wish to express my sincere gratitude to Professor E. W. Schroeder, Head of Agricultural Engineering Department, for his counsel and assistance concerning my program of study.

Appreciation is extended to Mr. William S. Abbott, Coordinator of International Programs, for all his help and especially for rendering me invaluable assistance in administrative affairs.

I am thankful to Mr. George W. A. Mahoney, Assistant Professor of Agricultural Engineering, for his guidance in the absence of my major adviser. His suggestions were very helpful.

Appreciation is extended to Mr. Jack Fryrear, Head Draftsman, and to Mr. Don McCrackin.

A word of gratitude goes to Mr. Romesh K. Munshi, Instructor of Civil Engineering, Dr. Dale D. Grosvenor, Director of Computer Center, and the operators of the Computer Center for their wonderful services.

To my program specialist, Mr. H. W. Dill of USDA, my program manager, Mr. Granville N. Bressler of AID, and my Technical Adviser, Mr. D. A. Ritter also of AID, I express my sincere gratitude.

Appreciation is also extended to my friends for their understanding and encouragement. I wish each and everyone of them success in their endeavors.

TABLE OF CONTENTS

Chapter	Page
I. INTRODUCTION . . . . .	1
II. REVIEW OF LITERATURE . . . . .	2
Introduction . . . . .	2
Cattle Housing . . . . .	2
Slats and the Slatted Floor . . . . .	4
Slatted Floors Versus Straw Bedding . . . . .	5
Design of Slats . . . . .	8
Grids and Gridded Floors . . . . .	13
III. THE STUDY . . . . .	17
Objectives . . . . .	17
Pertinent Quantities . . . . .	18
Discussion of Pertinent Quantities . . . . .	18
Formation of PI Terms . . . . .	22
Assumptions and Limitations . . . . .	23
Experimental Design . . . . .	24
IV. EXPERIMENTAL EQUIPMENT . . . . .	29
Model Grids . . . . .	29
Strain Gage Assembly . . . . .	29
Weights . . . . .	30
V. ANALYTICAL PROCEDURE . . . . .	36
Determination of Stiffness Index For Bending in Pro- totype . . . . .	36
Determination of Stiffness Index For Torsion in Pro- totype . . . . .	38
VI. EXPERIMENTAL PROCEDURE . . . . .	41
Determination of Stiffness Index For Bending in Model . . . . .	41
Determination of Animal Body Configurations and Weight Ratio of Weight Carried by Front Legs to Hind Legs . . . . .	43
Determination of Strain in the Model Grids . . . . .	44

Chapter		Page
VII.	ANALYSIS OF DATA . . . . .	48
	Calculation of the Bending Moment . . . . .	48
	Calculation of $\pi_{14}$ . . . . .	49
	Development of the Prediction Equation. . . . .	49
VIII.	DISCUSSION OF RESULTS. . . . .	61
	Comparison of Predicted $\pi_{14}$ To Observed $\pi_{14}$ . . . . .	61
	Application of Experimental Results . . . . .	61
	Example . . . . .	67
IX.	SUMMARY AND CONCLUSIONS. . . . .	72
	Suggestions For Further Study . . . . .	73
	SELECTED BIBLIOGRAPHY . . . . .	75
	APPENDIX A. Animal Configuration and Weight Measurements . . . . .	77
	APPENDIX B. Experimental and Computed Data . . . . .	79

LIST OF TABLES

Table	Page
I. Labor Requirement to Keep Cows in Slatted Floor or Conventional Barns, Man-Minutes/Cow/Day . . . . .	6
II. Labor Requirement For Manure Handling in Conventional Stall Barns and Those With Slatted Floor, Man-Minutes/Cow/Day .	6
III. Recommended Space Requirements For Cattle of Various Sizes	7
IV. Standard Design For Factory-Produced Floor Slats . . . . .	12
V. Design Specifications of Slats For Cattle . . . . .	13
VI. Pertinent Quantities . . . . .	19
VII. Relationship of Width at Shoulders and Distance Between Hoofs to Weight of Steer . . . . .	23
VIII. Values at Which Some Independent Parameters Were Held Constant . . . . .	27
IX. Schedule of Experiments . . . . .	28
X. Equivalent Loads in LbF. . . . .	45
XI. Parameter Combinations For Grid No. 1. . . . .	50
XII. Parameter Combinations For Grid No. 2. . . . .	51
XIII. Parameter Combinations For Grid No. 3. . . . .	52
XIV. Computed Values of Resisting Moment and Predicted Moment as Functions of the Effective Depth of a Grid Bar . . . . .	69

LIST OF FIGURES

Figure	Page
1. Some Slat Cross-sections . . . . .	4
2. Schematic Load Diagram . . . . .	9
3. Loading For Bending. . . . .	10
4. Loading For Shear. . . . .	10
5. Slat Cross-section . . . . .	10
6. Slat Cross-section . . . . .	13
7. General View at Shelter Roof and Cage. Cage was Completely Floored with Reinforced Concrete Precast Grids . . . . .	15
8. Waste Collection Tanks . . . . .	15
9. Typical Grid Floor . . . . .	15
10. General Floor and Animal Appearance. . . . .	16
11. Typical Hind-Quarter Appearance. . . . .	16
12. Corner Self-Feeder Installation. . . . .	16
13. Grid Configuration With Constant Cross-section . . . . .	18
14. Top View of Floor Composed of Eight Grids. . . . .	20
15. Side View of Grids and Upright Supports. . . . .	20
16. Animal Configuration . . . . .	21
17. Model Grid No. 1 . . . . .	31
18. Model Grid No. 2 . . . . .	32
19. Model Grid No. 3 . . . . .	33
20. View of Milling Machine Cutting Out Slots in a Model Grid. .	34
21. Typical Model Grid With Strain Gages and Lead Wires. . . . .	34



Figure	Page
22. Bridge Balancing Unit and Strain Indicator Used for Measuring Strain in Model Grids . . . . .	35
23. Prototype Cross-section. . . . .	36
24. Prototype Cross-section. . . . .	39
25. Designation of Loading Zones and Strain Gage Stations For A Typical Model Grid . . . . .	47
26. Plot of Bending Moment Parameter Versus Load Parameter For Station No. 1. . . . .	53
27. Plot of Bending Moment Parameter Versus Load Parameter For Station No. 2. . . . .	54
28. Plot of Bending Moment Parameter Versus Load Parameter For Station No. 3. . . . .	55
29. Plot of Bending Moment Parameter Versus Load Parameter For Station No. 4. . . . .	56
30. Plot of $\text{Ln}(1/\pi_2)$ Versus $\text{Ln}(1/A)$ . . . . .	58
31. Predicted Compared With Observed Values of $\pi_{14}$ Using EQ. (7-14a). . . . .	62
32. Predicted Compared With Observed Values of $\pi_{14}$ Using EQ. (7-14b). . . . .	63
33. Predicted Compared With Observed Values of $\pi_{14}$ Using EQ. (7-14c). . . . .	64
34. Predicted Compared With Observed Values of $\pi_{14}$ Using EQ. (7-14d). . . . .	65
35. Stress Distribution Diagram. . . . .	67
36. Plot of Resisting Moment and Predicted Moment For Station No. 1 Versus Depth of a 4 Inches Wide Reinforced Concrete Rectangular Section . . . . .	70

## CHAPTER I

### INTRODUCTION

The significant position of livestock production in the Agricultural Industry and the functional limitations of existing housing facilities have made the improvement of livestock housing a very important agricultural engineering problem. It is very well understood among agricultural engineers and agricultural experts that better housing equipped with environmental controls directly influences the quality as well as the quantity of agricultural products.

For complete environmental control, a shelter needs to be completely confined. For such a shelter, the use of slatted or gridded floors have produced quite favorable results.

Some of the advantages of slotted floors are: higher concentration of livestock, elimination of bending, reduction of labor required for cleaning, improved animal health and comfort, improved sanitation, improved control of disease and parasites, storage of manure for fertilizer, and easy adaptability of labor-saving automation equipment.

This study is concerned with the structural analysis for design of reinforced concrete floor grids under bending when loaded by beef cattle. The experimental investigations were performed on models.

## CHAPTER II

### REVIEW OF LITERATURE

#### Introduction

Most of the research with respect to slatted and gridded floors has been done to test their functional values. Some investigations were conducted primarily for the purpose of testing predetermined designs of slats. There is no evidence, however, of experimental investigations dealing with the structural analysis for design of reinforced concrete floor grids. The European countries have been pioneers in the use of slatted floors for livestock housing.

#### Cattle Housing

The big question at present is "which way to go in cattle housing?" Should livestock farmers stay with open sheds, go to partially confined sheds, or should they go to fully confined housing.

Malena, Van Fossen, and Mayer (13) reported that basic designs of beef cattle buildings fall into three different categories: Open-shed, under-roof confinement, and completely controlled environment buildings.

Open-shed housing. Generally, this building is an open area with feeding and watering areas out in the lot. Some partitioning is sometimes used to cut down drafts. Otherwise, no attempt is made to control environmental conditions.

Under-roof confinement. The main reason for using this type of housing is to eliminate weather problems. The roof keeps out most of the direct sunlight during the hot season, but at the same time is built so that the cattle receive a generous supply of warming sunlight in the winter. In this setup the cattle are confined within the shed for 24 hours a day. No attempt is made to control environmental conditions.

Environmental-controlled buildings. It seems that the trend in cattle housing is moving toward complete confinement with appropriate equipment to control the environmental conditions. Weather factors are eliminated with this type of building. It is temperature and humidity controlled. In areas where extreme weather conditions are prevalent, the animals need to be put in environmental-controlled housing so that optimum production efficiency could be achieved. In this type of housing the problems of bedding requirement, manure disposal, and space requirements become very significant.

Hence, to solve these problems the use of slatted floors was introduced. Hammer (7) reports that the original work with slatted floors was done in Iceland about 200 years ago. Later the Norwegian farmers adopted the idea for sheep and goat barns. It was not until 1952 that special attention was focused toward the improvement of slatted floors in the Institute of Farm Building Research of the Agricultural College of Norway at Vollebekk. Since 1956, Sweden, Britain, Belgium, Czechoslovakia, Austria, and Germany have undertaken similar trials. In the last few years, several research investigations have been conducted in the United States.

### Slats and the Slatted Floor

Slats could be considered as small floor beams. Slats could be made out of hardwood, concrete or steel. Compared to reinforced concrete or steel slats, wooden slats wear out fast and warp. Even though wooden slats are easy to handle and to replace, they are not as desirable as the other two.

There are several different cross-sections of slats that can be used. The most common shape is a trapezoidal cross-section with the bottom tapered so that the manure could easily slip down to the basin.

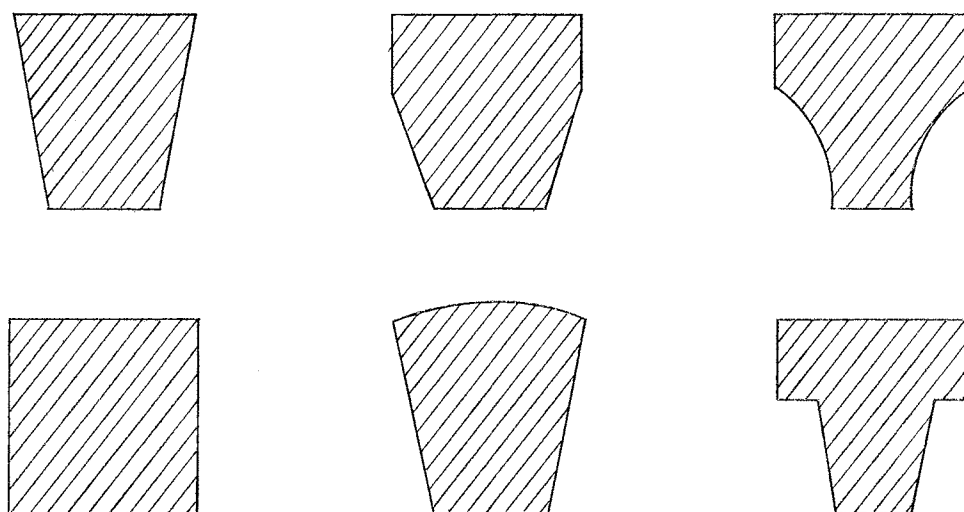


Figure 1. Some slat cross-sections

Slatted floors could be made either with individual slats spaced about 1"-2" apart, depending upon the size of the animals, or a grid floor could be formed. It is recommended that the top width of the slats should be 3-4 times the size of the top width of the slot.

## Slatted Floors Versus Straw Bedding

Sufficient evidence is available to indicate clearly that slatted floors have proven advantageous to the conventional straw bedding of cattle housing. Soutar (24), Nordbø (16), Hammer (7), Green (6), Lees (12), reported that among other important considerations, the most significant advantages of slatted floors over conventional floors are:

1. The saving of bedding. With slatted floors no straw was required for bedding. In many European countries, the availability of straw for bedding is quite critical.
2. The saving of labor. Since cleaning, bedding and brushing are not necessary, slatted floors require much less labor than conventional stanchion-type barns. Slatted floors clean themselves by the movement of hoofs. In cattle pens with slatted floors, the manure is collected in a basin directly beneath the floor. The manure could be handled in several ways. It could be removed by a tractor-operated shoveling bucket or else mixed with water and then pumped out. In Tables I and II from Hammer (7) we can see the saving of labor when slatted floors are used.
3. The saving in building cost. The use of slatted floors permits higher density or concentration of cattle in a given pen. Therefore, less space is required per head. Space requirements vary with the size of the animal and for cattle the following table by the Portland Cement Association (23) gives a fairly good estimate of density.

TABLE I  
LABOR REQUIREMENT TO KEEP COWS IN SLATTED FLOOR OR  
CONVENTIONAL BARNs, MAN-MINUTES/COW/DAY (17)

Type of Housing	Number of Cows		
	10	20	40
Stanchion	13.76	12.85	11.73
Enclosed loose housing with slatted floors	11.43	9.07	8.02

TABLE II  
LABOR REQUIREMENTS FOR MANURE HANDLING IN CONVENTIONAL-STALL  
BARNs AND THOSE WITH SLATTED FLOOR,  
MAN-MINUTES/COW/DAY ( 8 )

Type of Stall Barn	Number of Cows	Barn Cleaning	Manure Disposal	Total Manure Handling
Conventional Stanchion Barn	20	2.90	0.89	3.79
	50	2.92	0.89	3.81
Slatted Floor Stall Barns with T- shaped metal slats	20	0.53	0.75	1.28
	50	0.47	0.53	1.00

TABLE III  
RECOMMENDED SPACE REQUIREMENTS FOR CATTLE  
OF VARIOUS SIZES

Size of Animal	Square Feet
Calves under six months	10-15
Cattle six months to one year	15-25
Cattle one to two years	25-35
Mature beef cattle	30-40
Cows	35-45

The initial cost of the slatted floor is greater than the other types of floors. However, as Lees (12) reported, the capital cost can be recovered in no more than two seasons by the saving of straw alone.

4. The animals are clean, quiet, and thrifty. Since the manure is kicked under by the hoofs of the animals, the floor remains fairly clean and the animals stay clean. It seems that the slots keep the animals on their feet most of the time and there is not very much movement. In some instances beef cattle gained more weight because they were on their feet most of the time and thus ate more feed. Ventilation and other environmental controls could be installed to provide more comfort.



Other important aspects of slatted floors are: The improvement for sanitation, controlling disease, freedom from parasites, permitting manure to be stored and used for fertilizer, and adapting well to labor-saving automation equipment.

### Design of Slats

Several experiments have been conducted on slatted and grid floors to test their functional values. As indicated in the previous section, most of these investigations have shown quite favorable results.

Structural investigations, however, have been primarily tests on predetermined designs of slats. In Norway (3), the Voss School of Agriculture conducted structural tests on six different cross-sections of concrete floor slats in 1953. Two qualities of concrete with compressive specifications of 2840 psi and 4260 psi were used.

Using three slats of the same quality, cross-section, and length, tests were conducted to determine the average moments and shears at failure. Test loads were applied hydraulically as shown by the schematic diagram, Figure 2. This loading condition gave uniform shear stresses throughout approximately half of the slat length and uniform moment stresses throughout the other half. This way bending and shear capacities of the beam could be obtained simultaneously. Only one of the thirty-six slats failed in shear, and the rest failed in flexure.

From the results of these structural tests, slat designs were selected to fit the animal loadings expected on various spans. The slat cross-sections were chosen so that the minimum safety factor for any set of conditions was about 1.25. On this basis, the 3.94-inch deep slats were

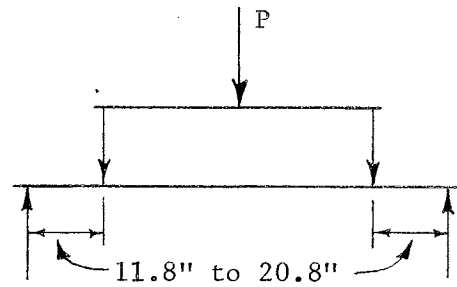


Figure 2. Schematic load diagram

considered usable on spans up to approximately five feet. The 4.72-inch deep slats were usable on spans up to approximately six and one-half feet and the 5.90-inch deep slats made with the high-quality concrete were usable on spans up to ten feet. The slats made with lower-quality concrete and with the narrow bottoms consistently gave lower load-carrying capacities than their test counterparts.

Based on the Norwegian tests and on current American practices with reinforced concrete, the following method of design was recommended for floor slats to carry cattle.

Loads: Assume individual hoof loads of one-fourth the animal weight. Assume the distance between an animal's hoofs as 1.0 feet and the distance between adjacent animals as 2 feet. Place on the chosen span the maximum number of hoof loads possible according to the above spacing. Arrange the loads to give maximum moment or shear. For moment calculations, use two superimposed hoof loads at midspan. See Figure 2. For shear computations, use two superimposed hoof loads at the support. See Figure 3. The weight of the slat may be considered as uniformly distributed load.

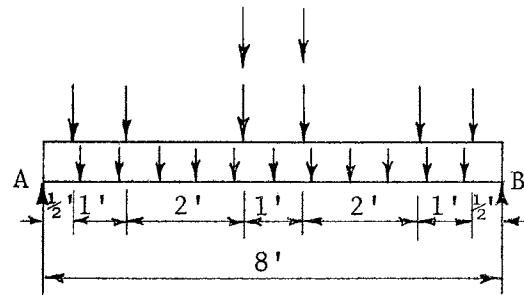


Figure 3. Loading for bending

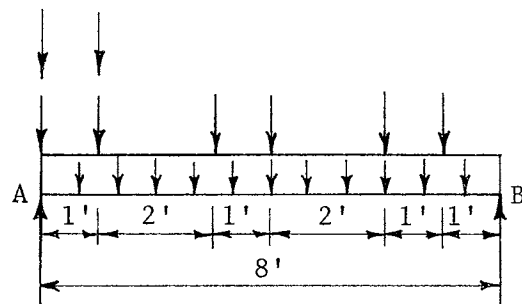


Figure 4. Loading for shear

Stresses: Stresses as allowed in ACI 318-63, "Building Code Requirements for Reinforced Concrete," are recommended.

Calculations: Determine unit shear by the formula

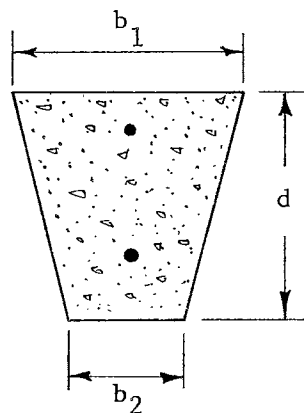


Figure 5. Slat cross-section

$$v = \frac{V}{bjd} \quad (2-1)$$

where,

$v$  = Unit shear, LbF/Sq.In.

$V$  = Total shear, LbF.

$b$  = Average width =  $\frac{b_1 + b_2}{2}$ , In.

$d$  = Depth, In.

$j$  = Ratio of distance between centroid of compression and centroid of tension to the depth,  $d$ .

To determine the cross-sectional area  $bd$ , use the above unit shear formula and the maximum allowable unit shear and a calculated total shear at the support as in Figure 4. The value of  $j$  could be calculated using the following formulas (25).

$$j = 1 - \frac{k}{3} \text{ and } k = \frac{n}{n+r} \quad (2-2)$$

where,

$n$  = Ratio of modulus of elasticity of steel to concrete

$r$  = Ratio of allowable tensile stress for steel,  $f_s$ , to compressive stress in extreme fiber,  $f_c$

from

$$M_o = \frac{1}{2} f_c j k b d^2 \quad (2-3)$$

where,

$M_o$  = Maximum bending moment, LbF.ft., as in the middle of span in Figure 3.

$f_c$  = compressive stress in extreme fiber, LbF/Sq.In.

$b d^2$  could be calculated.

Then using a suitable value for  $b$ ,  $d$  could be computed for both  $bd$  and  $bd^2$ .

Size of main reinforcement rod could be determined from

$$M_s = A_s f_s jd \quad (2-4)$$

where,

$M_s$  = Bending moment for steel which is the same as  $M_o$ ,  
LbF·ft.

$A_s$  = Cross-sectional area for tension reinforcement, Sq.In.

$f_s$  = Allowable tensile stress for steel, LbF/Sq.In.

Table IV shows a standard design for factory-produced floor slats which was prepared jointly by the University of Norway Institute of Building Construction and the Norwegian Cement Association in 1958 (3).

TABLE IV

STANDARD DESIGN FOR FACTORY-PRODUCED FLOOR SLATS

	Maximum slat length, (ft.)		
	5.4	7.2	10.8
Main reinforcement diameter, (In.)	0.51	0.51	0.63
Depth (In.)	3.54	4.72	5.90
Top Width (In.)	5.90	5.90	5.90
Bottom Width (In.)	4.14	3.54	2.95

Concrete Quality: 4,260 psi in 20 cm. Cube Test

A similar design specifications put out by the Portland Cement Association (23) in the United States is shown on Table V on the following page. Figure 6 shows a cross-section of the slats.

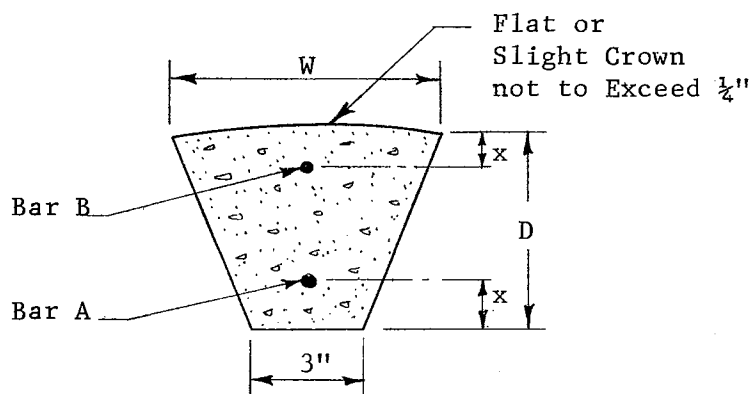


Figure 6. Slat cross-section

TABLE V

## DESIGN SPECIFICATIONS OF SLATS FOR CATTLE

Clear Span	Dimensions			Bar Size	
	D	W	X	A	B
6'-0"	6"	6"	1 1/2"	No. 5 (5/8")	No. 3 (3/8")
8'-0"	6"	6"	1 1/2"	No. 6 (3/4")	No. 3 (3/8")
10'-0"	7 1/2"	6"	1 1/2"	No. 6 (3/4")	No. 3 (3/8")
12'-0"	7 1/2"	6"	1 1/2"	No. 7 (7/8")	No. 3 (3/8")

## Grids and Gridded Floors

So far the discussion in this chapter has dealt with slats. However, the use of concrete grids as floor components is becoming popular. In a concrete grid floor the transverse bars provide complete continuity of all the longitudinal bars that make up the grid. A picture of a 5-bar gridwork is shown on Figure 9. For the same bar and slat cross-section, width of slot, and area of floor, grid floors can carry more load than a series of individual slats.

Professor G. L. Nelson of the Department of Agricultural Engineering at Oklahoma State University has conducted a preliminary test on "caged cattle feedlot pen system" (unpublished progress report - OAES Project 1208, July 31, 1965), using concrete grid floor system. The primary objectives of the test were to identify guidelines and any problems (cattle health, feeding, management) that might arise and need to be taken into account in subsequent, more definitive experiments with cattle confined closely on a gridded floor.

The specific objectives were:

1. To evaluate growth rate and feed conversion.
2. To identify any adverse effect of the cage system on the cattle.
3. To evaluate frequency of principal activities of the cattle (eating, drinking, standing, lying) and obtain data for subsequent design of cattle cages.
4. To evaluate cattle preferences for floor grid configuration (grid slat width, slot width).
5. To evaluate the effectiveness of waste transfer through the floor grids, and rate of waste accumulation in underfloor collection tanks.

In this preliminary test 10 steers were housed in a pen, Figure 7, enclosing an area of 16.94 ft. by 16.77 ft. The cattle were confined by a cable fence on steel angle posts. The cage was sheltered by a plywood roof 24 ft. by 32 ft.; and by partial walls on the north and west sides for a windbreak. Waste was collected by two concrete tanks, Figure 8, each approximately 7 ft. 4 in. by 17 ft. 8 in. Feed was offered free choice in 4 self-feeders, each with a 24 inch feeding space. A feeder and a water cup, Figure 12, were located in each corner of the cage.

Figures 9, 10, and 11 show the typical floor before occupation by cattle and conditions of the floor and animals after occupation.

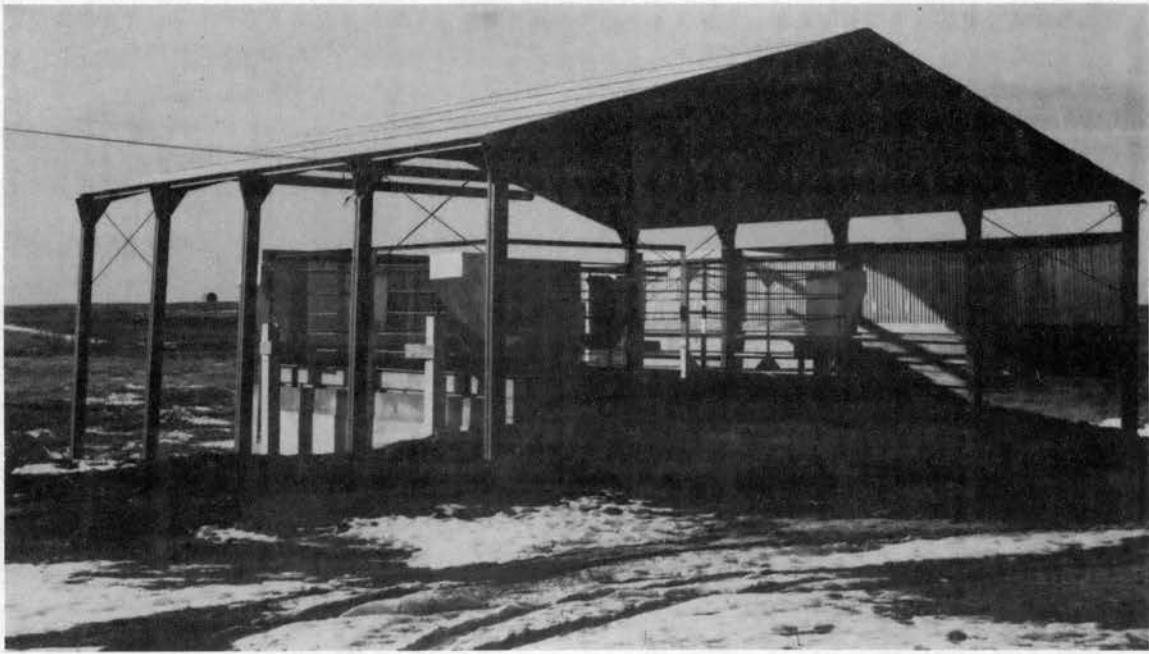


Figure 7. General View at Shelter Roof and Cage. Cage was completely floored with reinforced concrete precast grids.



Figure 8. Waste collection tanks.

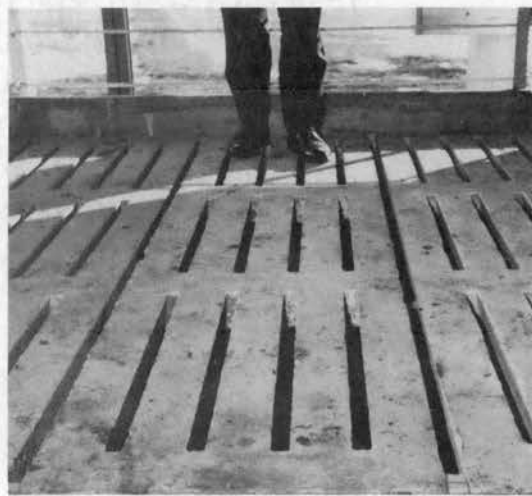


Figure 9. Typical grid floor.



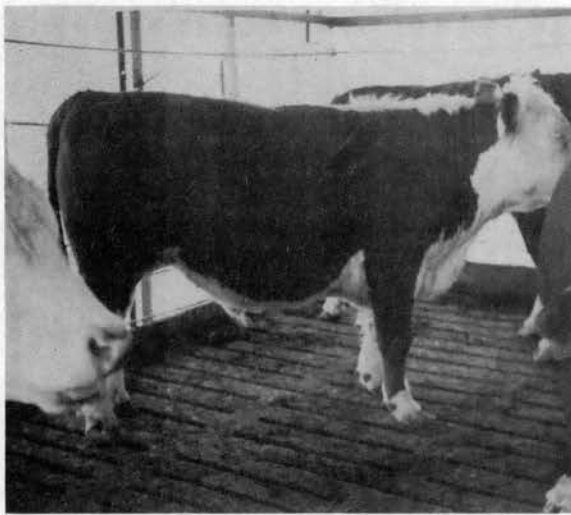


Figure 10. General floor and animal appearance.

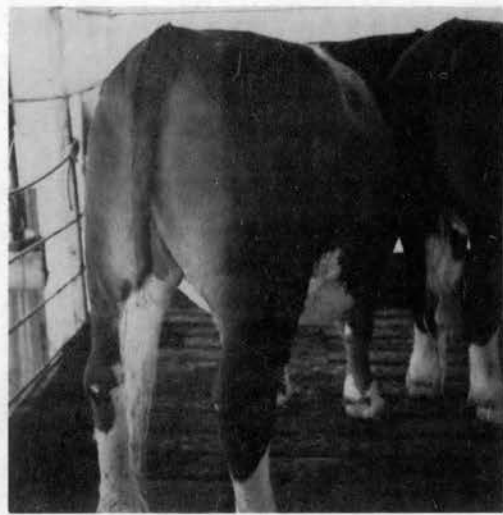


Figure 11. Typical hind-quarter appearance

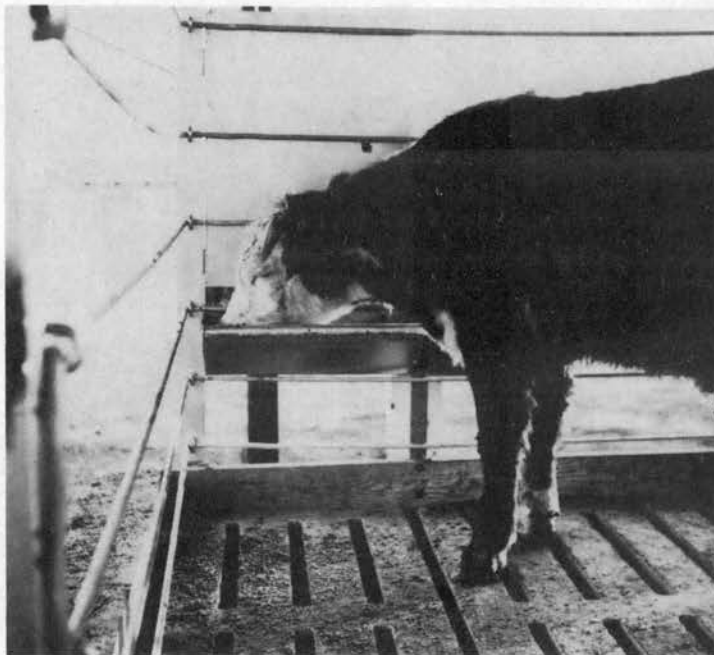


Figure 12. Corner self-feeder installation.

## CHAPTER III

### THE STUDY

A model study was proposed because the use of prototype grids with the cattle moving around presents considerable difficulties in observation. A model study also reduces the cost of construction and assembly, and it provides a saving of time and money.

#### Objectives

The objectives of the study were as follows:

1. Determine the model requirements for investigating bending stresses in a floor grid for beef cattle.
2. Develop an experimental bending stress equation that could be used for the design of floor grids.

The factors that were thought to affect the bending stresses were those physical quantities that characterize:

1. The grid configuration and mechanical properties of materials, E and G.
2. The animal configuration and its weight.
3. The arrangement of the animals with respect to an individual grid.

### Pertinent Quantities

In order to apply the concept of dimensional analysis, the first step is to list all of the physical quantities that are thought to affect the problem under study.

The quantities that affect the bending stresses on floor grids subjected to live loads of beef cattle are listed on Table VI.

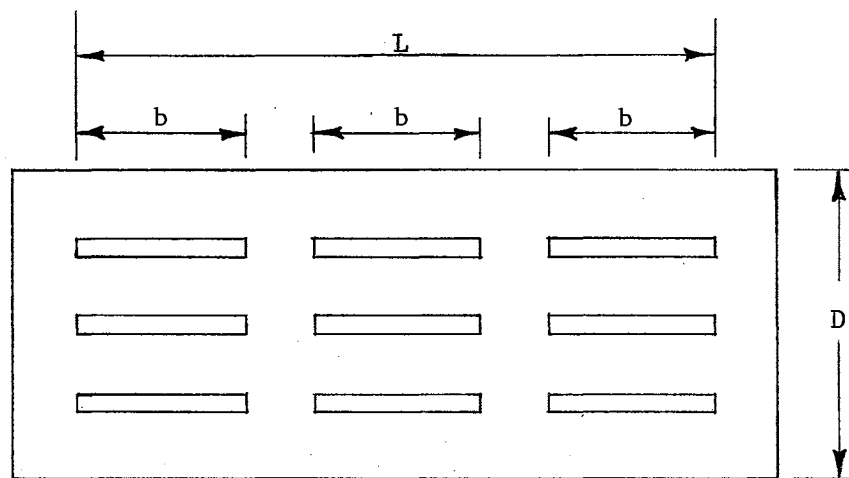


Figure 13. Grid Configuration with Constant Cross-section

The grids will be placed side by side separated by a distance equal to the width of the slots in a grid and each grid will be supported at both ends. Figures 14 and 15 show the arrangement of the grids to form a floor.

### Discussion of Pertinent Quantities

$b$ , the length of a bar, and  $L$ , the length of the grid have a direct relationship with the bending moment of the grid.

TABLE VI  
PERTINENT QUANTITIES

<u>No.</u>	<u>Symbol</u>	<u>Description</u>	<u>Units</u>	<u>Dimensional Symbol</u>
1.	b	Bar Length	In.	L
2.	L	Effective Grid Length	In.	L
3.	D	Grid Width	In.	L
4.	n	Number of Bars	---	---
5.	EI	Stiffness Index for Bending for One Bar	LbF·Sq.In.	FL
6.	GJ	Stiffness Index for Torsion for One Bar	LbF·Sq.In.	FL
7.	M	Bending Moment at Mid Span of Middle Bar	LbF·Ft.	FL
8.	P	Weight of Steer	LbF	F
9.	Q	Weight Ratio	---	---
10.	$\alpha$	Length From Nose to Front Legs	In.	L
11.	$\beta$	Length From Front Legs to Hind Legs	In.	L
12.	$\lambda$	Over all length of Steer	In.	L
13.	$\gamma$	Distance Between Front Hoofs, Center to Center	In.	L
14.	$\omega_1$	Width at Hips	In.	L
15.	$\omega_2$	Width at the Middle	In.	L
16.	$\omega_3$	Width at Shoulders	In.	L

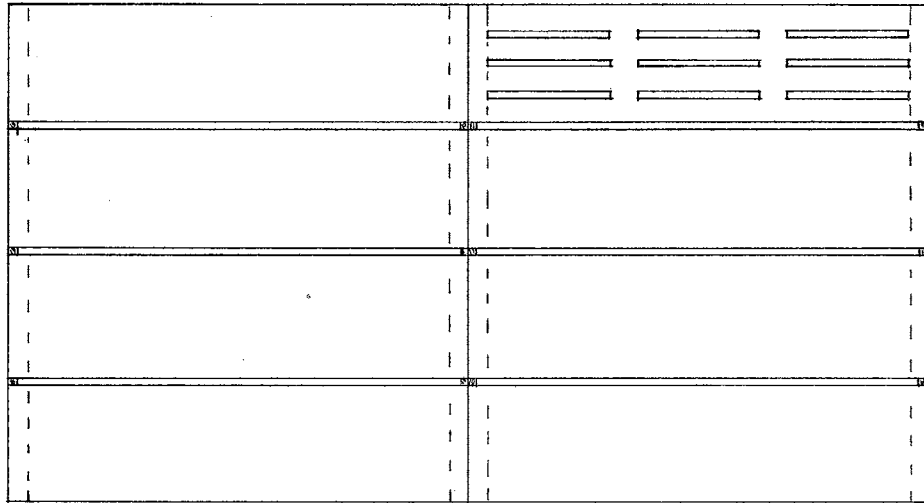


Figure 14. Top View of Floor Composed of Eight Grids

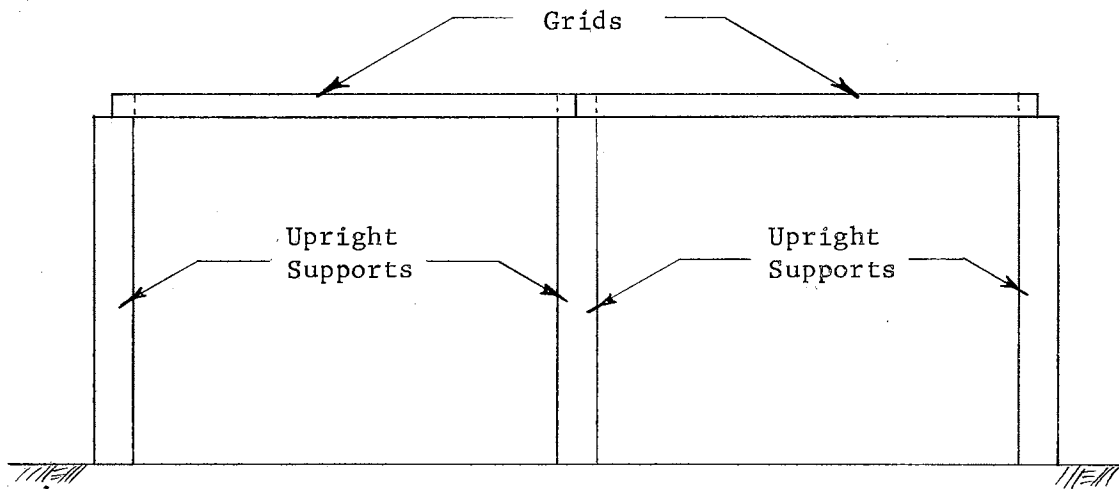


Figure 15. Side View of Grids and Upright Supports

$D$ , the width of the grid, has a direct relationship with the stiffness of the grid for bending as well as torsion.

$n$ , the number of bars, affects the width,  $d$ , of the grid.

$EI$ , is the stiffness index for bending for one bar.

$GJ$ , is the stiffness index for torsion for one bar.

$EI$  and  $GJ$  were considered pertinent because the bending and torsional stresses are functions of  $EI$  and  $GJ$  respectively. The grids used in this study are statically indeterminate with a large number of redundants. This makes it very involved to determine the bending stresses analytically.

$M$ , the bending moment, is the dependent variable that is to be evaluated.

$P$ , is the weight to be applied by a steer.

$Q$ , is the ratio of the weight applied through the front legs to the weight applied through the hind legs.

$\alpha$ ,  $\beta$ ,  $\lambda$ ,  $\omega_1$ ,  $\omega_2$ ,  $\omega_3$  are the body-configuration quantities pertaining to the animal. See Figure 16.

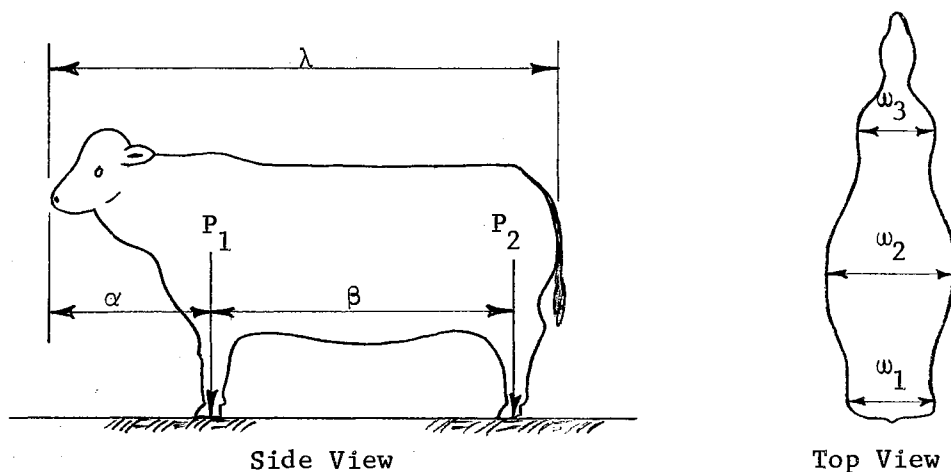


Figure 16. Animal Configuration

These values would influence the configuration and arrangement of the animals in the pen.

$\gamma$ , is the distance between the front hoofs of the animal. This value will determine the number and positioning of the front hoofs along the length of the grid.

#### Formation of PI Terms

There were 16 quantities which were described in two basic dimensions. According to Buckingham PI Theorem (15), the number of dimensionless and independent parameters required to express a relationship among the variables in any phenomenon is equal to the number of quantities involved, minus the number of basic dimensions in which those quantities may be measured. Hence, in this study there are several combinations of 14 dimensionless and independent parameters.

The 14 parameters that are most convenient to use in the experiment design and analysis of this study are:

$$\begin{array}{lll}
 \pi_1 = b/L & \pi_6 = \alpha/\lambda & \pi_{11} = Q \\
 \pi_2 = D/L & \pi_7 = \beta/\lambda & \pi_{12} = PL^2/EI \\
 \pi_3 = \gamma/L & \pi_8 = \omega_1/\lambda & \pi_{13} = EI/GJ \\
 \pi_4 = \omega_3/L & \pi_9 = \omega_1/\omega_2 & \pi_{14} = ML/EI \\
 \pi_5 = n & \pi_{10} = \omega_3/\omega_2 &
 \end{array}$$

Hence, the bending stress parameter expressed as a function of the other PI terms will give the general prediction equation

$$\pi_{14} = f(\pi_1, \pi_2, \pi_3, \pi_4, \pi_5, \pi_6, \pi_7, \pi_8, \pi_9, \pi_{10}, \pi_{11}, \pi_{12}, \pi_{13}) \quad (3-1)$$

## Assumptions and Limitations

Because of the unavailability of information concerning the relationship of weight of a beef animal to its body configurations, the following assumptions listed on Table VII were made:

TABLE VII  
RELATIONSHIP OF WIDTH AT SHOULDERS AND DISTANCE  
BETWEEN HOOFS TO WEIGHT OF STEER

<u>Weight of Steer</u>	<u>Width at Shoulders</u>	<u>Distance Between Hoofs</u>
600 lb.	18 in.	10 in.
800 lb.	20 in.	10 in.
1000 lb.	22 in.	12 in.
1200 lb.	24 in.	12 in.

The only such information available is reported by Brody (2) in which the width at the hips of dairy cattle increases by approximately 2 inches for each 200 lbs. of gain in weight.

Since there was not enough time to study all of the possibilities of arrangements of cattle in a pen, only one arrangement was taken. This arrangement, where the steers are lined up shoulder to shoulder facing in alternating directions, was thought to produce the highest possible longitudinal loading. In this case all of the bars along only one free longitudinal side will be loaded. This system of loading is expected to exert the most severe possible condition of bending stresses in the grid floors.



### Experimental Design

To evaluate the function  $f$ , would require holding all the independent PI terms except one constant, and varying that one to establish a relationship between it and the dependent PI term in turn, and the resulting relationships between the dependent PI terms and the other individual PI terms combined to give a general relationship. Since this method of study could be rather involved, it was reduced to manageable proportions. To do this, experiments were conducted at selected values of the independent PI terms to correspond to typical prototype conditions.

The dependent PI term is the bending moment parameter,  $\pi_{14} = M/EI$ . This parameter was evaluated in each experiment as a function of one of the independent variables.

$\pi_1 = b/L$ , the bar length parameter, was evaluated for each model grid. However, since there was no bar length variation within a grid and since it was secondary to the grid length parameter,  $D/L$ , it was deleted from the design of experiments.

$\pi_2 = D/L$  is the grid length parameter.  $\pi_2$  was evaluated for a constant value of  $D = 6 \frac{1}{8}$  in. and effective lengths of 16 in., 19 in., and 22 in.

$\pi_3 = \gamma/L$  is the load spacing parameter. Because of lack of pertinent information concerning the relationship of weight to body configurations of an animal, values of  $\gamma$  were assumed as 10.0 inches for the 600 LB and 800 LB weight classes and 12.0 inches for the 1000 LB and 1200 LB weight classes.

$\pi_4 = \omega_3/L$  is the parameter determining the number of animals that can be placed on a grid according to the specification mentioned on the

last paragraph of page 24. For the same reasons mentioned above, values of  $\omega_3$  were assumed as 18.0 inches, 20.0 inches, 22.0 inches, and 24.0 inches corresponding to weight classes of 600 Lb, 800 Lb, 1000 Lb, and 1200 Lb, respectively.

$\pi_{12} = PL^2/EI$ , the load parameter, was evaluated for each grid by varying the load, P. The value of EI was constant for the model and the prototype. For load, four prototype animal weights were selected. The prototype values of P were: 600 Lb, 800 Lb, 1000 Lb, and 1200 Lb. These loads were reduced to the corresponding model loads by the following dimensionless relationship.

$$\left(\frac{PL^2}{EI}\right)_m = \left(\frac{PL^2}{EI}\right)_p \quad (3-2)$$

$$\frac{P_m L_m^2}{(EI)_m} = \frac{P_p L_p^2}{(EI)_p} \quad (3-3)$$

$$P_m = \left(\frac{L_p}{L_m}\right)^2 \left[\frac{(EI)_m}{(EI)_p}\right] P_p \quad (3-4)$$

In the calculation of EQ. (3-4), values of  $(EI)_m = 1064.83 \text{ LbF}\cdot\text{Sq}\cdot\text{In.}$  and  $(EI)_p = 46,908,000 \text{ LbF}\cdot\text{Sq}\cdot\text{In.}$  were used.

The animal configuration parameters  $\pi_6 = \alpha/\lambda$ ,  $\pi_7 = \beta/\lambda$ ,  $\pi_8 = \omega_1/\lambda$ ,  $\pi_9 = \omega_1/\omega_2$ ,  $\pi_{10} = \omega_3/\omega_2$  were found to be constants at values of  $\pi_6 = 0.3906$ ,  $\pi_7 = 0.5680$ ,  $\pi_8 = 0.2863$ ,  $\pi_9 = 0.8444$ , and  $\pi_{10} = 0.8134$ . The animal front weight to hind weight ratio-parameter  $\pi_{11} = Q$  was constant at 1.2502. These values were calculated from measurements of length, width, and weight of 10 steers according to Figure 16. From the

dimensions tabulated on Appendix A, each parameter was evaluated for each animal and then an average of 10 such values was computed for each independent PI term.

$\pi_5 = n$  is the bar-number parameter taken along the transverse line of the grid.  $\pi_5 = 4$ .

$\pi_{13} = EI/GJ$ , the stiffness parameter was evaluated for the prototype grid. The stiffness index for bending, EI, and the stiffness index for torsion, GJ, were evaluated for a reinforced medium-strength concrete of a typical trapezoidal cross-section. The prototype section dimensions were: top width of 5 inches, bottom width of 3 inches, and depth of 3.5 inches. Reinforcement rods of 3/4 inches in the bottom and 3/8 inches in the top were used. The stiffness index for bending was 46,908,000 LbF·Sq.In. The approximate stiffness index for torsion was 47,718,720 LbF·Sq.In. Therefore the value of  $\pi_{13} = 0.9830$ .

The constant parameters are listed on Table VIII. Table IX shows the schedule of experiments that were conducted in this study.

Since  $\pi_1$  was deleted, and  $\pi_5, \pi_6, \pi_7, \pi_8, \pi_9, \pi_{10}, \pi_{11}$ , and  $\pi_{13}$  were held constant throughout the experiments, the prediction equation reduces to:

$$\pi_{14} = f(\pi_2, \pi_3, \pi_4, \pi_{12}) \quad (3-5)$$

TABLE VIII

VALUES AT WHICH SOME INDEPENDENT PARAMETERS WERE HELD CONSTANT

$\pi_5 = n$	$\pi_6 = \frac{\alpha}{\lambda}$	$\pi_7 = \frac{\beta}{\lambda}$	$\pi_8 = \frac{\omega_1}{\lambda}$	$\pi_9 = \frac{\omega_1}{\omega_2}$	$\pi_{10} = \frac{\omega_3}{\omega_2}$	$\pi_{11} = Q$	$\pi_{13} = \frac{EI}{GJ}$
4	0.3906	0.5680	0.2863	0.8444	0.8134	1.2502	0.9830

TABLE IX  
SCHEDULE OF EXPERIMENTS

Exp. No.	$\pi_{14} = \frac{ML}{EI}$	$\pi_2 = \frac{D}{L}$	$\pi_3 = \frac{y}{L}$	$\pi_4 = \frac{\omega_3}{L}$	$\pi_{12} = \frac{PL^2}{EI}$
1	Measure	0.3828	0.1562	0.2812	0.0524
2	Measure		0.1875	0.3125	0.0699
3	Measure			0.3438	0.0873
4	Measure		0.3750	0.1048	
5	Measure	0.3224	0.1315	0.2368	0.0739
6	Measure		0.1579	0.2632	0.0985
7	Measure			0.2895	0.1232
8	Measure		0.3158	0.1478	
9	Measure	0.2784	0.1136	0.2045	0.0990
10	Measure		0.1364	0.2273	0.1321
11	Measure			0.2500	0.1651
12	Measure		0.2727	0.1981	

## CHAPTER IV

### EXPERIMENTAL EQUIPMENT

#### Model Grids

Three model grids were constructed out of 0.10 in. thick aluminum sheet metal. Rectangular plates were cut first with the exact width and length dimensions. In each grid, slots of 3/8" were cut out by a milling machine. A steel file was used to finish rough edges. Every grid had a constant bar cross-section 1 1/4" wide by 0.10" deep. Variation in grids was obtained by using three different lengths of 18 in., 21 in., and 24 in. Allowing an inch on both ends for support, the effective length for each grid was 16 in., 19 in., and 22 in., respectively. A dimension sketch of each grid is presented in Figures 17, 18, and 19.

#### Strain Gage Assembly

SR-4 strain gages were mounted on both faces of each middle bar. The gages were of Baldwin-Lima-Hamilton, Type FAP-25-12, gage factor of 2.04  $\pm$  1%, and gage resistance of 120.0  $\pm$  0.5 ohms.

Strain was measured by a Baldwin strain gage indicator calibrated in micro-inches per inch of length. Since it was required to read the strain from more than one strain gage at any one time, a switching and balancing unit was connected to the strain indicating device. A picture of the strain indicator with the switching and balancing unit is shown on Figure 22.

## Weights

A toledo laboratory computagram balancing scale calibrated to 0.01 of a pound weight was used to measure the equivalent model weights. Fine sand was used for weight components. An animal weight component exerted through one front hoof was represented by the combined weight of a one-pint can, a strong nylon string, and a fish hook. Each load was applied by hanging the combined weight from the grid. The fish hooks were blunted slightly so they would not make a dent in the aluminum grid thus causing variation in the cross-section of the bar. The fish hooks were used to simulate point leading.

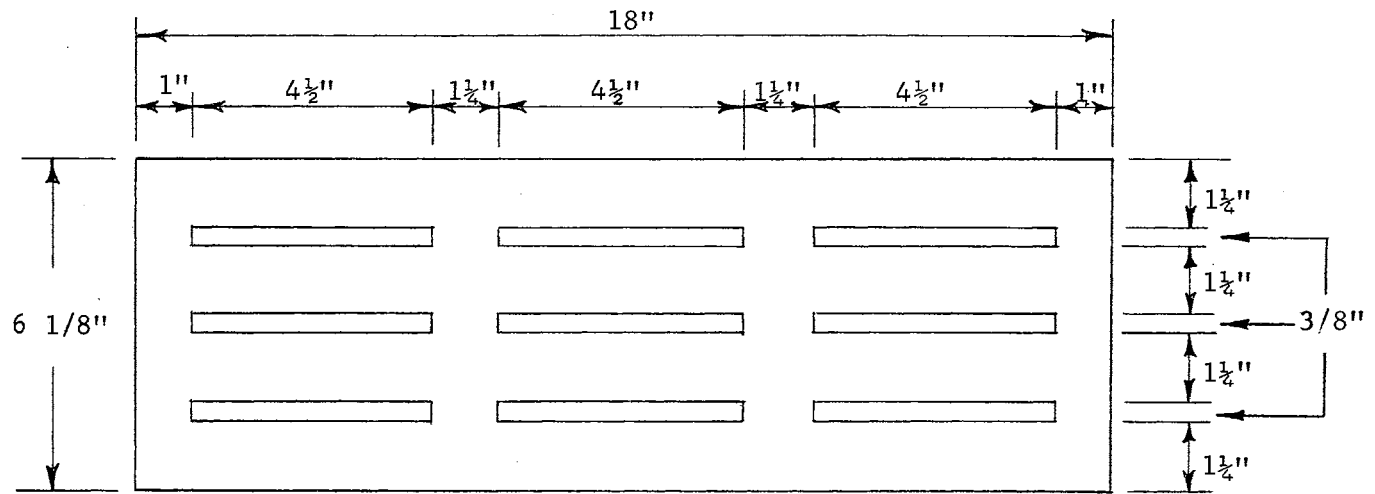


Figure 17. Model Grid No. 1



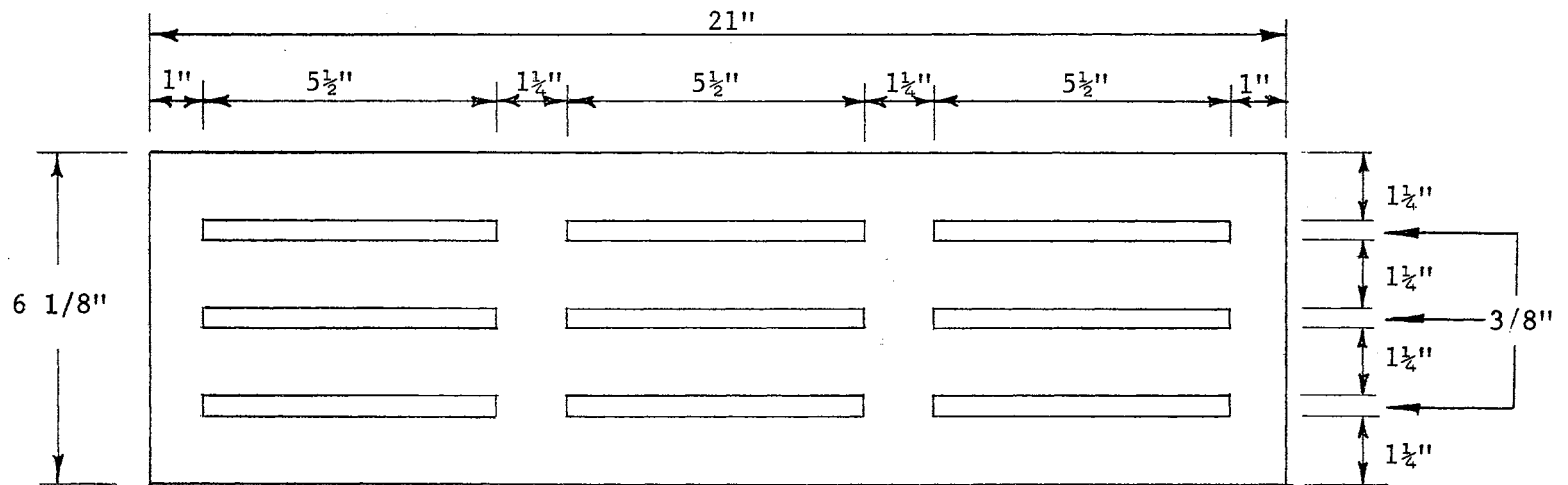


Figure 18. Model Grid No. 2

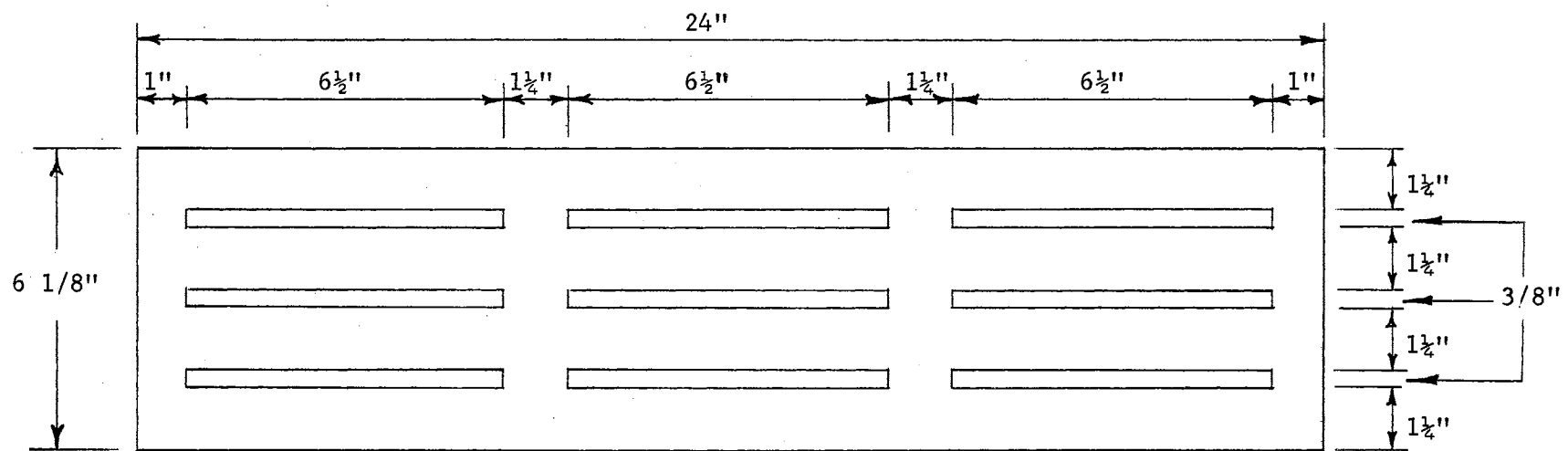


Figure 19. Model Grid No. 3

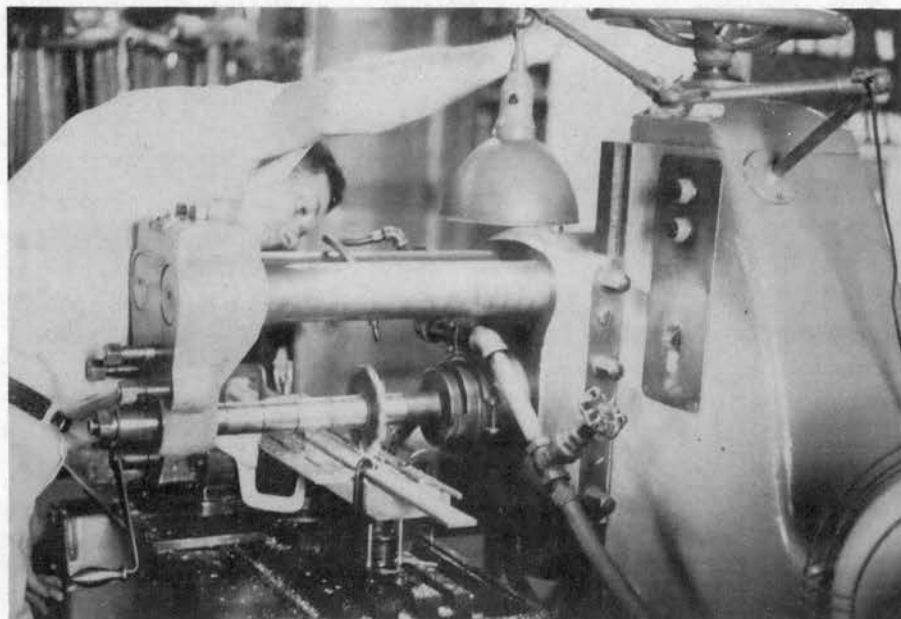


Figure 20. View of milling machine cutting out slots in a model grid.

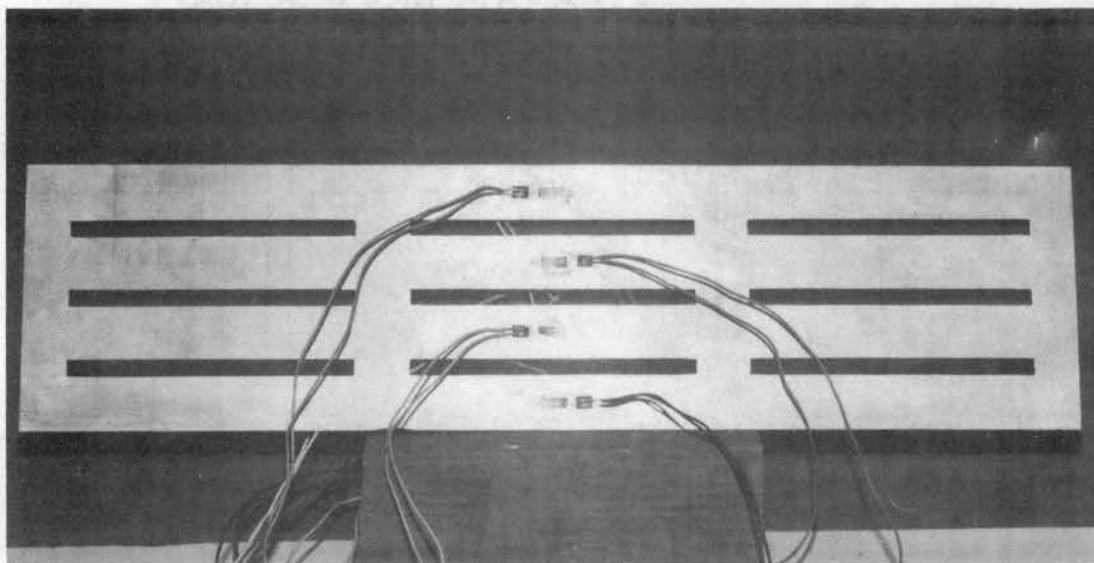


Figure 21. Typical model grid with strain gages and lead wires.

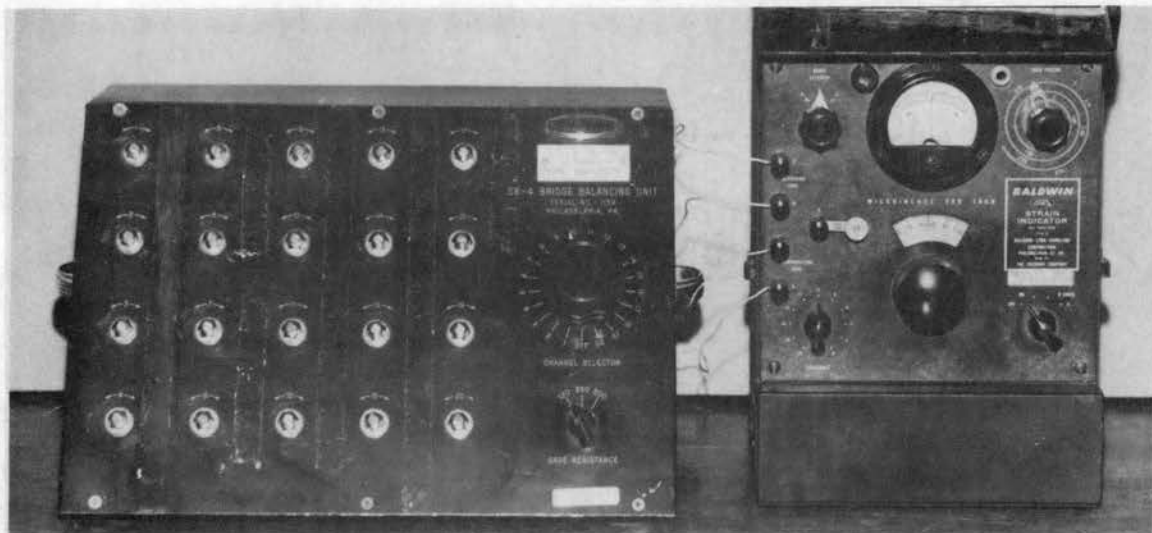


Figure 22. Bridge balancing unit and strain indicator used for measuring strain in model grids.

## CHAPTER V

### ANALYTICAL PROCEDURE

#### Determination of Stiffness Index For Bending in Prototype

The moment of inertia for bending was determined on a trapezoidal cross-section of medium strength reinforced concrete. For dimensions of the cross-section and size of reinforcement bars see Figure 23 below.

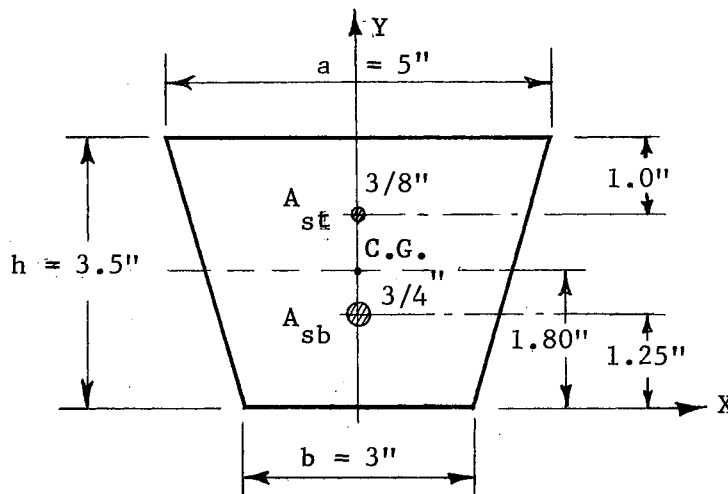


Figure 23. Prototype Cross-section

#### Moment of Inertia

$A_c$  = Area of concrete cross-section

$A_{st}$  = Area of cross-section of top rod

$A_{sb}$  = Area of cross-section of bottom rod

$n$  = Ratio of modulus of elasticity of steel ( $E_s$ ) to that of medium strength concrete ( $E_c$ )

Center of gravity,  $\bar{Y}$

$$\bar{Y}_c = \frac{h}{3} \left( \frac{2a + b}{a + b} \right) = \frac{3.5}{3} \left( \frac{10 + 3}{5 + 3} \right) = 1.90 \text{ In.}$$

$$A_c = \frac{h}{2}(a + b) = \frac{3.5}{2}(5 + 3) = 14.0 \text{ Sq.In.}$$

$$A_{st} = \frac{1}{4} \left( \frac{3}{8} \right)^2 \pi = 0.1105 \text{ Sq.In.}$$

$$A_{sb} = \frac{1}{4} \left( \frac{3}{4} \right)^2 \pi = 0.4420 \text{ Sq.In.}$$

$$\bar{Y} = \frac{(A_c)(\bar{Y}_c) + (A_{st})(n-1)(h-1.0) + (A_{sb})(n-1)(1.25)}{A_c + (A_{st})(n-1) + (A_{sb})(n-1)}$$

$$\bar{Y} = \frac{14.0 \times 1.90 + 0.1105(9-1)(2.5) + 0.4420(9-1)(1.25)}{14.0 + (0.1105)(9-1) + 0.4420(9-1)}$$

$$\bar{Y} = 1.80 \text{ In.}$$

$$I_{xc} = \frac{h^3(a^2 + 4ab + b^2)}{36(a + b)}$$

$$I_{xc} = \frac{(3.5)^3 [(5)^2 + (4)(5)(3) + (3)^2]}{36(5 + 3)}$$

$$I_{xc} = 13.993 \text{ In.}^4$$

$$I'_{xc} = I_{xc} + A_c(\bar{Y}_c - \bar{Y})^2 + A_{st}(n-1)(3.5 - 1.0 - \bar{Y})^2 + A_{sb}(n-1)(\bar{Y} - 1.25)^2$$

$$I'_{xc} = 13.993 + 14.0(0.10)^2 + 0.1105(8)(0.70)^2 + 0.4420(8)(0.55)^2$$

$$I'_{xc} = 15.636 \text{ In.}^4$$

For medium strength concrete — compressive strength of 3000 psi and 140 Lb/cu. ft. (11).

$$E = 3.0 \times 10^6 \text{ psi}$$

Therefore,

$$EI = (3.0 \times 10^6)(15.636)$$

$$EI = 46,908,000 \text{ LbF}\cdot\text{Sq. In.}$$

Determination of Stiffness Index For  
Torsion in Prototype

The analysis of shearing stress distribution in non-circular cross-sections of bars under torsion is complex. Through analytical evidence and many experiments, it has been found that in non-circular sections the shearing unit stresses are not proportional to their distances from the axis. Some knowledge of the location of maximum and minimum shearing stresses in non-circular sections may be obtained from the application of the membrane analogy (21). The membrane analogy is derived from the observation that the differential equation of the deflection of a membrane has the same form as the theoretical equation (from the theory of elasticity) for the shearing stresses in any uniform rod subjected to twisting moments. Therefore, the use of the polar moment of inertia in a trapezoidal cross-section provides only an approximation of the stiffness index for torsion.

The polar moment of inertia was determined on the same trapezoidal cross-section without reinforcement. Tensile reinforcement, used in the construction of prototype grids, would only have a slight effect in reducing torsional stresses. Hence, the effect of reinforcement in the computation of polar moment of inertia will be neglected.

Divide the trapezoid into one rectangle and two congruent triangles.

Polar Moment of Inertia

$$A_1 = A_3 = \frac{3.5 \times 1}{2} = 1.75 \text{ Sq. In.}$$

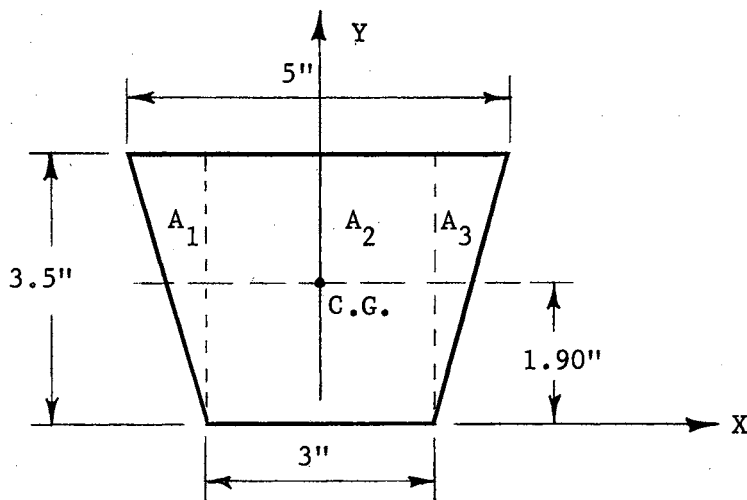


Figure 24. Prototype Cross-section

$$A_2 = 3.5 \times 3 = 10.5 \text{ Sq. In.}$$

Static moment of the three areas

$$2(1.75) \times \frac{2}{3}(3.5) = 8.17 \text{ In.}^3$$

$$10.5 \times \frac{3.5}{2} = 18.4 \text{ In.}^3$$

$$\text{Center of gravity} = \frac{8.17 + 18.4}{14.0} = 1.90 \text{ In.}$$

Moment of inertia of rectangle about center of gravity

$$I_{xcr} = \frac{3 \times (3.5)^3}{12} + 10.5(1.75-1.9)^2$$

$$I_{xcr} = 10.7 + 0.236 = 10.936 \text{ In.}^4$$

Moment of inertia of rectangle about axis of symmetry

$$I_{yr} = \frac{3.5 \times (3)^3}{12} = 7.875 \text{ In.}^4$$

Moment of inertia of both triangles about center of gravity

$$I_{xct} = 2 \left[ \frac{1 \times (3.5)^3}{36} + (1.75)(2.33-1.90)^2 \right]$$



$$I_{xct} = 2 (1.191 + 0.324) = 3.030 \text{ In.}^4$$

Moment of inertia of both triangles about axis of symmetry

$$I_{yt} = 2 \left[ \frac{(3.5)(1)^3}{36} + (1.75)(1.5 + 0.33)^2 \right]$$

$$I_{yt} = 2(0.972 + 5.86) = 13.664 \text{ In.}^4$$

$$J = I_{xcr} + I_{yr} + I_{xct} + I_{yt} \quad (5-1)$$

$$J = 10.936 + 7.875 + 3.030 + 13.664$$

$$J = 35.505 \text{ In.}^4$$

For the same strength and weight of concrete the modulus of rigidity is

$$G = \frac{E}{2(1 + \mu)} \quad (5-2)$$

For concrete, values of  $\mu$  could be assumed from 0.10 to 0.15

Taking  $\mu = 0.125$

$$G = \frac{3.0 \times 10^6}{2(1 + 0.125)}$$

$$G = 1.344 \times 10^6 \text{ Psi}$$

Stiffness index for torsion, GJ

$$GJ = (1.344 \times 10^6)(35.505)$$

$$GJ = 47,718,720 \text{ lbF}\cdot\text{Sq. In.}$$

## CHAPTER VI

### EXPERIMENTAL PROCEDURE

It was explained in Chapter III that the weight of an animal was reduced to the model size by the formula  $P_m = (L_p^2/L_m^2) [(EI)_m/(EI)_p](P_p)$ . To use this relationship, it was necessary to compute the stiffness index for bending for the material from which the model grids were constructed.

#### Determination of Stiffness Index

##### For Bending in Model

Two groups of three strips 1.0 inches, 1.25 inches and 1.5 inches wide and 6.0 inches, 10.0 inches, and 18.0 inches long respectively were cut from the actual experimental 0.10 inches thick aluminum plate. The samples were tested for E, modulus of elasticity, using two methods.

##### A. Simply Supported Beam

1. Two SR-4 strain gages were mounted at the center of both sides of each strip and lead wires were soldered to each terminal of a strain gage. Temperature compensation and double strain reading were achieved by the use of strain gages on both sides.
2. Each strip was simply supported by mounting on rigidly anchored steel supports.

3. The lead wires were hooked to the active and compensating terminals of a strain recorder.
4. Three loads of 1 LbF, 2 LbF, and 3 LbF were applied at mid span.
5. The strain was read and recorded in micro-inches per inch of length.
6. The stiffness index was computed from the following equation

$$EI = \frac{PLd}{8\epsilon} \quad (6-1)$$

where,

P = load applied at mid span, LBF

L = length of strip, In.

d = depth or thickness of strip, In.

$\epsilon$  = strain, micro-inches per inch of length

7. The modulus of elasticity was calculated for each strip by dividing the EI value by the corresponding moment of inertia, I.

#### B. Cantilevered Beam

1. Each strip was fixed on one end to a rigidly anchored steel beam.
2. Loads of 1 LbF, 2 LbF, and 3 LbF were applied at the free end of a bar and the deflections were measured at the point where the load was applied. An Ames dial indicator was used to measure the deflections.
3. The stiffness index was computed from the following equation.

$$EI = \frac{PL^3}{3\delta} \quad (6-2)$$

where,

$P$  = load applied at free end, LbF

$L$  = length of strip from fixed end to point of load application, In.

$\delta$  = deflection at point of load application, In.

4. The modulus of elasticity was calculated for each strip by dividing the EI value by the corresponding moment of inertia, I.

Finally, taking the average E from the sum of the values of E from both methods, the stiffness index was determined for a 1.25" x 0.10" cross-section that was used in the main model grid experiment. The resulting value of EI was 1064.83 LbF·Sq.In.

#### Determination of Animal Body Configuration and Weight Ratio of Load Carried by Front Legs to Hind Legs

A flat platform scale was used to measure the weight of the animal. The scale was fenced-in and had only one gate. The area around the scale platform was of the same level as the scale platform so that the animal would not sense any difference in elevation. The first weight was taken with the animal's front legs only resting on the scale platform and the second weight was taken with its hind legs only resting on the scale platform. Then the total weight was taken.

The linear dimensions were measured by a tape measure for lengths, such as  $\alpha$ ,  $\beta$ , and  $\lambda$  and a simple caliper was used for width, such as  $\omega_1$ ,  $\omega_2$ , and  $\omega_3$ .

The values for the weights and linear dimensions are tabulated in Appendix A.

#### Determination of Strain in Model Grids

1. Load spacings were marked on both of the free longitudinal edges. Spacing was governed by the distance between the front hoofs,  $\gamma$ , and the width at the shoulders of the animal,  $\omega_3$ . The distance,  $D'$ , between the adjacent hoofs of two animals A and B was:

$$D' = \left( \frac{\omega_3 - \gamma}{2} \right)_A + \left( \frac{\omega_3 - \gamma}{2} \right)_B \quad (6-3)$$

2. One strain gage was mounted on each of the four middle bars. Each strain gage was placed on the bar centered transversely and longitudinally. For a symmetrically loaded bar, it was expected that the maximum bending moment will occur in the middle of the bar.
3. Lead wires were soldered to each strain gage.
4. The grids were then mounted one at a time on rigidly anchored beam supports. The grids were simply supported on both ends.
5. Since the original model weights were too small to obtain an appreciable reading on the strain recorder, a load to strain relationship was established by loading each grid by seven loads of 1.0 LbF, 2.0 LbF, 3.0 LbF, 4.0 LbF, 5.0 LbF, 6.0 LbF, and 7.0 LbF. Five replications were taken for every load applied on a grid.
6. The equivalent model weight for one hoof was determined by using a ratio of  $1\frac{1}{2}$  to 1 of load carried by the front legs to

that carried by the hind legs. Table XIII shows the equivalent loads.

TABLE X  
EQUIVALENT LOADS IN Lbf

<u>Prototype Weight of Animal</u>	<u>Model Weight of Animal</u>	<u>Load Exerted By One Front Hoof</u>
600	0.2182	0.0606
800	0.2909	0.0808
1000	0.3636	0.1010
1200	0.4364	0.1212

7. An equivalent hoof weight was represented by the combined weight of a one-pint can, fine sand used as weight components, a strong nylon string used for hanging the load from the grid-bar and lightweight fish-hook for applying the weight as point load on the middle of a bar. A toledo laboratory computagram balancing scale was used to measure the weight. The scale was calibrated to 0.01 of a pound weight.
8. According to the load spacing specifications, each class of load was applied on every grid. First, one free longitudinal edge was loaded. This was designated as Zone AA. Five replications were taken on Zone AA. The same load was then applied on the other free longitudinal edge of the same face. This edge was labeled Zone BB and five replications were taken on it.
9. Starting from Zone AA, each strain gage was labeled Station No. 1, Station No. 2, Station No. 3, and Station No. 4. The designation of the stations remained the same when the load

was applied on Zone BB. Figure 25 shows the position of the strain gages labeled as stations and Zones AA and BB.

10. A replication consisted of (1) balancing the strain indicator on 1000, (2) applying the load on the grid, (3) recording the strain under load, and (4) removing the load.

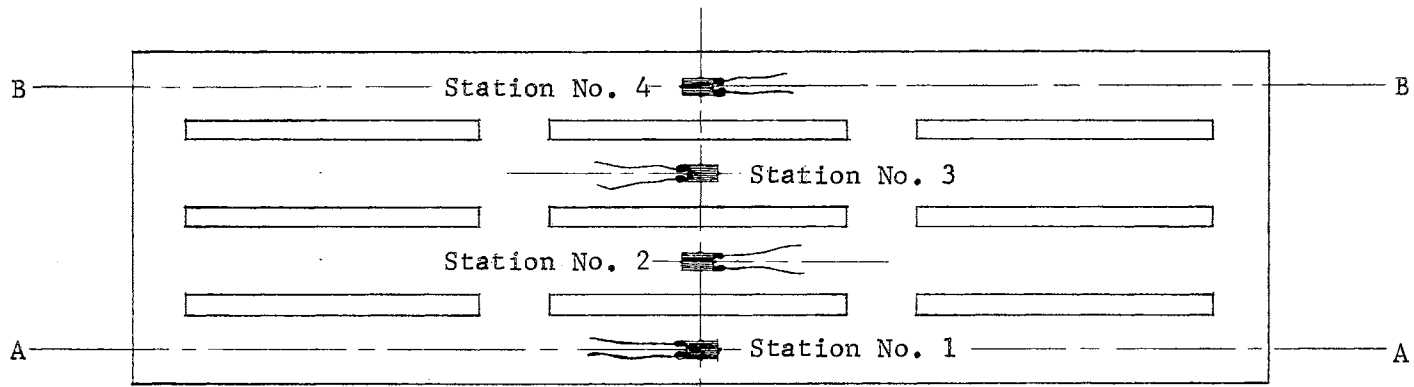


Figure 25. Designation of Loading Zones and Strain Gage Stations For A Typical Model Grid



## CHAPTER VII

### ANALYSIS OF DATA

#### Calculation of the Bending Moment

Using the observed strain readings obtained from the experiments, the corresponding bending moments were calculated for the model grids. The calculations were performed by an IBM 7040 computer using Fortran IV Language.

The flexural equation

$$\sigma = \frac{My}{I} \quad (7-1)$$

where,

$\sigma$  = normal stress in LbF/Sq.In. at a distance  $y$  from the neutral surface and on a transverse plane

$M$  = resisting moment of the section in LbF·In.

$I$  = centroidal moment of inertia in In.<sup>4</sup>

and the equation of Young's Modulus of Elasticity

$$E = \frac{\sigma}{\epsilon} \quad (7-2)$$

where,

$E$  = Young's Modulus of Elasticity in LbF/Sq.In.

$\epsilon$  = strain in micro-inches per inch of length

combine to give the equation

$$M = \frac{\epsilon(EI)}{y} \quad (7-3)$$

Equation (7-3) was used in the calculation of the bending moments for the model grids. The EI value for the model was 1064.83 LbF·Sq.In.

To calculate the corresponding bending moments in the prototype grids, the following model-to-prototype relationship was used:

$$\left(\frac{ML}{EI}\right)_m = \left(\frac{ML}{EI}\right)_p \quad (7-4)$$

Hence,

$$M_p = \frac{L_m}{L_p} \frac{(EI)_p}{(EI)_m} M_m \quad (7-5)$$

The values for the strain and bending moments are tabulated in Appendix B.

#### Calculation of $\pi_{14}$

The values of  $\pi_{14} = ML/EI$  were calculated for the bending moment of each replication. These values along with corresponding values of  $\pi_2$ ,  $\pi_3$ ,  $\pi_4$ , and  $\pi_{12}$  are indicated on Tables XI, XII, and XIII. A value in a replication is an average of Zone AA and Zone BB.

#### Development of the Prediction Equation

Using the average of five replications for each station, values of  $\pi_{14}$  were plotted against the corresponding values of  $\pi_{12}$ , the load parameter. The natural logarithm of the reciprocal values of these PI terms plotted as straight lines for each grid as shown on Figures 26, 27, 28, and 29. The straight lines in these graphs are linear regression lines of the form  $\ln(1/\pi_{14}) = \ln(1/A) + b \cdot \ln(1/\pi_{12})$  with  $\ln(1/A)$  as the intercept and  $b$  as the slope.  $A$  is the value of  $\pi_{14}$  at the intercept for  $\pi_{12} = 1.0$ . The linear regression analysis was based on the method of least squares.

TABLE XI

## PARAMETER COMBINATIONS FOR GRID NO. 1

Exp. No.	Load in LbF	$\pi_2 = \frac{D}{L}$	$\pi_3 = \frac{V}{L}$	$\pi_4 = \frac{\omega_3}{L}$	$\pi_{12} = \frac{PL^2}{EI}$	Rep.	$\pi_{14} = \frac{ML^*}{EI}$			
							Sta. No. 1	Sta. No. 2	Sta. No. 3	Sta. No. 4
1	0.0606	0.3828	0.1562	0.2812	0.0524	1	0.0047	0.0035	0.0032	0.0030
						2	0.0047	0.0035	0.0032	0.0031
						3	0.0047	0.0035	0.0032	0.0031
						4	0.0047	0.0035	0.0031	0.0031
						5	0.0047	0.0035	0.0031	0.0030
2	0.0808	0.3828	0.1562	0.3125	0.0699	1	0.0055	0.0041	0.0037	0.0036
						2	0.0054	0.0040	0.0036	0.0035
						3	0.0054	0.0041	0.0037	0.0035
						4	0.0054	0.0041	0.0036	0.0035
						5	0.0054	0.0041	0.0037	0.0035
3	0.1010	0.3828	0.1875	0.3438	0.0873	1	0.0063	0.0047	0.0042	0.0040
						2	0.0063	0.0047	0.0042	0.0040
						3	0.0063	0.0047	0.0042	0.0040
						4	0.0063	0.0047	0.0042	0.0041
						5	0.0062	0.0047	0.0042	0.0040
4	0.1212	0.3828	0.1875	0.3750	0.1048	1	0.0068	0.0051	0.0046	0.0045
						2	0.0068	0.0051	0.0046	0.0045
						3	0.0068	0.0051	0.0046	0.0044
						4	0.0069	0.0051	0.0046	0.0044
						5	0.0069	0.0051	0.0046	0.0044

\*This value of  $\pi_{14}$  is an average of Zone AA and Zone BB.

TABLE XII  
PARAMETER COMBINATIONS FOR GRID NO. 2

Exp. No.	Load in LbF	$\pi_2 = \frac{D}{L}$	$\pi_3 = \frac{Y}{L}$	$\pi_4 = \frac{\omega_3}{L}$	$\pi_{12} = \frac{PL^2}{EI}$	Rep.	$\pi_{14} = \frac{ML^*}{EI}$			
							Sta. No. 1	Sta. No. 2	Sta. No. 3	Sta. No. 4
1	0.0606	0.3224	0.1315	0.2368	0.0739	1	0.0072	0.0056	0.0052	0.0050
						2	0.0072	0.0056	0.0051	0.0050
						3	0.0072	0.0056	0.0051	0.0050
						4	0.0072	0.0056	0.0052	0.0050
						5	0.0072	0.0056	0.0052	0.0050
2	0.0808	0.3224	0.1315	0.2632	0.0985	1	0.0084	0.0066	0.0061	0.0059
						2	0.0085	0.0068	0.0061	0.0059
						3	0.0085	0.0066	0.0061	0.0059
						4	0.0085	0.0066	0.0061	0.0058
						5	0.0085	0.0066	0.0061	0.0059
3	0.1010	0.3224	0.1579	0.2895	0.1231	1	0.0101	0.0078	0.0072	0.0070
						2	0.0100	0.0078	0.0072	0.0070
						3	0.0100	0.0078	0.0072	0.0070
						4	0.0100	0.0078	0.0072	0.0070
						5	0.0100	0.0078	0.0071	0.0069
4	0.1212	0.3224	0.1579	0.3158	0.1478	1	0.0107	0.0082	0.0076	0.0073
						2	0.0106	0.0083	0.0076	0.0073
						3	0.0107	0.0082	0.0076	0.0074
						4	0.0106	0.0082	0.0076	0.0073
						5	0.0107	0.0082	0.0076	0.0074

\*This value of  $\pi_{14}$  is an average of Zone AA and Zone BB.

TABLE XIII

PARAMETER COMBINATIONS FOR GRID NO. 3

Exp. No.	Load in LbF	$\pi_2 = \frac{D}{L}$	$\pi_3 = \frac{Y}{L}$	$\pi_4 = \frac{\omega_3}{L}$	$\pi_{12} = \frac{PL^2}{EI}$	Rep.	$\pi_{14} = \frac{ML^*}{EI}$			
							Sta. No. 1	Sta. No. 2	Sta. No. 3	Sta. No. 4
1	0.0606	0.2784	0.1136	0.2045	0.0990	1	0.0112	0.0086	0.0080	0.0080
						2	0.0112	0.0085	0.0080	0.0080
						3	0.0112	0.0085	0.0080	0.0081
						4	0.0111	0.0086	0.0081	0.0081
						5	0.0111	0.0085	0.0080	0.0081
2	0.0808	0.2784	0.1136	0.2273	0.1321	1	0.0129	0.0102	0.0096	0.0095
						2	0.0130	0.0102	0.0096	0.0096
						3	0.0129	0.0101	0.0095	0.0095
						4	0.0129	0.0101	0.0096	0.0095
						5	0.0130	0.0102	0.0096	0.0095
3	0.1010	0.2784	0.1364	0.2500	0.1651	1	0.0150	0.0118	0.0110	0.0108
						2	0.0150	0.0118	0.0111	0.0108
						3	0.0151	0.0118	0.0111	0.0108
						4	0.0151	0.0118	0.0110	0.0108
						5	0.0151	0.0117	0.0111	0.0108
4	0.1212	0.2784	0.1364	0.2727	0.1981	1	0.0163	0.0130	0.0122	0.0118
						2	0.0164	0.0130	0.0122	0.0120
						3	0.0164	0.0130	0.0123	0.0120
						4	0.0164	0.0130	0.0122	0.0119
						5	0.0163	0.0129	0.0121	0.0119

\*This value of  $\pi_{14}$  is an average of Zone AA and Zone BB.

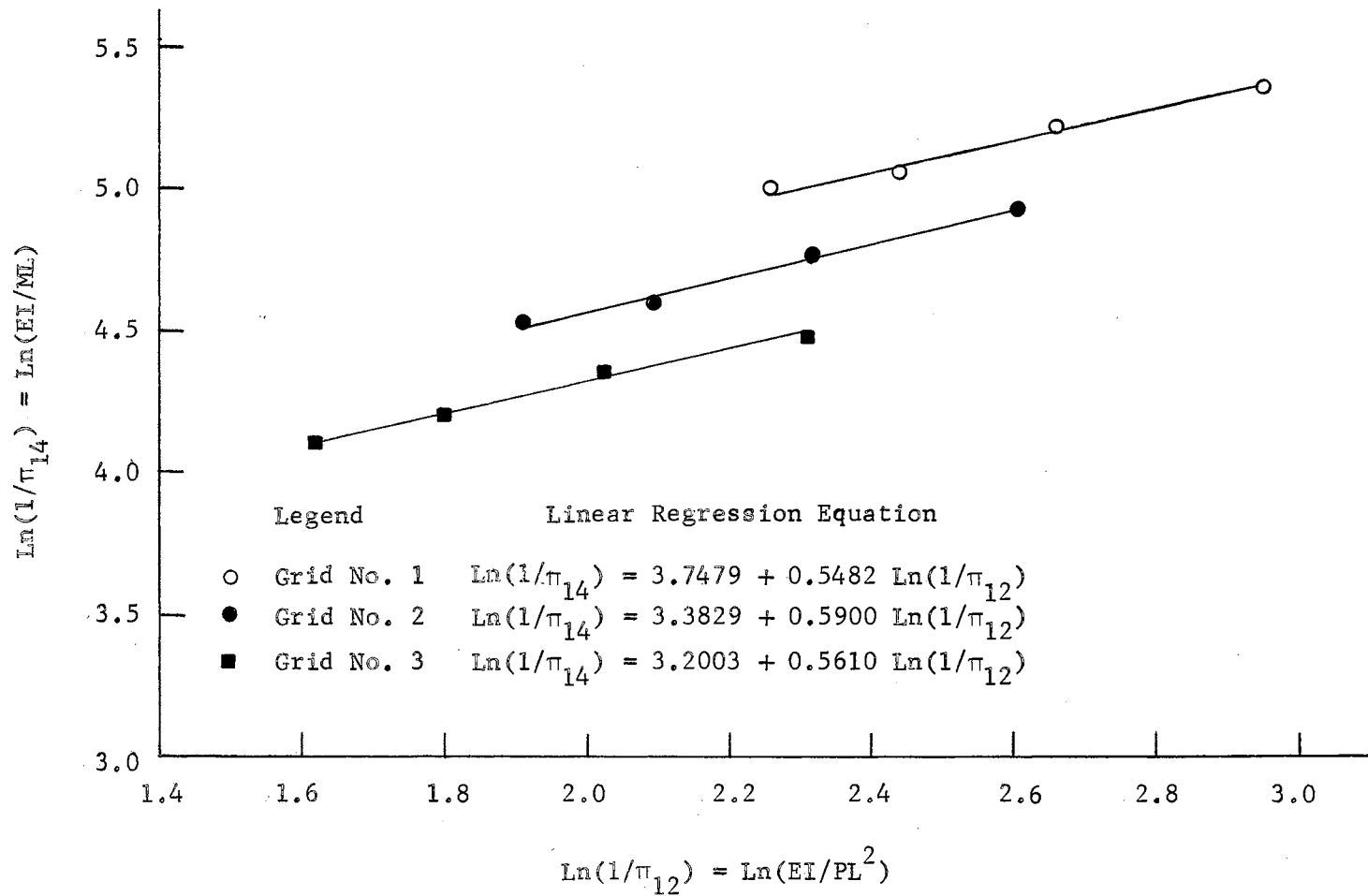


Figure 26. Plot of Bending Moment Parameter Versus Load Parameter for Station No. 1

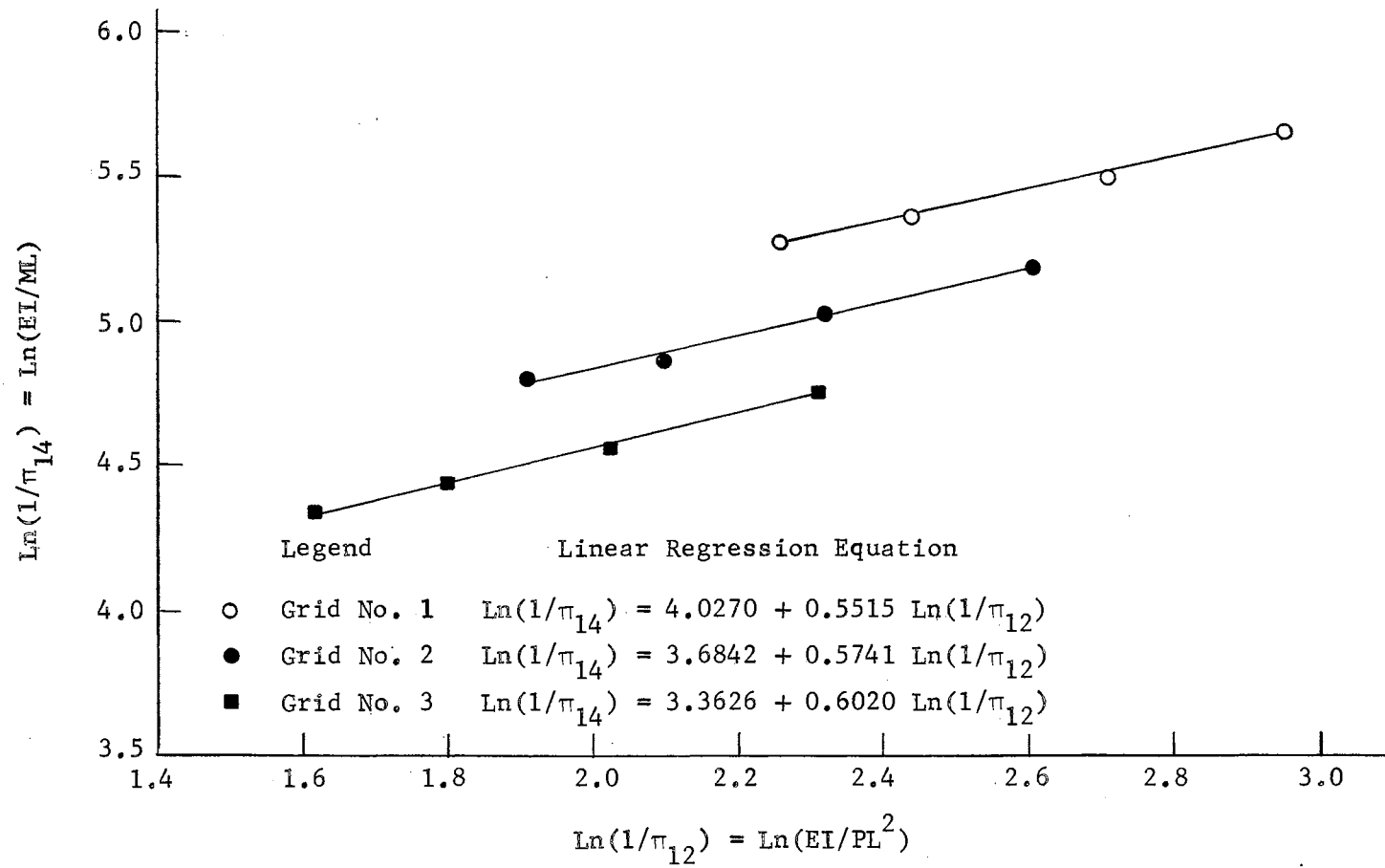


Figure 27. Plot of Bending Moment Parameter Versus Load Parameter for Station No. 2.

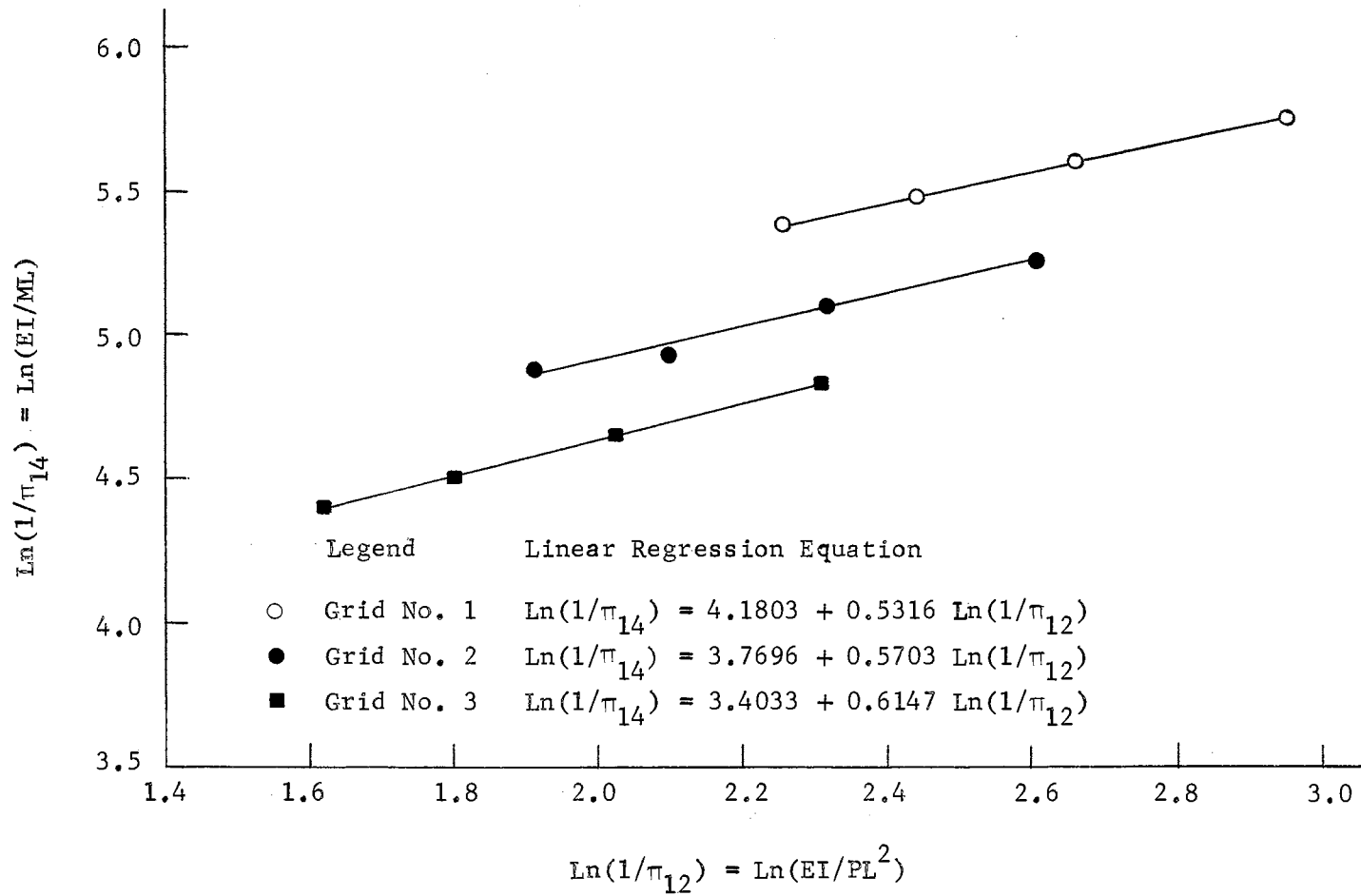


Figure 28. Plot of Bending Moment Parameter Versus Load Parameter for Station No. 3



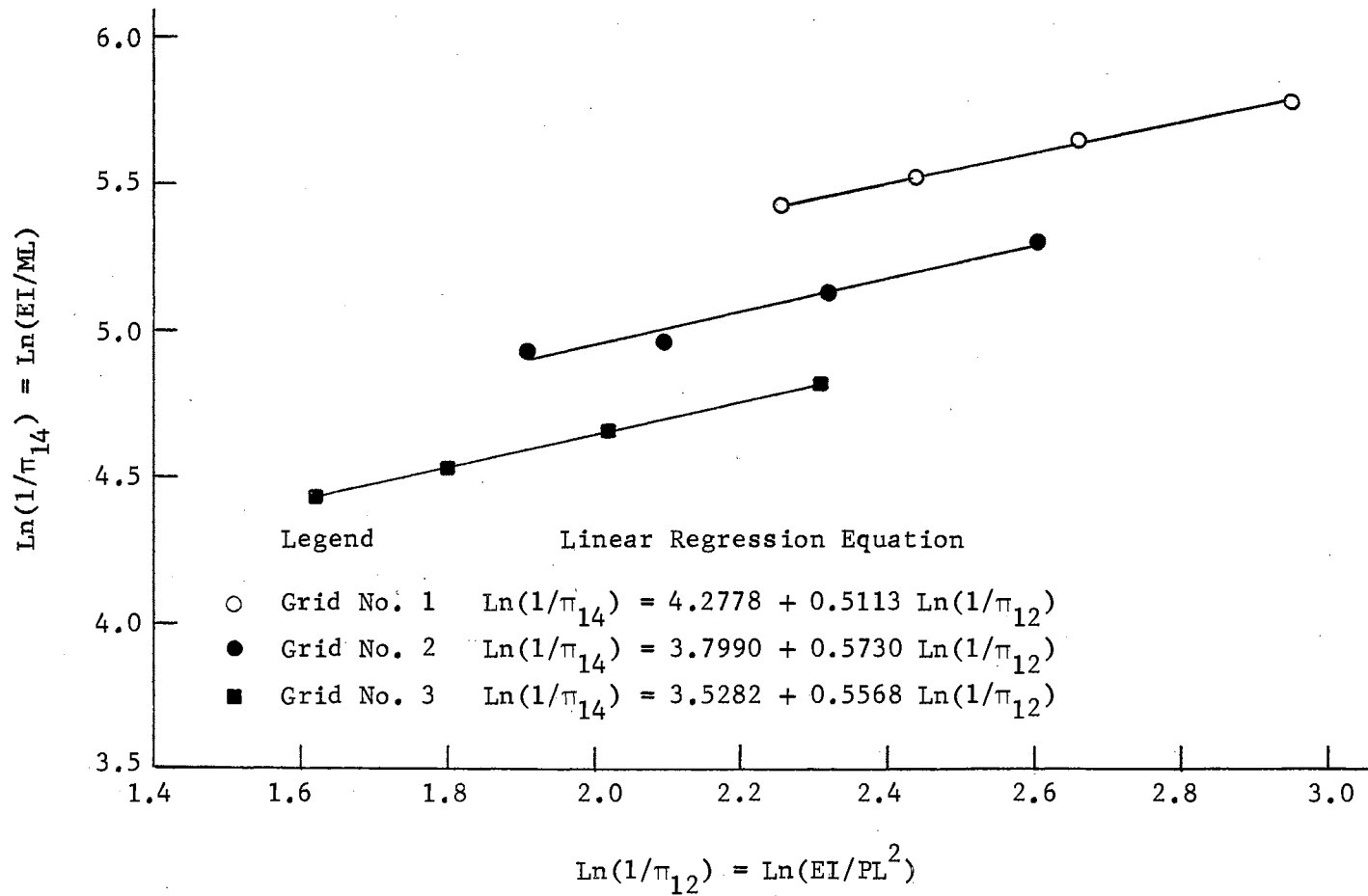


Figure 29. Plot of Bending Moment Parameter Versus Load Parameter for Station No. 4.

The slopes pertaining to each grid were pooled by taking the average of the three slopes. The result was one regression equation for each station as follows:

$$\text{Station No. 1 } \ln(1/\pi_{14}) = \ln(1/B_1) + 0.5664 \ln(1/\pi_{12}) \quad (7-6a)$$

$$\text{Station No. 2 } \ln(1/\pi_{14}) = \ln(1/B_2) + 0.5759 \ln(1/\pi_{12}) \quad (7-6b)$$

$$\text{Station No. 3 } \ln(1/\pi_{14}) = \ln(1/B_3) + 0.5722 \ln(1/\pi_{12}) \quad (7-6c)$$

$$\text{Station No. 4 } \ln(1/\pi_{14}) = \ln(1/B_4) + 0.5470 \ln(1/\pi_{12}) \quad (7-6d)$$

The  $\ln(1/B_i)$  was evaluated for each station by plotting the  $\ln(1/\pi_2)$ , the logarithm of the reciprocal of the grid length parameter, against the  $\ln(1/A)$  for each grid. From the linear regression analysis, Figure 30, the values of  $\ln(1/B_i)$  were:

$$\text{Station No. 1 } \ln(1/B_1) = 5.3884 - 1.7308 \ln(1/\pi_2) \quad (7-7a)$$

$$\text{Station No. 2 } \ln(1/B_2) = 6.0323 - 2.0835 \ln(1/\pi_2) \quad (7-7b)$$

$$\text{Station No. 3 } \ln(1/B_3) = 6.5240 - 2.4382 \ln(1/\pi_2) \quad (7-7c)$$

$$\text{Station No. 4 } \ln(1/B_4) = 6.5265 - 2.3658 \ln(1/\pi_2) \quad (7-7d)$$

Combining equations (7-6) and (7-7) and expressing the equations in terms of the pertinent quantities, we get the following prediction equations:

$$\text{Station No. 1 } \frac{ML}{EI} = 0.00457 \left(\frac{D}{L}\right)^{-1.7308} \left(\frac{PL}{EI}\right)^{2 \cdot 0.5664} \quad (7-8a)$$

$$\text{Station No. 2 } \frac{ML}{EI} = 0.00240 \left(\frac{D}{L}\right)^{-2.0835} \left(\frac{PL}{EI}\right)^{2 \cdot 0.5759} \quad (7-8b)$$

$$\text{Station No. 3 } \frac{ML}{EI} = 0.00147 \left(\frac{D}{L}\right)^{-2.4382} \left(\frac{PL}{EI}\right)^{2 \cdot 0.5722} \quad (7-8c)$$

$$\text{Station No. 4 } \frac{ML}{EI} = 0.00146 \left(\frac{D}{L}\right)^{-2.3658} \left(\frac{PL}{EI}\right)^{2 \cdot 0.5470} \quad (7-8d)$$

To determine the degree of association of  $\pi_{14}$  as a function of  $\pi_{12}$ , a correlation analysis was performed on the linear regression values of

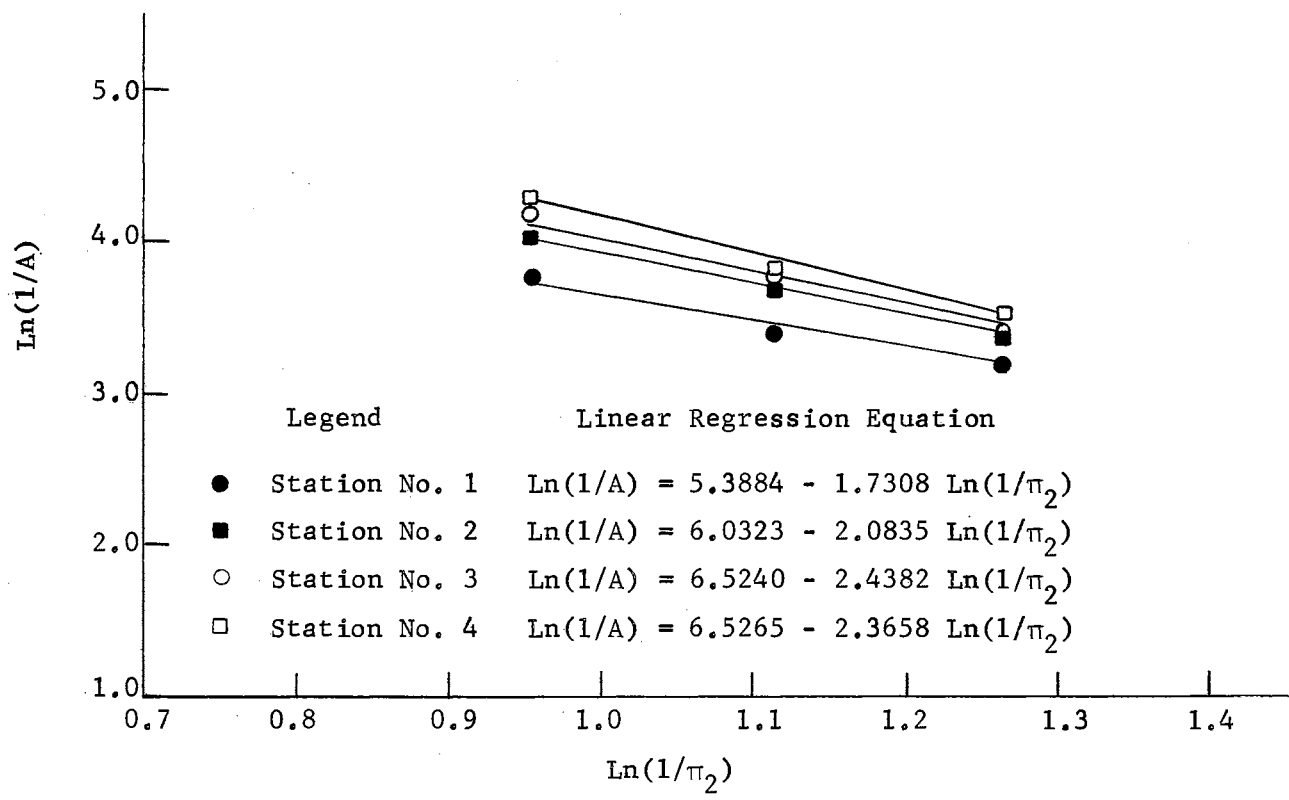


Figure 30. Plot of  $\ln(1/\pi_2)$  Versus  $\ln(1/A)$

$\pi_{12}$  and  $\pi_{14}$ . The resulting correlation coefficients for Station No. 1 were: 0.9964 for Grid No. 1, 0.9830 for Grid No. 2, and 0.9977 for Grid No. 3.

Since there was a high degree of association between  $\pi_{12}$  and  $\pi_{14}$ , it could be assumed that the effects of  $\pi_2$ ,  $\pi_3$ , and  $\pi_4$  could be neglected. However, it was hypothesized that the introduction of  $\pi_2$  and  $\pi_4$  would improve the degree of association and thus provide a more inclusive prediction equation.  $\pi_4$  was introduced into the prediction equation because it is the parameter that determines the number of animals that can be placed on a grid.  $\pi_3$  is an index of spacing between the front hoofs of an animal. Therefore, it was hypothesized to be of secondary effect and not included in the analysis. The final prediction equation was hypothesized to be of the form:

$$\left(\frac{ML}{EI}\right)_i = \bar{\Phi} \left(\frac{D}{L}\right)^{n_1} \left(\frac{\omega_3}{L}\right)^{n_2} \left(\frac{PL^2}{EI}\right)^{n_3} \quad (7-9)$$

where,

$\bar{\Phi}$  = dimensionless coefficient

$i$  = station designation number

$n_1, n_2, n_3$  = dimensionless exponents

The values of  $n_1$  and  $n_3$  are already known for each station from Eq. (7-8). This leaves only  $\bar{\Phi}$  and  $n_2$  to be evaluated.

For each value of  $\pi_4$  we get one equation involving  $\bar{\Phi}$  and  $n_2$  as variables in the form of:

$$\left(\frac{ML}{EI}\right)_{OBS.} = \bar{\Phi} \left(\frac{\omega_3}{L}\right)^{n_2} \left(\frac{D}{L}\right)^{n_1} \left(\frac{PL^2}{EI}\right)^{n_3} \quad (7-10)$$

$$\bar{\phi} \left( \frac{\omega_3}{L} \right)^{n_2} = \frac{\left( \frac{ML}{EI} \right)_{\text{OBS.}}}{\left( \frac{D}{L} \right)^{n_1} \left( \frac{PL^2}{EI} \right)^{n_2}} \quad (7-11)$$

The value on the right side of equation (7-11) is known. Let this value be K.

Therefore,

$$\bar{\phi} \left( \frac{\omega_3}{L} \right)^{n_2} = K \quad (7-12)$$

$$\text{Log}_{10} \bar{\phi} + n_2 \text{Log}_{10} \left( \frac{\omega_3}{L} \right) = \text{Log}_{10} K \quad (7-13)$$

For each value of  $\left( \frac{\omega_3}{L} \right)$  there is a corresponding value of K. This gives twelve equations of the form of equation (7-13) for each station.

With the simultaneous solution of these equations a final prediction equation was computed for every station. The four final prediction equations are:

$$\left( \frac{ML}{EI} \right)_1 = 0.0054 \left( \frac{D}{L} \right)^{-1.7308} \left( \frac{\omega_3}{L} \right)^{0.1264} \left( \frac{PL^2}{EI} \right)^{0.5664} \quad (7-14a)$$

$$\left( \frac{ML}{EI} \right)_2 = 0.0037 \left( \frac{D}{L} \right)^{-2.0835} \left( \frac{\omega_3}{L} \right)^{0.3424} \left( \frac{PL^2}{EI} \right)^{0.5759} \quad (7-14b)$$

$$\left( \frac{ML}{EI} \right)_3 = 0.0032 \left( \frac{D}{L} \right)^{-2.4382} \left( \frac{\omega_3}{L} \right)^{0.5931} \left( \frac{PL^2}{EI} \right)^{0.5772} \quad (7-14c)$$

$$\left( \frac{ML}{EI} \right)_4 = 0.0024 \left( \frac{D}{L} \right)^{-2.3658} \left( \frac{\omega_3}{L} \right)^{0.3793} \left( \frac{PL^2}{EI} \right)^{0.5470} \quad (7-14d)$$

## CHAPTER VIII

### DISCUSSION OF RESULTS

#### Comparison of Predicted $\pi_{14}$ to Observed $\pi_{14}$

It was not possible to compare the results of this study with other previous work because similar information was not available at the time this study was conducted. However, a comparison was made between the predicted values and observed values of the bending moment parameter for each station. Mean error sum of squares were calculated for each station to give 0.0000000015 for Station No. 1, 0.0000000019 for Station No. 2, 0.0000000012 for Station No. 3, and 0.0000000053 for Station No. 4. From this and a visual inspection of Figures 31, 32, 33, and 34, it can be seen that there is good agreement between the predicted and observed values of  $\pi_{14}$ .

#### Application of Experimental Results

From the prediction equations developed in this study, four bending moments could be determined for each grid at the points designated as Station No. 1, Station No. 2, Station No. 3, and Station No. 4. Of the four prediction equations, Eq. (7-14a) gives the maximum bending moment that can be used for an entire grid.

For reinforced concrete grid, the main problem is the design of a bar that could support a given normal load. This could be done according

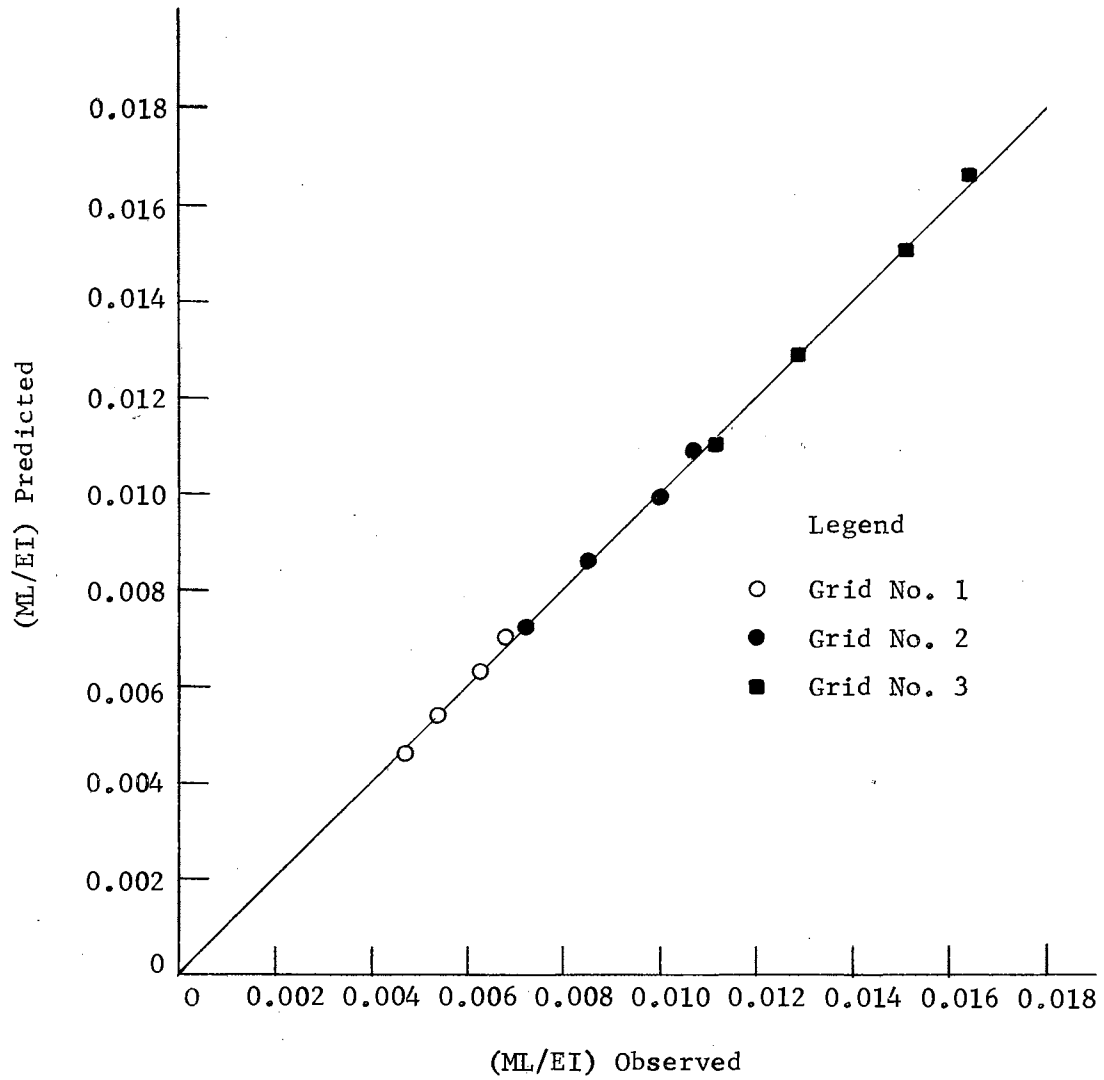


Figure 31. Predicted Compared with Observed Values of  $\pi_{14}$  Using Eq. (7-14a)

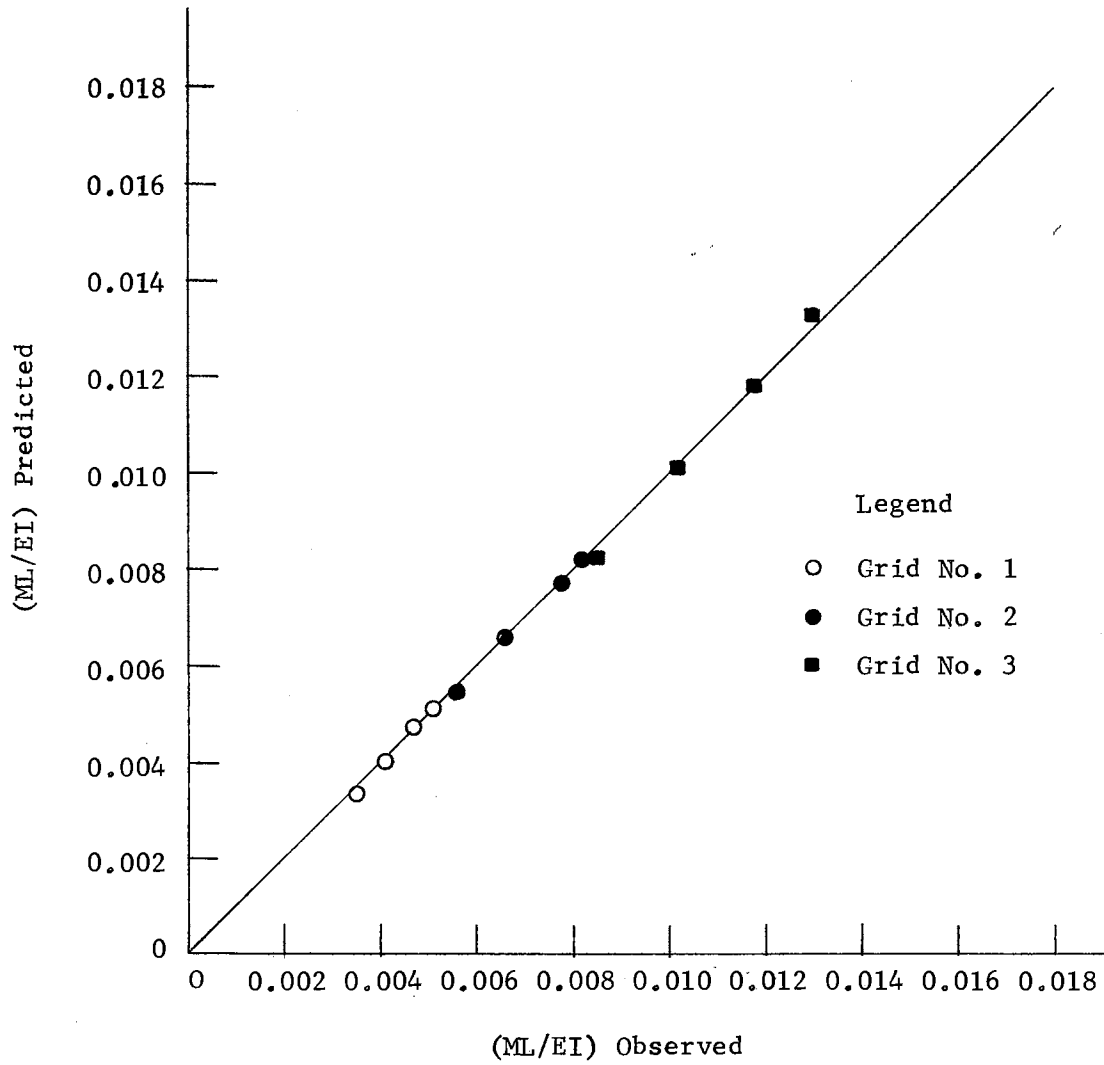


Figure 32. Predicted Compared with Observed Values of  $\pi_{14}$  Using Eq. (7-14b)



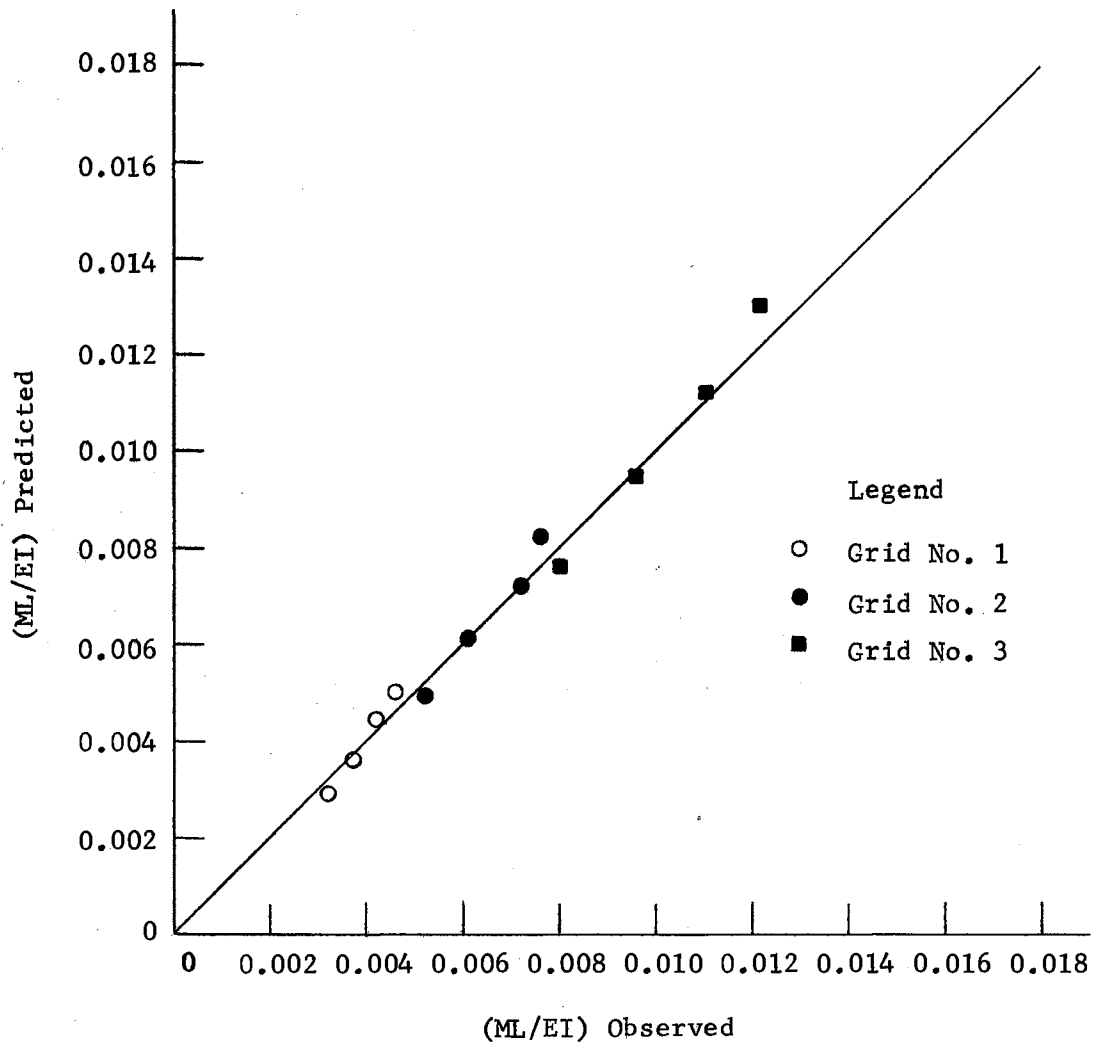


Figure 33. Predicted Compared with Observed Values of  $\pi_{14}$  Using Eq. (7-14c)

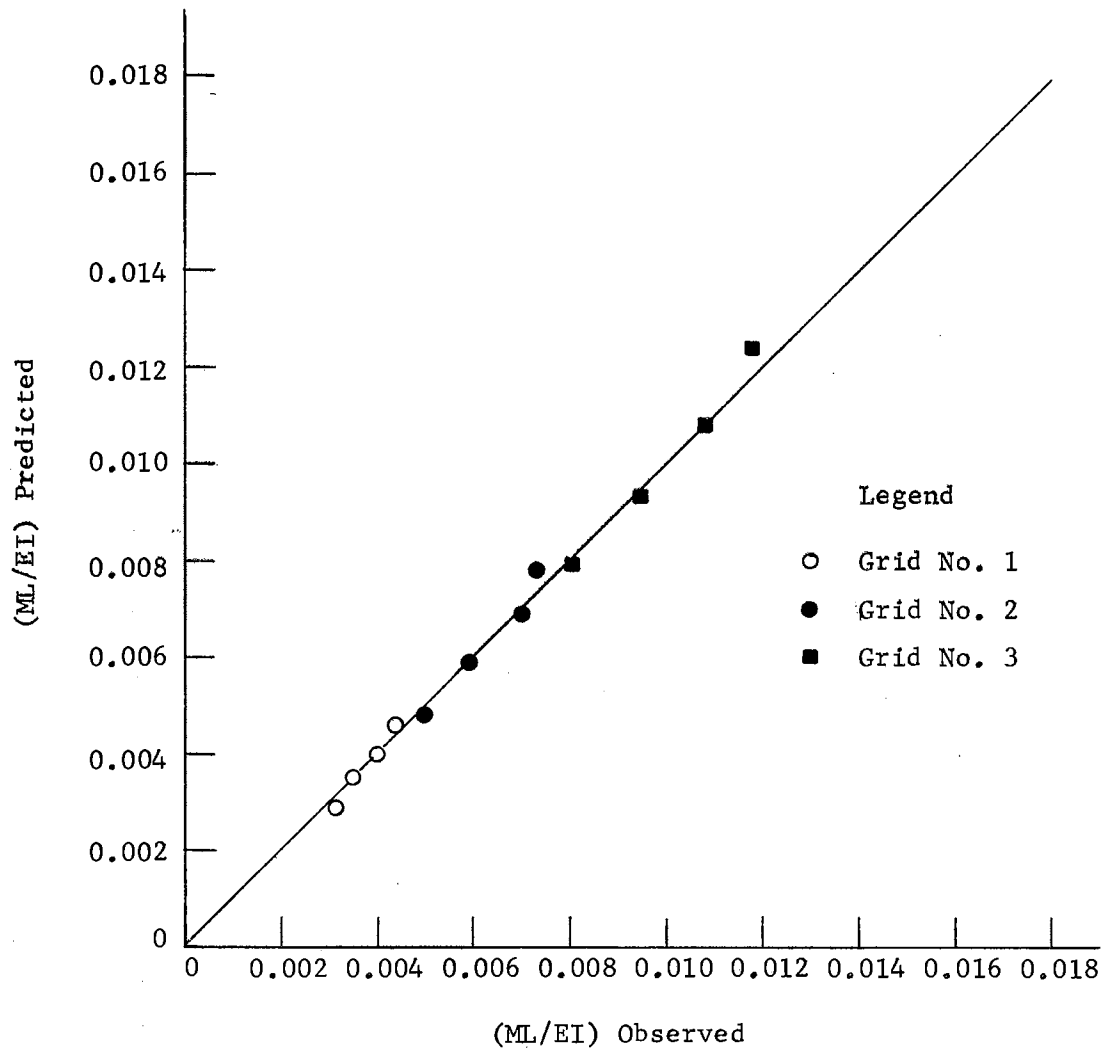


Figure 34. Predicted Compared with Observed Values of  $\pi_{14}$  Using Eq. (7-14d)

to the following procedure:

1. Select a range of animal weights,  $P_i$ , that may be placed on a floor grid.
2. Select the suitable grid length,  $L$ , grid width,  $D$ , and bar width,  $b$ .
3. Select the quality of the concrete to be used; i.e., select the  $f_c$ , compressive stress in extreme fiber, and  $f_c^u$ , ultimate compressive strength of concrete.
4. Select the  $f_s$ , stress in tensile reinforcement.
5. From a table of coefficients ( $K, k, j, p$ ) for rectangular sections -- based on cracked concrete -- find  $K, k$ , and  $p$ .
6. Select a suitable range of depth,  $d$ , of a bar cross-section.
7. Using the Equation ( $M_r = Kbd^2$ ) for the resisting moment, calculate the value of  $M_r$  for each value of  $d$ .
8. Plot the values of  $M_r$  against the values of  $d$ .
9. Using the prediction equation for Station No. 1 --

$$\frac{ML}{EI} = 0.0054 \left( \frac{D}{L} \right)^{-1.7308} \left( \frac{\omega_3}{L} \right)^{0.1264} \left( \frac{PL^2}{EI} \right)^{0.5664} \quad \text{-- calculate the}$$

predicted moment for the values of  $P, \omega_3, L, D, b, k, p$ , and  $d$ .

There is a value of  $\omega_3$  associated with each value of  $P$ .

10. Plot the values of the predicted moment for each value of  $P$  against the values of  $d$ .
11. From the plot of  $M_r, M_{pred.}$ , and  $d$ , the value of  $d$  at the point of intersection of the  $M_r$  and  $M_{pred.}$  curves for a particular value of  $P$ , would be the correct and most economical to use for the design of the cross-section. Any value of  $d$  to

the right of the point of intersection would be valid but less economical.

Example:

Design a reinforced concrete floor grid that will support beef cattle with the following weight classes: 600 Lb, 800 Lb, 1000 Lb, and 1200 Lb.

The Problem: Determine a rectangular section with tensile reinforcement that will support the given weight.

Solution:

Selection of grid dimensions

$$D = 24 \text{ in.}$$

$$L = 88 \text{ in. (Total length of grid = 96 in.)}$$

$$b = 4 \text{ in.}$$

Selection of concrete and steel qualities

$$f_c = 1050 \text{ psi}$$

$$f'_c = 3000 \text{ psi (Determine by 6 x 12 inch cylinders)}$$

$$f_s = 20,000 \text{ psi}$$

$$n = 9.2$$

For a balanced design, where the compressive stresses at the extreme top fiber of the concrete and the tensile stresses of the reinforcing steel reach their allowable values at the same time, we find values of

$$K = 152$$

$$k = 0.326$$

$$p = 0.0085$$

where,

$$K = \frac{f_c}{2} k j \quad (8-1)$$

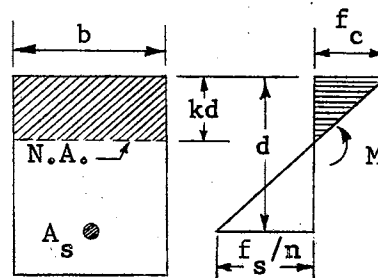


Figure 35. Stress Distribution Diagram

$$j = 1 - 1/3 k \quad (8-2)$$

$$k = \frac{1}{1 + f_s/nf_c} \quad (8-3)$$

$$p = \frac{A_s}{bd} \quad (8-4)$$

The effective moment of inertia will be

$$I = 1/3 (b) \left[ (k)(d) \right]^3 + (p)(bd)(n) \left[ (1-k)(d) \right]^2 \quad (8-5)$$

For values of d equal to:

1.50 in., 1.75 in., 2.00 in., 2.25 in., 2.50 in., 2.75 in., 3.00 in.,  
3.25 in., 3.50 in., 3.75 in., and 4.00 in.

The effective moment of inertia in  $\text{In.}^4$  will be, 0.6355, 1.0091, 1.5063,  
2.1447, 2.9420, 3.9158, 5.0838, 6.4636, 8.0728, 9.9292 and 12.0504.

For a unit weight of 150 Lb/cu.ft. of concrete

$$E_c = 3.0 \times 10^6 \text{ psi}$$

This will give bending stiffness index,  $EI \times 10^6$ , values of:

1.9065, 3.0273, 4.5189, 6.4341, 8.8260, 11.7374, 15.2514, 19.3908,  
24.2184, 29.7876 and 36.1512.

Determine the predicted bending moment,  $M_{\text{pred.}}$ , using EQ. (7-14a)

with the above values of EI.

Determine the resisting moment,  $M_r$ , using the equation

$$M_r = Kbd^2 \quad (8-6)$$

Values of  $M_{\text{pred.}}$ , and  $M_r$  are listed on Table XIV.

From Figure 36, the value of d at the point of intersection for each weight class is 1.65 in. for 600 Lb, 2.15 in. for 800 Lb, 2.65 in. for 1000 Lb, and 3.15 in. for 1200 Lb.

TABLE XIV  
 COMPUTED VALUES OF RESISTING MOMENT AND PREDICTED  
 MOMENT AS FUNCTIONS OF THE EFFECTIVE DEPTH  
 OF A GRID BAR

d in inches	M <sub>r</sub> in LbF·In.	M <sub>pred.</sub> in LbF·In.			
		600 Lb	800 Lb	1000 Lb	1200 Lb
1.50	1368	1497	1785	2050	2298
1.75	1862	1829	2182	2505	2809
2.00	2432	2176	2595	2981	3341
2.25	3078	2536	3025	3474	3895
2.50	3800	2909	3469	3984	4467
2.75	4598	3293	3927	4510	5056
3.00	5472	3687	4398	5051	5662
3.25	6422	4092	4881	5605	6284
3.50	7448	4506	5374	6172	6920
3.75	8550	4929	5879	6752	7569
4.00	9728	5361	6394	7343	8232

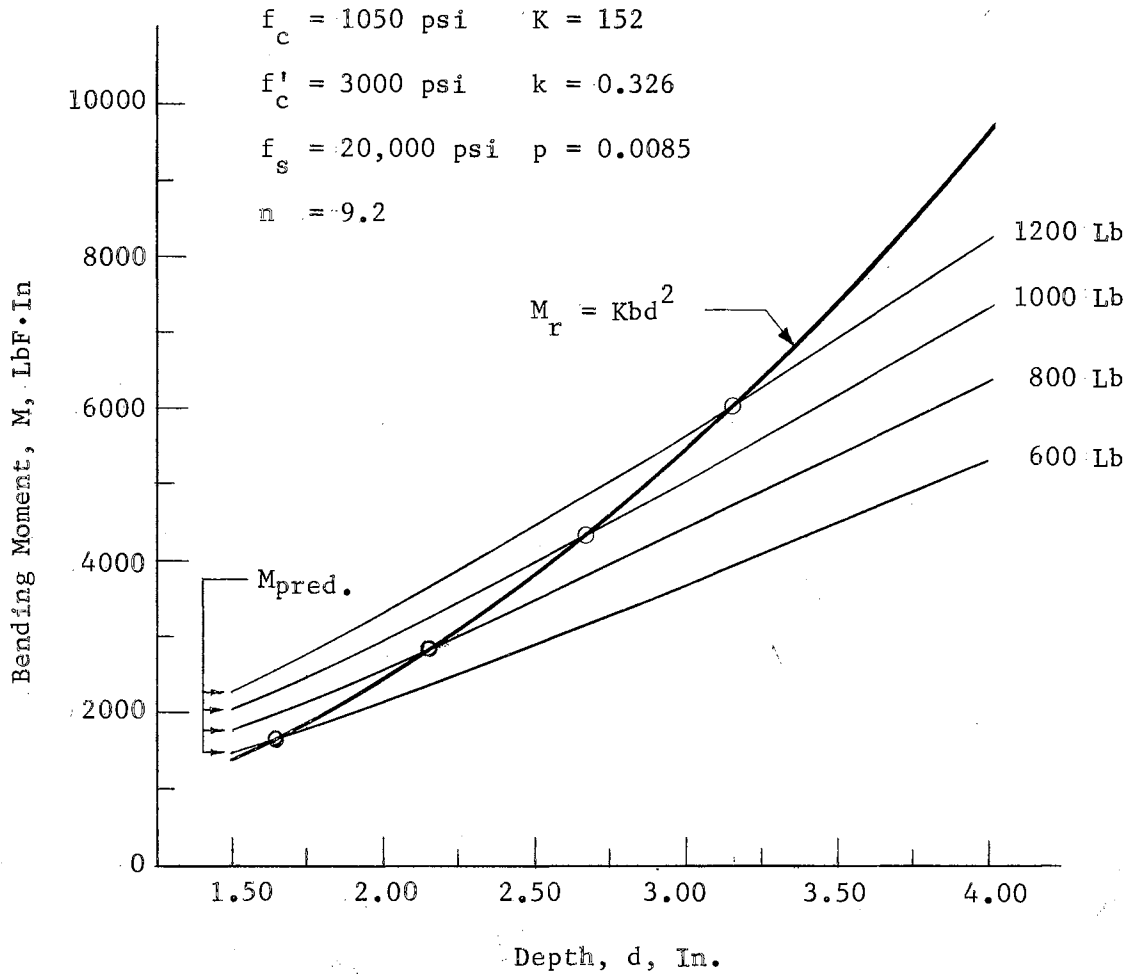


Figure 36. Plot of Resisting Moment and Predicted Moment for Station No. 1 Versus Depth of a 4 Inches Wide Reinforced Concrete Rectangular Section

For farm structures purposes a 3/4 inch covering of concrete below the tensile reinforcement rod would be sufficient.

A comprehensive reinforcement rod smaller than the tensile reinforcement rod could be used for grid handling purposes.

Since a trapezoidal cross-section is better than a rectangular cross-section for ease of waste disposal from the surface of the grid into the collection basin, the top width of the rectangular section could be increased by one inch and the bottom width decreased also by one inch. This rearrangement of the section width will not reduce its ability to resist the bending stresses. In fact it could make it stronger because the concrete below the neutral axis does not have any effect on the value of the effective moment of inertia of the section for a condition of cracked concrete and tensile reinforcing. The cracks could be microscopic in size.



## CHAPTER IX

### SUMMARY AND CONCLUSIONS

An experimental model analysis was conducted with the objective of developing a prediction equation to determine the maximum possible bending stresses that could be induced in a floor grid under the loads of beef cattle. The principles of dimensional analysis and similitude were employed in the investigation of this study.

The quantities pertinent to this study were those characterizing the dimensions of the grid and the mechanical properties of materials, E and G, the animal configuration and its weight, and the arrangement of animals with respect to one grid.

The loading pattern was designed to provide maximum loading by taking maximum concentration. This was done by aligning the animals shoulder to shoulder and facing in alternating directions. For load positioning, the front hoof spacing and the shoulder width were taken. The load was applied on the free longitudinal edge of a grid.

Animal configuration measurements and weights were taken from 10 heads of steers.

The following conclusions were drawn from this experimental study:

1. Bending moment induced at midspan of each bar in a 4-bar grid-work can be predicted by an equation of the form:

$$\frac{ML}{EI} = \Phi \left(\frac{D}{L}\right)^{n_1} \left(\frac{w_3}{L}\right)^{n_2} \left(\frac{PL^2}{EI}\right)^{n_3} \quad (9-1)$$

where,

$M$  = Bending moment at midspan of the middle bar, LbF·In.

$EI$  = Bending stiffness index for a bar, LbF·Sq.In.

$\phi$  = Dimensionless coefficient (Eq. 7-14)

$D$  = Width of grid, In.

$L$  = Effective length of grid, In.

$w_3$  = Width at shoulders of steer, In.

$P$  = Steer weight, LbF

$n_1$ ,  $n_2$ , and  $n_3$  = Dimensionless exponents (Eq. 7-14)

2. From prediction Equation (7-14a), the maximum bending moment can be computed. This prediction equation is usable for the design of reinforced concrete floor grids.
3. With mean error sum of squares range of 0.0000000015-0.000000012, the four prediction equations describe the system sufficiently.
4. Since Figures 31, 32, 33, and 34 show very good fit, the effect of the hoof spacing index could be neglected.
5. From the animal configuration and weight measurements, it was found that the ratio of the animal weight exerted through the front legs to that exerted through the hind legs is approximately  $1\frac{1}{4}$  to 1.

#### Suggestions for Further Study

1. It should be interesting to investigate the possibility of conducting a similar study using prototype conditions. This would provide the situation of live loads from the cattle and dead loads from the weight of the floor grids.

2. In line with the present study, a more rigorous investigation could be conducted by applying several possible animal arrangements and introducing more variables in the model-grid dimensions; such as, variable slot and variable width of grids.
3. An auxiliary investigation that could expedite research in grid floors for cattle would be the establishment of a relationship of animal configurations to total body weight.
4. Another experimental project could be the building and load testing of some prototype grids designed according to the procedure explained in Chapter VIII.

#### SELECTED BIBLIOGRAPHY

1. Baxter, S. H. and D. S. Soutar. "Slatted Floors for Intensive Beef." Farm Buildings. No. 4, London: Autumn, 1964.
2. Brody, Samuel. "Linear Growth, Form, and Function." Bioenergetics and Growth. Hafner Publishing Company, Inc., New York: 1964.
3. Burgener, M. L. "Design For Concrete Slatted Floors For Livestock." American Society of Agricultural Engineers. Paper No. 61-407. St. Joseph, Michigan: June 25-28, 1961. (Mimeo.)
4. Cooper, T. H. "Slatted Floors." Farmer and Stock Breeder. October, 1960.
5. Den Hartog, J. P. Advanced Strength of Materials. McGraw-Hill Book Company, Inc., New York: 1952.
6. Green, N. K. "Slatted Floor Housing For Cattle." Agricultural Land Service. England. Ca. 1961.
7. Hammer, W. "European Experience With Slatted Floors For Livestock." American Society of Agricultural Engineers. Paper No. 60-922. Memphis, Tennessee: December, 1960. (Mimeo.)
8. Hammer, W. and P. Czepluch. "Erfahrungen Mit Der Schwemmentmistung." (Experiences With Barn Cleaning by Flooding) Lanttechnik (Germany) Volume 15. No. 11. June, 1960. (Not Seen)
9. Higdon, Archie, Edward H. Ohlsen, and William B. Stiles. Mechanics of Materials. John Wiley and Sons, Inc., New York: November, 1962.
10. Kiosterman, E. W. and W. L. Roller. "Steel Slotted Floors Reduce Costs." The Farm Spokesman. Ca. 1964.
11. Kunze, Walter E., Comm. Chairman, and others. Reinforced Concrete Design Handbook. American Concrete Institute Publication SP-3. Detroit, Michigan: 1965.
12. Lees, J. L. "Slatted Feeding Platform For Dairy Cows." Publication of the University College of Wales. Aberystwyth: 1961.
13. Malena, D., L. D. Van Fossen, and V. M. Meyer. "Total Confinement For Beef." Successful Farming. Volume 62, No. 11, Meredith Publishing Co., November, 1964.

14. Morris, W. H. M. "Slatted Floors and Free-Stalls For Cattle." Review of British and Norwegian Developments. March, 1963.
15. Murphy, Glen. Similitude in Engineering. The Ronald Press Company. New York: 1950.
16. Nordbø, H. "Loose Housing Barns With Slatted Floors." Translation of a Norwegian Article Entitled "Bingefos Med Spaltegolf." Farm Building Research Institute, Vollebeich, Norway. 1960.
17. Nordbø, H. "Norke Forsok Og Erfaringer Med Nye Fjóstyper." (Norwegian Experiments and Experiences with New Types of Livestock Housing). (Mimeo., not seen) Ca. 1960.
18. Palmer, L. M. "Slat-Floor Barn For All Types of Stock." Farm Journal. August, 1963.
19. Reese, Raymond C., Comm. Chairman, and others. Building Code Requirements For Reinforced Concrete. ACJ 318-63. June, 1963.
20. Schulz, A. H. "Building and Equipment System For Cattle Feeding." Paper presented to Midwest Farm Editors. North Dakota State University. June, 1961.
21. Seely, Fred B. and James O. Smith. Advanced Mechanics of Materials. John Wiley and Sons, Inc., London: August, 1961.
22. "Slotted Floors For Cattle." Wallace Farm. 1962.
23. "Slotted Floors For Efficient Livestock Production." Concrete For Agriculture. F170. Portland Cement Association Publication. Chicago: 1964.
24. Soutar, D. S. "The Housing of Livestock on Slatted Floors. Reprinted from the "Transactions of the Royal Highlands and Agricultural Society of Scotland." 1961.
25. Winter, G., L. C. Urquhart, C. E. O'Rourke, and H. A. Nilson. "Beams." Design of Concrete Structures. McGraw Hill Book Company, New York: 1964.

APPENDIX A  
ANIMAL CONFIGURATIONS AND WEIGHT MEASUREMENTS

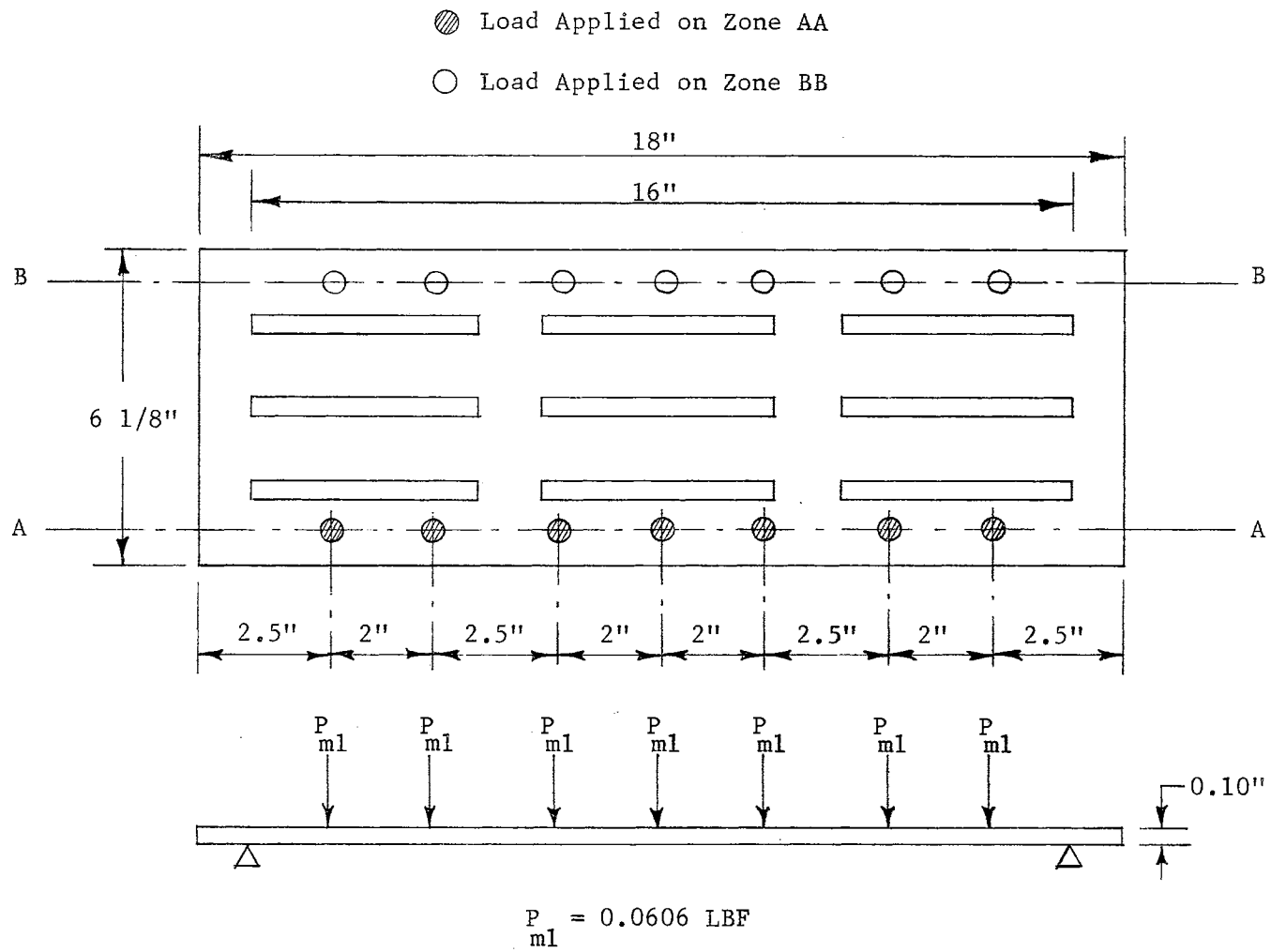
APPENDIX A  
BEEF CATTLE MEASUREMENTS

No.	Length in Inches			Width in Inches			Weight in Lbs.		Total
	Nose to Front Legs	Front Legs to Hind Legs	Nose to Tail	Hips	Middle	Shoulder	Front* Legs	Hind* Legs	
1	26	39 3/4	67 3/4	18 3/4	22 1/2	18	397	315	690
2	25 1/2	36	67	20 1/4	23 1/2	19 1/2	408	352	726
3	28 1/8	41	69 1/2	19 1/8	23 1/4	18 3/4	434	340	740
4	28 1/2	39 1/2	72	21 5/8	24	20 1/4	468	380	741
5	27	39	68 3/4	19 3/4	22 1/2	20 1/2	429	334	751
6	25 1/2	39 1/2	68 1/2	18 3/4	22 3/4	18 1/4	421	345	767
7	28	42 1/2	72 1/2	19 3/4	24 1/4	18 1/4	460	362	809
8	27 1/2	40	72 1/4	19 1/2	24 1/4	19	470	380	838
9	28 1/2	41 1/2	71	21 1/2	24	20 1/4	462	385	855
10	29	39	71	21 1/2	26 1/4	20 1/4	500	387	861

\*The animal was able to recognize the difference in the hardness of the surface of the scale platform and the surface outside the scale. This could be seen by the difference in the total weight and the sum of the weight exerted by the front and hind legs.

APPENDIX B  
EXPERIMENTAL AND COMPUTED DATA





$\gamma = 10 \text{ In.}$

$\omega_3 = 18 \text{ In.}$

Figure B-01. Model Grid Loading Diagram

TABLE B-I

STRAIN IN MICRO-INCHES PER INCH OF LENGTH

LOAD NO. 1 APPLIED ON GRID NO. 1

REP.	LOAD APPLIED ON ZONE AA				LOAD APPLIED ON ZONE BB			
	STATION				STATION			
	1	2	3	4	1	2	3	4
1	14.3750	10.5000	10.1250	9.1875	9.3125	9.8125	11.2500	15.0000
2	14.3750	10.7500	10.3125	10.0000	9.4375	9.7500	11.3125	15.0000
3	14.5000	10.7500	10.0000	9.8125	9.5000	9.8750	11.3750	15.1250
4	14.3750	10.8125	10.0000	9.8750	9.3125	9.5625	11.1250	14.9375
5	14.3750	10.6250	10.0000	9.6875	9.3125	9.5000	11.1875	15.1250

TABLE B-II

BENDING MOMENT IN MODEL IN LBF-IN.

LOAD NO. 1 APPLIED ON GRID NO. 1

REP.	LOAD APPLIED ON ZONE AA				LOAD APPLIED ON ZONE BB			
	STATION				STATION			
	1	2	3	4	1	2	3	4
1	0.3061	0.2236	0.2156	0.1957	0.1983	0.2090	0.2396	0.3194
2	0.3061	0.2289	0.2196	0.2130	0.2010	0.2076	0.2409	0.3194
3	0.3088	0.2289	0.2130	0.2090	0.2023	0.2103	0.2422	0.3221
4	0.3061	0.2303	0.2130	0.2103	0.1983	0.2036	0.2369	0.3181
5	0.3061	0.2263	0.2130	0.2063	0.1983	0.2023	0.2383	0.3221

TABLE B-III

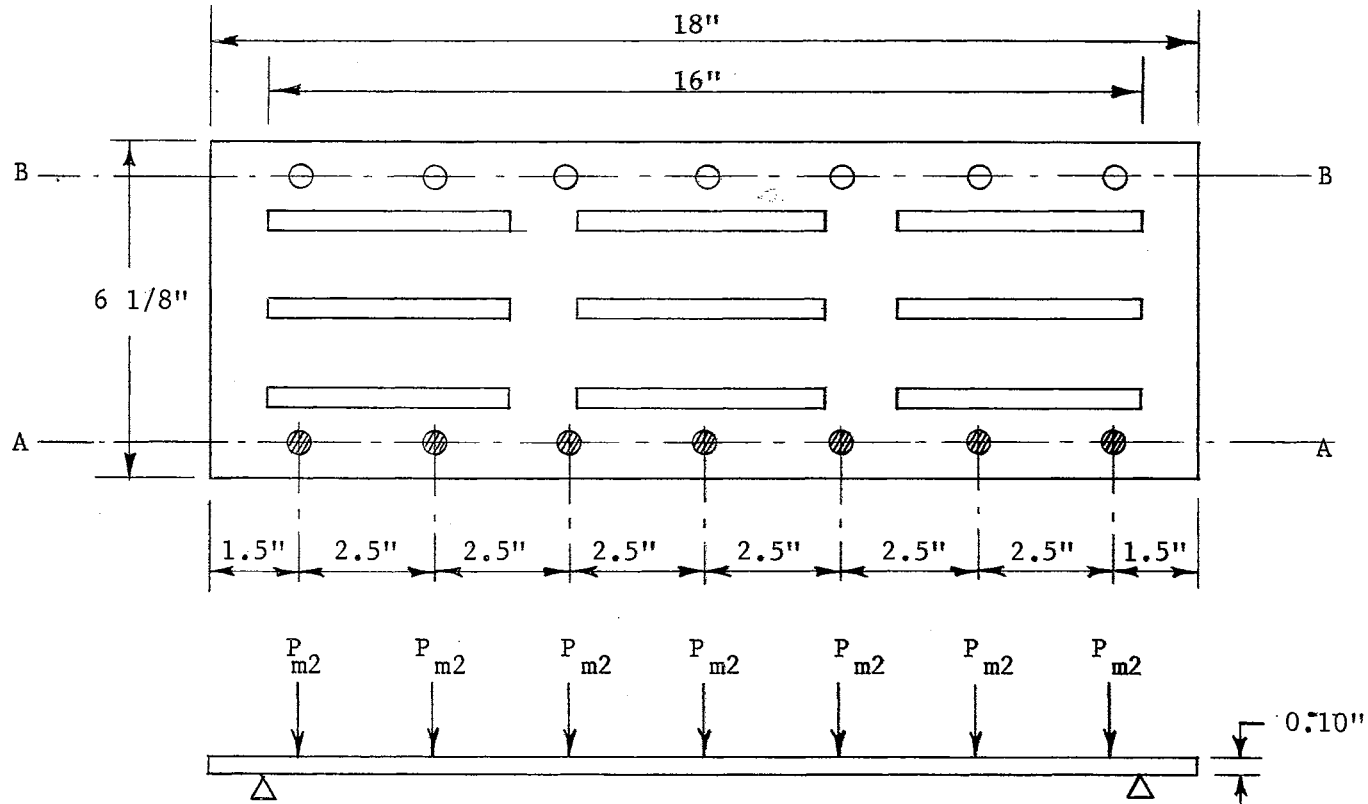
BENDING MOMENT IN PROTOTYPE IN LBF-IN.

LOAD NO. 1 APPLIED ON GRID NO. 1

REP.	LOAD APPLIED ON ZONE AA				LOAD APPLIED ON ZONE BB			
	STATION				STATION			
	1	2	3	4	1	2	3	4
1	3371.5124	2462.6699	2374.7174	2154.8362	2184.1537	2301.4236	2638.5749	3518.0999
2	3371.5124	2521.3049	2418.6937	2345.3999	2213.4711	2286.7649	2653.2337	3518.0999
3	3400.8299	2521.3049	2345.3999	2301.4236	2228.1299	2316.0824	2667.8924	3547.4174
4	3371.5124	2535.9637	2345.3999	2316.0824	2184.1537	2242.7887	2609.2574	3503.4412
5	3371.5124	2491.9874	2345.3999	2272.1062	2184.1537	2228.1299	2623.9161	3547.4174

⊗ Load Applied on Zone AA

○ Load Applied on Zone BB



$$P_{m2} = 0.0808 \text{ LBF}$$

$$\gamma = 10 \text{ In.}$$

$$\omega_3 = 20 \text{ In.}$$

Figure B-02. Model Grid Loading Diagram

TABLE B-IV

STRAIN IN MICRO-INCHES PER INCH OF LENGTH

LOAD NO. 2 APPLIED ON GRID NO. 1

REP.	LOAD APPLIED ON ZONE AA				LOAD APPLIED ON ZONE BB			
	STATION				STATION			
	1	2	3	4	1	2	3	4
1	16.7500	12.5000	11.7500	11.2500	11.0000	11.2500	13.0000	17.4375
2	16.3125	12.1875	11.3750	11.3125	10.8125	11.1875	13.0000	17.1875
3	16.7500	12.5000	11.7500	11.3125	10.6875	11.1875	13.0000	17.1875
4	16.7500	12.5000	11.6250	11.4375	10.6875	11.1250	12.9375	17.1875
5	16.8750	12.5000	11.7500	11.2500	10.6875	11.2500	13.0000	17.1875

TABLE B-V

BENDING MOMENT IN MODEL IN LBF-IN.

LOAD NO. 2 APPLIED ON GRID NO. 1

REP.	LOAD APPLIED ON ZONE AA				LOAD APPLIED ON ZONE BB			
	STATION				STATION			
	1	2	3	4	1	2	3	4
1	0.3567	0.2662	0.2502	0.2396	0.2343	0.2396	0.2769	0.3714
2	0.3474	0.2596	0.2422	0.2409	0.2303	0.2383	0.2769	0.3660
3	0.3567	0.2662	0.2502	0.2409	0.2276	0.2383	0.2769	0.3660
4	0.3567	0.2662	0.2476	0.2436	0.2276	0.2369	0.2755	0.3660
5	0.3594	0.2662	0.2502	0.2396	0.2276	0.2396	0.2769	0.3660

TABLE B-VI

BENDING MOMENT IN PROTOTYPE IN LBF-IN.

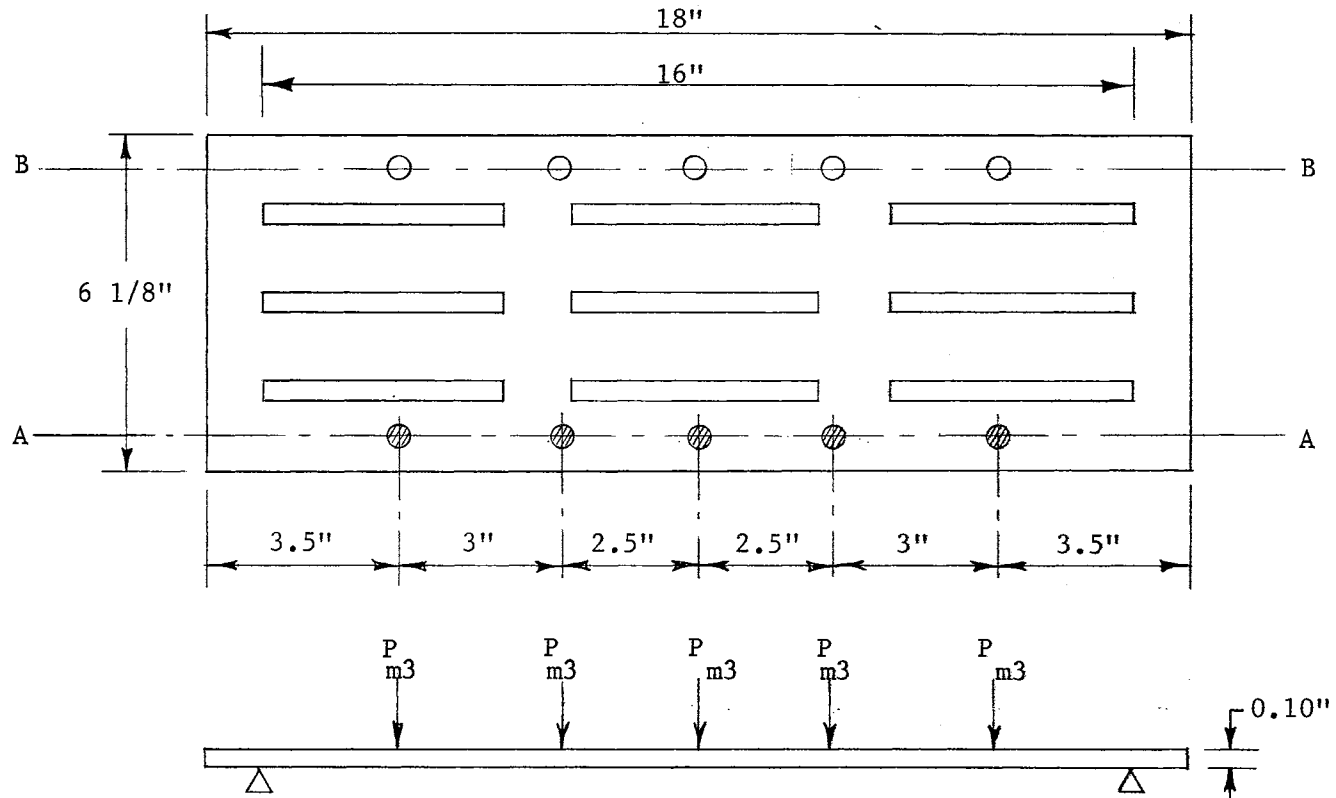
LOAD NO. 2 APPLIED ON GRID NO. 1

REP.	LOAD APPLIED ON ZONE AA				LOAD APPLIED ON ZONE BB			
	STATION 1	STATION 2	STATION 3	STATION 4	STATION 1	STATION 2	STATION 3	STATION 4
1	3928.5449	2931.7499	2755.8449	2638.5749	2579.9399	2638.5749	3049.0199	4089.7911
2	3825.9336	2858.4562	2667.8924	2653.2337	2535.9637	2623.9161	3049.0199	4031.1561
3	3928.5449	2931.7499	2755.8449	2653.2337	2506.6462	2623.9161	3049.0199	4031.1561
4	3928.5449	2931.7499	2726.5274	2682.5511	2506.6462	2609.2574	3034.3611	4031.1561
5	3957.8623	2931.7499	2755.8449	2638.5749	2506.6462	2638.5749	3049.0199	4031.1561



⊗ Load Applied on Zone AA

○ Load Applied on Zone BB



$$P_{m3} = 0.1010 \text{ LBF}$$

$$\gamma = 12 \text{ In.}$$

$$\omega_3 = 22 \text{ In.}$$

Figure B-03. Model Grid Loading Diagram

TABLE B-VII

STRAIN IN MICRO-INCHES PER INCH OF LENGTH

LOAD NO. 3 APPLIED ON GRID NO. 1

REP.	LOAD APPLIED ON ZONE AA				LOAD APPLIED ON ZONE BB			
	STATION				STATION			
	1	2	3	4	1	2	3	4
1	19.2500	20.6250	13.3125	12.8125	12.4375	12.7500	15.0000	20.0625
2	19.2500	14.2500	13.2500	12.8125	12.5000	12.9375	15.0000	20.0625
3	19.3125	14.2500	13.2500	12.9375	12.3750	13.0000	14.9375	20.0625
4	19.4375	14.3125	13.3750	13.0000	12.4375	12.9375	15.0000	20.0625
5	19.3750	14.3125	13.5000	12.9375	12.3125	12.6250	14.8125	19.6875

TABLE B-VIII

BENDING MOMENT IN MODEL IN LBF-IN.

LOAD NO. 3 APPLIED ON GRID NO. 1

REP.	LOAD APPLIED ON ZONE AA				LOAD APPLIED ON ZONE BB			
	STATION				STATION			
	1	2	3	4	1	2	3	4
1	0.4100	0.4392	0.2835	0.2729	0.2649	0.2715	0.3194	0.4273
2	0.4100	0.3035	0.2822	0.2729	0.2662	0.2755	0.3194	0.4273
3	0.4113	0.3035	0.2822	0.2755	0.2635	0.2769	0.3181	0.4273
4	0.4140	0.3048	0.2848	0.2769	0.2649	0.2755	0.3194	0.4273
5	0.4126	0.3048	0.2875	0.2755	0.2622	0.2689	0.3155	0.4193

TABLE B-IX

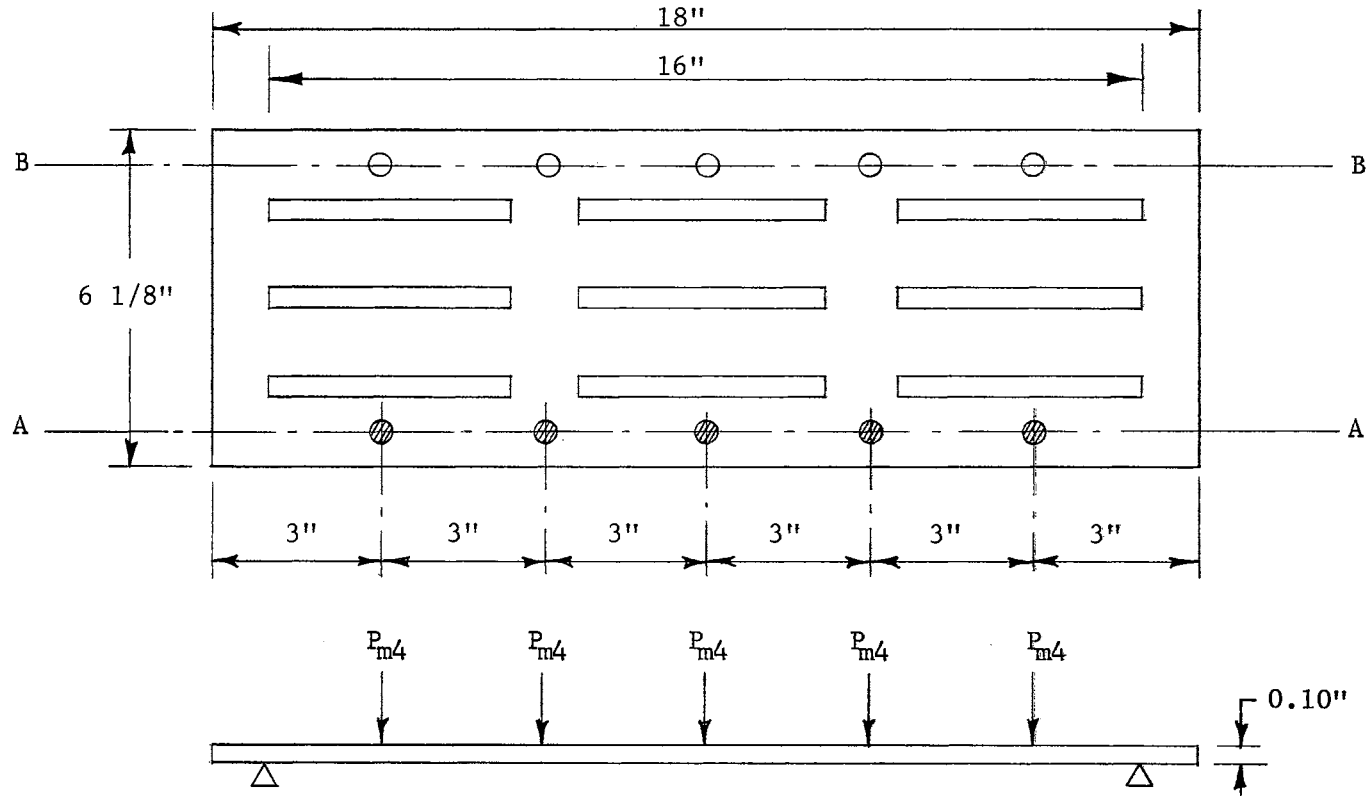
BENDING MOMENT IN PROTOTYPE IN LBF-IN.

LOAD NO. 3 APPLIED ON GRID NO. 1

REP.	LOAD APPLIED ON ZONE AA				LOAD APPLIED ON ZONE BB			
	STATION				STATION			
	1	2	3	4	1	2	3	4
1	4514.8948	4837.3873	3122.3137	3005.0437	2917.0912	2990.3849	3518.0999	4705.4586
2	4514.8948	3342.1949	3107.6549	3005.0437	2931.7499	3034.3611	3518.0999	4705.4586
3	4529.5536	3342.1949	3107.6549	3034.3611	2902.4324	3049.0199	3503.4412	4705.4586
4	4558.8711	3356.8537	3136.9724	3049.0199	2917.0912	3034.3611	3518.0999	4705.4586
5	4544.2123	3356.8537	3166.2899	3034.3611	2887.7737	2961.0674	3474.1237	4617.5061

⊗ Load Applied on Zone AA

○ Load Applied on Zone BB



$$P_{m4} = 0.1212 \text{ LBF}$$

$$\gamma = 12 \text{ In.}$$

$$\omega_3 = 24 \text{ In.}$$

Figure B-04. Model Grid Loading Diagram

TABLE B-X  
 STRAIN IN MICRO-INCHES PER INCH OF LENGTH  
 LOAD NO. 4 APPLIED ON GRID NO. 1

REP.	LOAD APPLIED ON ZONE AA				LOAD APPLIED ON ZONE BB			
	STATION				STATION			
	1	2	3	4	1	2	3	4
1	20.9375	15.6250	14.6875	14.3750	13.7500	14.1875	16.2500	21.8750
2	21.0000	15.6250	14.6875	14.3125	13.5625	13.8750	16.1250	21.6250
3	20.9375	15.6250	14.6875	14.2500	13.3750	13.9375	16.3125	21.8750
4	21.1250	15.5000	14.5625	14.2500	13.2500	14.1250	16.1875	21.7500
5	21.1250	15.5625	14.6875	14.2500	13.5000	13.9375	16.1250	21.9375

TABLE B-XI

BENDING MOMENT IN MODEL IN LBF-IN.

LOAD NO. 4 APPLIED ON GRID NO. 1

REP.	LOAD APPLIED ON ZONE AA				LOAD APPLIED ON ZONE BB			
	STATION				STATION			
	1	2	3	4	1	2	3	4
1	0.4459	0.3328	0.3128	0.3061	0.2928	0.3021	0.3461	0.4659
2	0.4472	0.3328	0.3128	0.3048	0.2888	0.2955	0.3434	0.4605
3	0.4459	0.3328	0.3128	0.3035	0.2848	0.2968	0.3474	0.4659
4	0.4499	0.3301	0.3101	0.3035	0.2822	0.3008	0.3447	0.4632
5	0.4499	0.3314	0.3128	0.3035	0.2875	0.2968	0.3434	0.4672

TABLE B-XII

BENDING MOMENT IN PROTOTYPE IN LBF-IN.

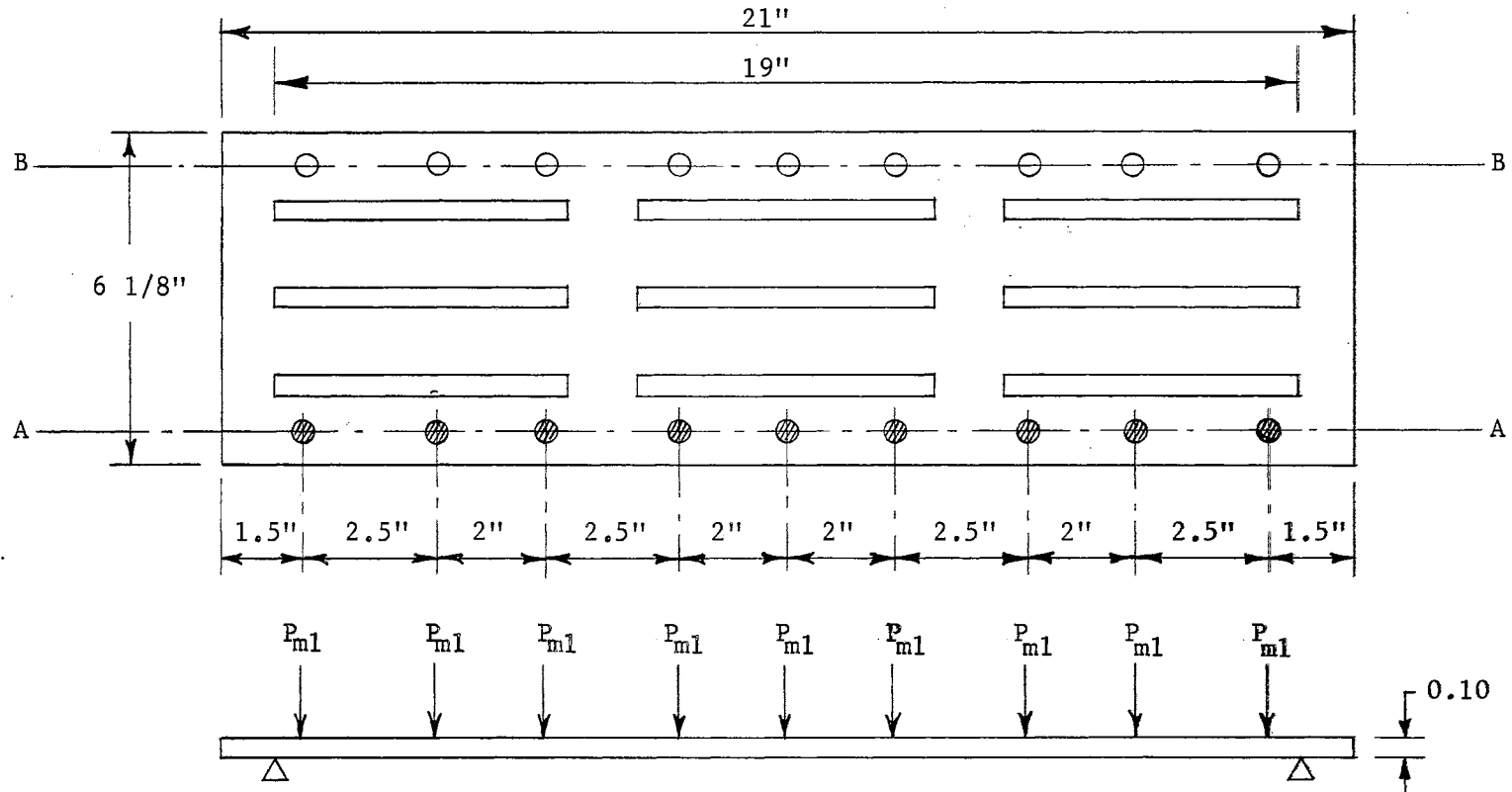
LOAD NO. 4 APPLIED ON GRID NO. 1

REP.	LOAD APPLIED ON ZONE AA				LOAD APPLIED ON ZONE BB			
	STATION				STATION			
	1	2	3	4	1	2	3	4
1	4910.6810	3664.6874	3444.8062	3371.5124	3224.9249	3327.5362	3811.2749	5130.5624
2	4925.3398	3664.6874	3444.8062	3356.8537	3180.9486	3254.2424	3781.9574	5071.9274
3	4910.6810	3664.6874	3444.8062	3342.1949	3136.9724	3268.9012	3825.9336	5130.5624
4	4954.6573	3635.3699	3415.4886	3342.1949	3107.6549	3312.8774	3796.6161	5101.2448
5	4954.6573	3650.0286	3444.8062	3342.1949	3166.2899	3268.9012	3781.9574	5145.2211



⊗ Load Applied on Zone AA

○ Load Applied on Zone BB



$$P_{m1} = 0.0606 \text{ LBF}$$

$$\gamma = 10 \text{ In.}$$

$$\omega_3 = 18 \text{ In.}$$

Figure B-05. Model Grid Loading Diagram

TABLE B-XIII

STRAIN IN MICRO-INCHES PER INCH OF LENGTH

LOAD NO. 1 APPLIED ON GRID NO. 2

REP.	LOAD APPLIED ON ZONE AA				LOAD APPLIED ON ZONE BB			
	STATION				STATION			
	1	2	3	4	1	2	3	4
1	18.8750	14.2500	13.5000	12.8750	13.6250	13.6875	15.1250	19.1875
2	18.9375	14.3125	13.4375	12.8750	13.5625	13.5625	15.1250	19.0000
3	18.8750	14.2500	13.3750	12.7500	13.5000	13.6250	15.1250	19.1875
4	18.8750	14.2500	13.5625	13.0000	13.4375	13.6250	15.1250	19.3125
5	18.9375	14.3125	13.6250	13.1250	13.5000	13.6250	15.1875	18.9375

TABLE B-XIV

BENDING MOMENT IN MODEL IN LBF-IN.

LOAD NO. 1 APPLIED ON GRID NO. 2

REP.	LOAD APPLIED ON ZONE AA				LOAD APPLIED ON ZONE BB			
	STATION				STATION			
	1	2	3	4	1	2	3	4
1	0.4020	0.3035	0.2875	0.2742	0.2902	0.2915	0.3221	0.4086
2	0.4033	0.3048	0.2862	0.2742	0.2888	0.2888	0.3221	0.4046
3	0.4020	0.3035	0.2848	0.2715	0.2875	0.2902	0.3221	0.4086
4	0.4020	0.3035	0.2888	0.2769	0.2862	0.2902	0.3221	0.4113
5	0.4033	0.3048	0.2902	0.2795	0.2875	0.2902	0.3234	0.4033

TABLE B-XV

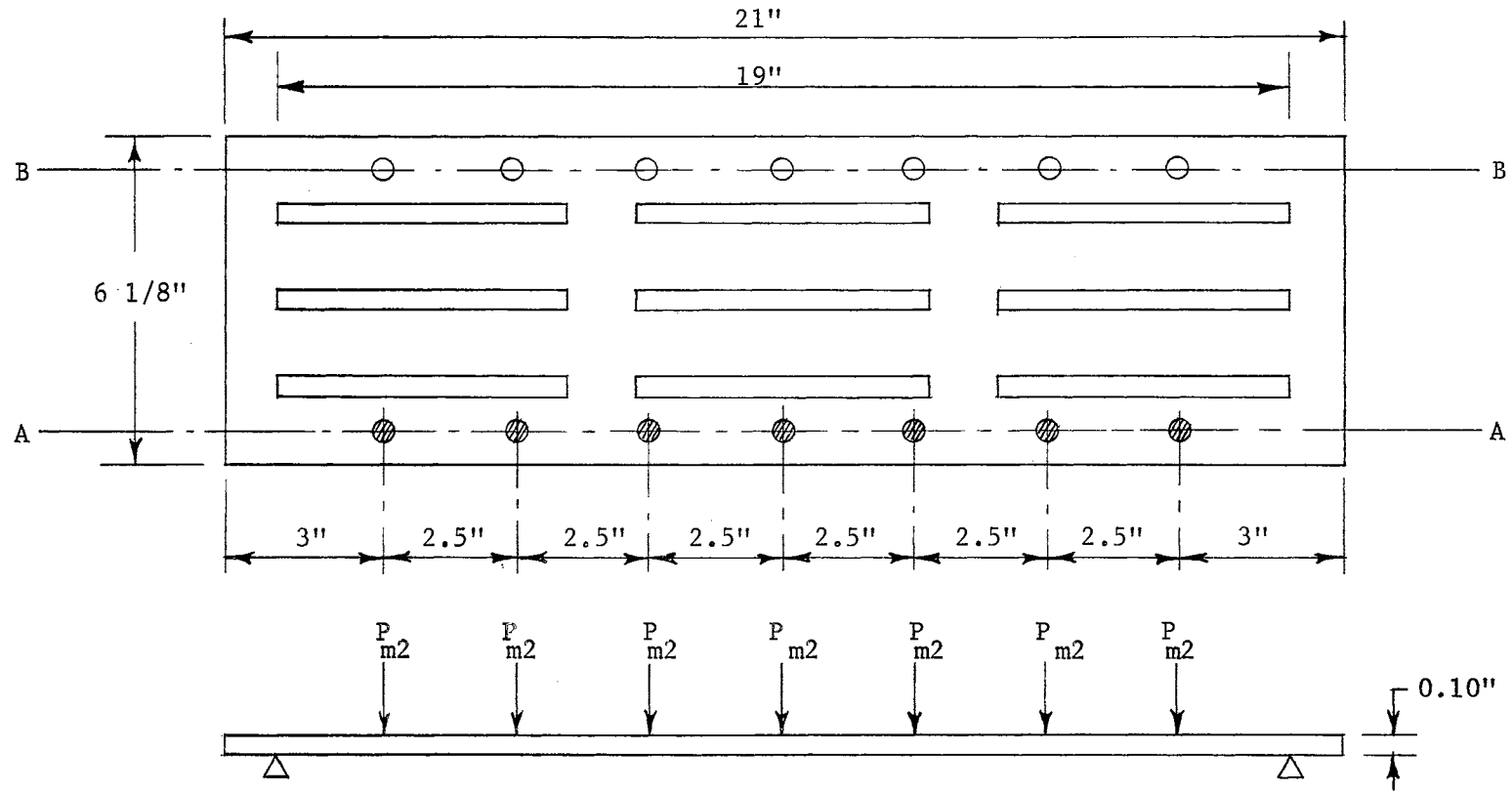
BENDING MOMENT IN PROTOTYPE IN LBF-IN.

LOAD NO. 1 APPLIED ON GRID NO. 2

REP.	LOAD APPLIED ON ZONE AA				LOAD APPLIED ON ZONE BB			
	1	2	3	4	1	2	3	4
1	4313.4310	3256.4976	3085.1030	2942.2741	3113.6688	3127.9517	3456.4579	4384.8455
2	4327.7139	3270.7805	3070.8201	2942.2741	3099.3859	3099.3859	3456.4579	4341.9968
3	4313.4310	3256.4976	3056.5373	2913.7084	3085.1030	3113.6688	3456.4579	4384.8455
4	4313.4310	3256.4976	3099.3859	2970.8399	3070.8201	3113.6688	3456.4579	4413.4113
5	4327.7139	3270.7805	3113.6688	2999.4057	3085.1030	3113.6688	3470.7409	4327.7139

⊗ Load Applied on Zone AA

○ Load Applied on Zone BB



$$P_{m2} = 0.0808 \text{ LBF/m}^2$$

$$\gamma = 10 \text{ In.}$$

$$\omega_3 = 20 \text{ In.}$$

Figure B-06. Model Grid Loading Diagram

TABLE B-XVI

STRAIN IN MICRO-INCHES PER INCH OF LENGTH

LOAD NO. 2 APPLIED ON GRID NO. 2

REP.	LOAD APPLIED ON ZONE AA				LOAD APPLIED ON ZONE BB			
	STATION				STATION			
	1	2	3	4	1	2	3	4
1	22.1250	16.8750	16.0625	15.3750	15.8125	16.0000	17.8125	22.4375
2	22.3750	17.6250	16.0625	15.4375	15.9375	16.2500	18.0625	22.5000
3	22.4375	16.8750	16.0625	15.3750	15.8125	16.1875	17.8125	22.4375
4	22.3750	16.9375	16.0625	15.3125	15.6875	16.0625	17.8750	22.5000
5	22.3750	16.9375	16.1250	15.3750	15.8750	16.0625	17.8125	22.5000

TABLE B-XVII

BENDING MOMENT IN MODEL IN LBF-IN.

LOAD NO. 2 APPLIED ON GRID NO. 2

REP.	LOAD APPLIED ON ZONE AA				LOAD APPLIED ON ZONE BB			
	STATION				STATION			
	1	2	3	4	1	2	3	4
1	0.4712	0.3594	0.3421	0.3274	0.3368	0.3407	0.3793	0.4778
2	0.4765	0.3754	0.3421	0.3288	0.3394	0.3461	0.3847	0.4792
3	0.4778	0.3594	0.3421	0.3274	0.3368	0.3447	0.3793	0.4778
4	0.4765	0.3607	0.3421	0.3261	0.3341	0.3421	0.3807	0.4792
5	0.4765	0.3607	0.3434	0.3274	0.3381	0.3421	0.3793	0.4792

TABLE B-XVIII

BENDING MOMENT IN PROTOTYPE IN LBF-IN.

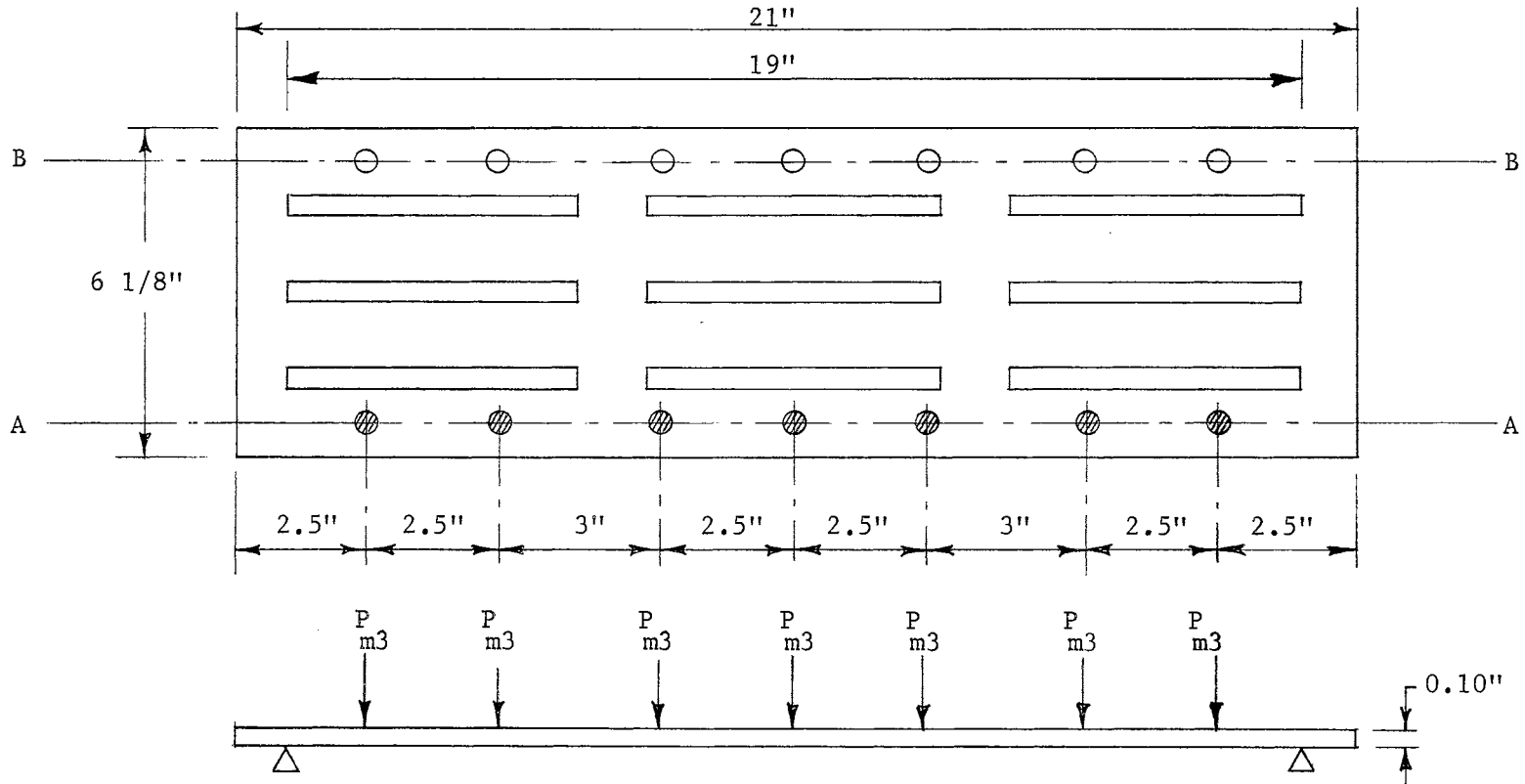
LOAD NO. 2 APPLIED ON GRID NO. 2

REP.	LOAD APPLIED ON ZONE AA				LOAD APPLIED ON ZONE BB			
	STATION				STATION			
	1	2	3	4	1	2	3	4
1	5056.1411	3856.3787	3670.7012	3513.5895	3613.5697	3656.4184	4070.6220	5127.5554
2	5113.2725	4027.7734	3670.7012	3527.8724	3642.1355	3713.5499	4127.7535	5141.8384
3	5127.5554	3856.3787	3670.7012	3513.5895	3613.5697	3699.2670	4070.6220	5127.5554
4	5113.2725	3870.6617	3670.7012	3499.3066	3585.0039	3670.7012	4084.9049	5141.8384
5	5113.2725	3870.6617	3684.9841	3513.5895	3627.8525	3670.7012	4070.6220	5141.8384



⊗ Load Applied on Zone AA

○ Load Applied on Zone BB



$$P_{m3} = 0.1010 \text{ LBF}$$

$$\gamma = 12 \text{ In.}$$

$$\omega_3 = 22 \text{ In.}$$

Figure.B-07. Model Grid Loading Diagram

TABLE B-XIX  
 STRAIN IN MICRO-INCHES PER INCH OF LENGTH  
 LOAD NO. 3 APPLIED ON GRID NO. 2

REP.	LOAD APPLIED ON ZONE AA				LOAD APPLIED ON ZONE BB			
	STATION				STATION			
	1	2	3	4	1	2	3	4
1	26.4375	20.0000	18.9375	18.0000	18.6875	18.9375	21.1250	26.5625
2	26.3125	19.8750	18.8125	18.0000	18.6875	18.9375	21.0625	26.3750
3	26.3125	19.9375	18.8125	18.1875	18.6875	18.9375	21.1250	26.6250
4	26.2500	19.8750	18.8750	18.0000	18.7500	18.8750	20.9375	26.6250
5	26.2500	19.8750	18.8125	18.0000	18.6250	18.8125	21.1875	26.5625

TABLE B-XX

BENDING MOMENT IN MODEL IN LBF-IN.  
 LOAD NO. 3 APPLIED ON GRID NO. 2

REP.	LOAD APPLIED ON ZONE AA				LOAD APPLIED ON ZONE BB			
	STATION				STATION			
	1	2	3	4	1	2	3	4
1	0.5630	0.4259	0.4033	0.3833	0.3980	0.4033	0.4499	0.5657
2	0.5604	0.4233	0.4006	0.3833	0.3980	0.4033	0.4486	0.5617
3	0.5604	0.4246	0.4006	0.3873	0.3980	0.4033	0.4499	0.5670
4	0.5590	0.4233	0.4020	0.3833	0.3993	0.4020	0.4459	0.5670
5	0.5590	0.4233	0.4006	0.3833	0.3966	0.4006	0.4512	0.5657

TABLE B-XXI

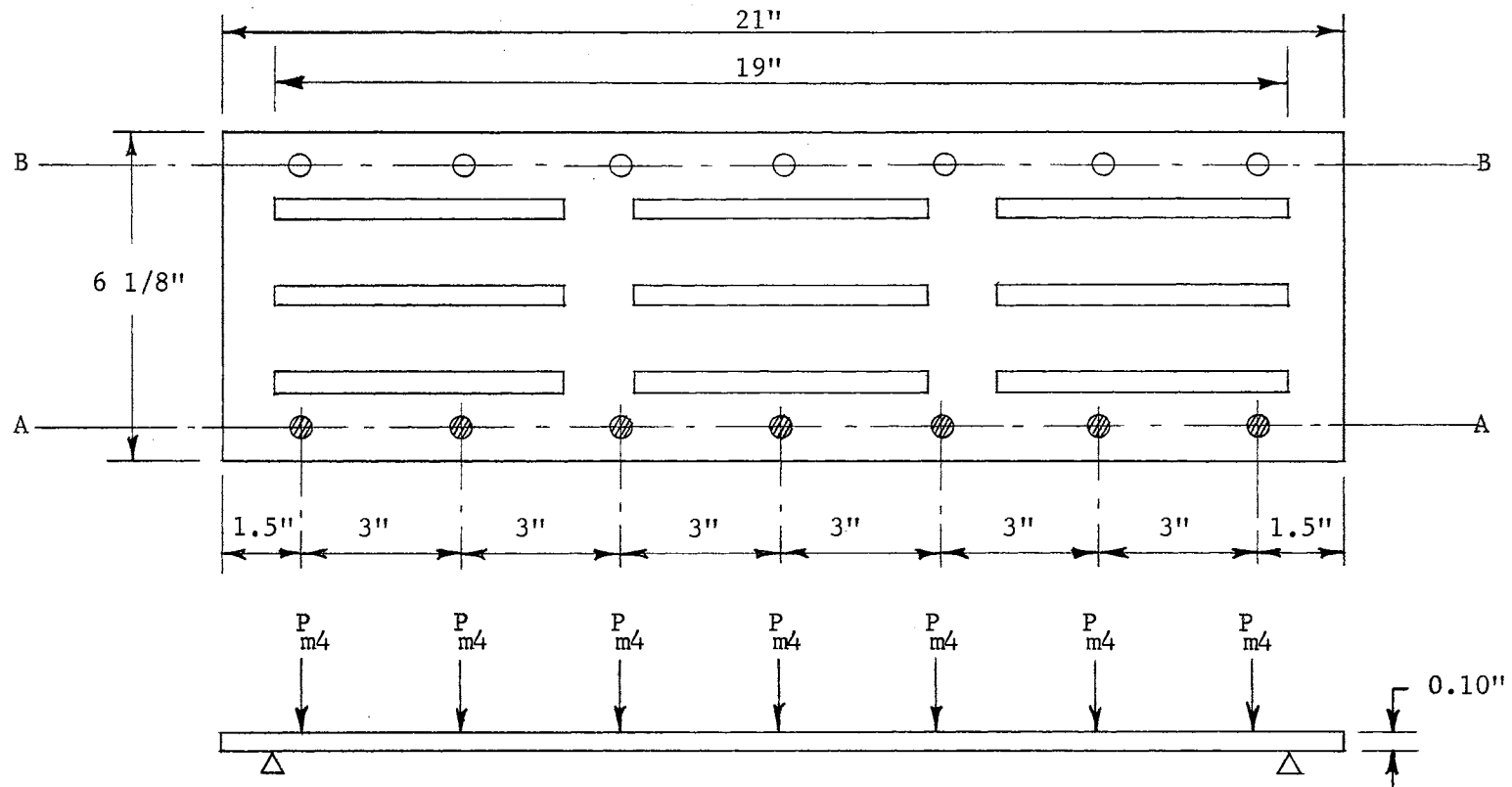
BENDING MOMENT IN PROTOTYPE IN LBF-IN.

LOAD NO. 3 APPLIED ON GRID NO. 2

REP.	LOAD APPLIED ON ZONE AA				LOAD APPLIED ON ZONE BB			
	1	2	3	4	1	2	3	4
1	6041.6601	4570.5230	4327.7139	4113.4707	4270.5823	4327.7139	4827.6149	6070.2258
2	6013.0942	4541.9572	4299.1481	4113.4707	4270.5823	4327.7139	4813.3320	6027.3771
3	6013.0942	4556.2401	4299.1481	4156.3193	4270.5823	4327.7139	4827.6149	6084.5087
4	5998.8115	4541.9572	4313.4310	4113.4707	4284.8653	4313.4310	4784.7662	6084.5087
5	5998.8115	4541.9572	4299.1481	4113.4707	4256.2995	4299.1481	4841.8978	6070.2258

⊗ Load Applied on Zone AA

○ Load Applied on Zone BB



$$P_{m4} = 0.1212 \text{ LBF}$$

$$\gamma = 12 \text{ In.}$$

$$\omega_3 = 24 \text{ In.}$$

Figure B-08. Model Grid Loading Diagram

TABLE B-XXII

STRAIN IN MICRO-INCHES PER INCH OF LENGTH

LOAD NO. 4 APPLIED ON GRID NO. 2

REP.	LOAD APPLIED ON ZONE AA				LOAD APPLIED ON ZONE BB			
	STATION				STATION			
	1	2	3	4	1	2	3	4
1	27.9375	20.9375	19.9375	18.8750	19.6875	20.0000	22.3750	28.1250
2	27.9375	21.1250	20.0000	18.8750	19.6875	20.0000	22.4375	28.0000
3	27.9375	21.0625	20.0000	19.1875	19.8125	20.0000	22.3125	28.3750
4	27.8125	20.8125	19.8750	18.8125	19.6875	20.0000	22.3125	28.1250
5	28.1875	21.1250	20.1250	19.1875	19.5625	20.0000	22.2500	28.2500

TABLE B-XXIII

BENDING MOMENT IN MODEL IN LBF-IN.

LOAD NO. 4 APPLIED ON GRID NO. 2

REP.	LOAD APPLIED ON ZONE AA				LOAD APPLIED ON ZONE BB			
	STATION	STATION	STATION	STATION	STATION	STATION	STATION	STATION
	1	2	3	4	1	2	3	4
1	0.5950	0.4459	0.4246	0.4020	0.4193	0.4259	0.4765	0.5990
2	0.5950	0.4499	0.4259	0.4020	0.4193	0.4259	0.4778	0.5963
3	0.5950	0.4486	0.4259	0.4086	0.4219	0.4259	0.4752	0.6043
4	0.5923	0.4432	0.4233	0.4006	0.4193	0.4259	0.4752	0.5990
5	0.6003	0.4499	0.4286	0.4086	0.4166	0.4259	0.4738	0.6016

TABLE B-XXIV

BENDING MOMENT IN PROTOTYPE IN LBF-IN.

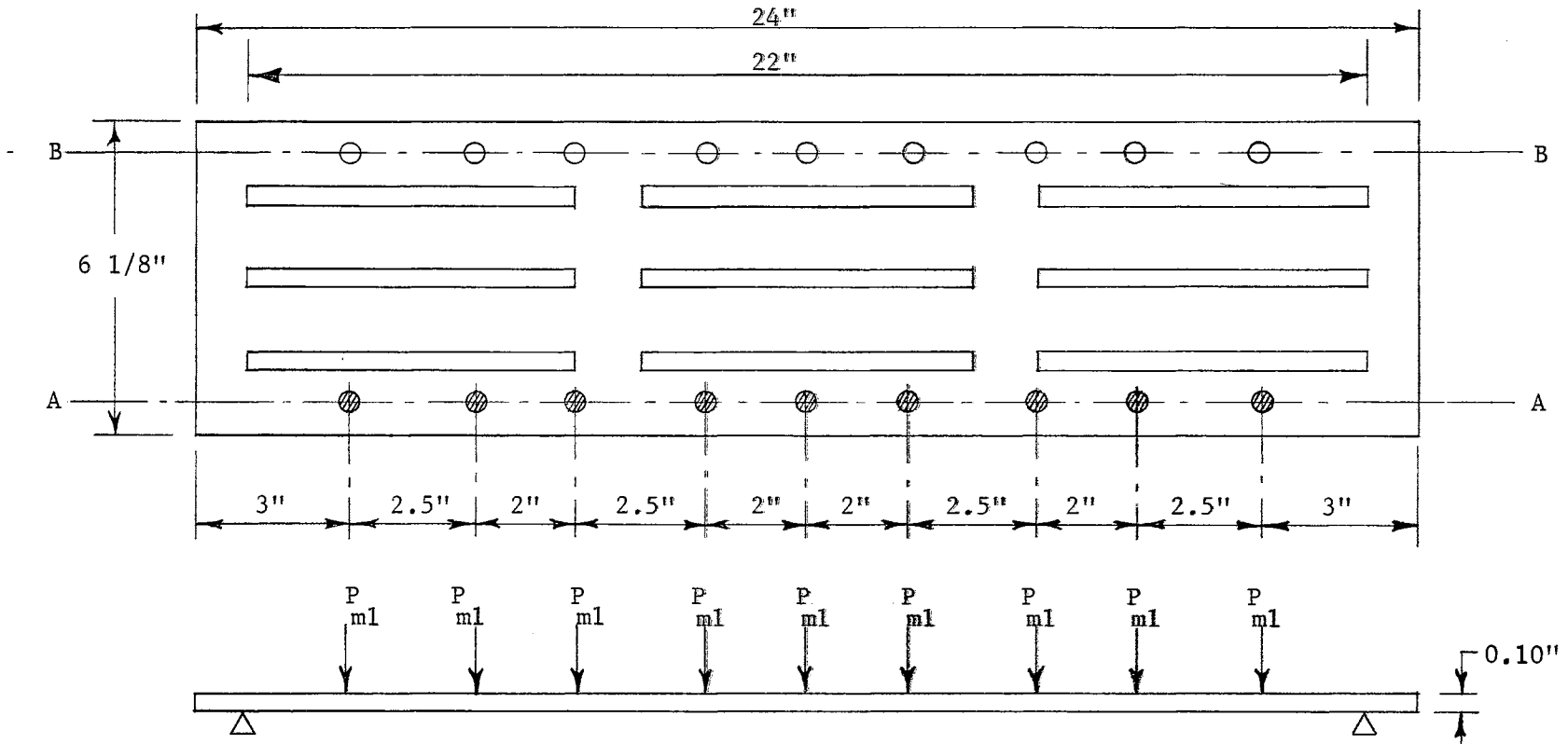
LOAD NO. 4 APPLIED ON GRID NO. 2

REP.	LOAD APPLIED ON ZONE AA				LOAD APPLIED ON ZONE BB			
	STATION				STATION			
	1	2	3	4	1	2	3	4
1	6384.4493	4784.7662	4556.2401	4313.4310	4499.1085	4570.5230	5113.2725	6427.2980
2	6384.4493	4827.6149	4570.5230	4313.4310	4499.1085	4570.5230	5127.5554	6398.7322
3	6384.4493	4813.3320	4570.5230	4384.8455	4527.6743	4570.5230	5098.9896	6484.4294
4	6355.8835	4756.2004	4541.9572	4299.1481	4499.1085	4570.5230	5098.9896	6427.2980
5	6441.5808	4827.6149	4599.0886	4384.8455	4470.5427	4570.5230	5084.7068	6455.8636



⊗ Load Applied on Zone AA

○ Load Applied on Zone BB



$$P_{ml} = 0.0606 \text{ LBF}$$

$$\gamma = 10 \text{ In.}$$

$$\omega_3 = 18 \text{ In.}$$

Figure B-09. Model Grid Loading Diagram

TABLE B-XXV

STRAIN IN MICRO-INCHES PER INCH OF LENGTH

LOAD NO. 1 APPLIED ON GRID NO. 3

REP.	LOAD APPLIED ON ZONE AA				LOAD APPLIED ON ZONE BB			
	STATION				STATION			
	1	2	3	4	1	2	3	4
1	25.5625	19.6875	18.3750	18.6250	18.0625	18.2500	19.2500	25.3125
2	25.1875	19.5625	18.3125	18.6250	18.0625	18.2500	19.2500	25.6250
3	25.1250	19.6250	18.3125	18.7500	18.0625	18.2500	19.1875	25.5000
4	25.1250	19.8750	18.4375	18.8125	18.0000	18.2500	19.1875	25.4375
5	24.9375	19.6250	18.3125	18.6875	18.0625	18.1875	19.1875	25.5000

TABLE B-XXVI

BENDING MOMENT IN MODEL IN LBF-IN.

LOAD NO. 1 APPLIED ON GRID NO. 3

REP.	LOAD APPLIED ON ZONE AA				LOAD APPLIED ON ZONE BB			
	STATION				STATION			
	1	2	3	4	1	2	3	4
1	0.5444	0.4193	0.3913	0.3966	0.3847	0.3887	0.4100	0.5391
2	0.5364	0.4166	0.3900	0.3966	0.3847	0.3887	0.4100	0.5457
3	0.5351	0.4179	0.3900	0.3993	0.3847	0.3887	0.4086	0.5431
4	0.5351	0.4233	0.3927	0.4006	0.3833	0.3887	0.4086	0.5417
5	0.5311	0.4179	0.3900	0.3980	0.3847	0.3873	0.4086	0.5431

TABLE B-XXVII

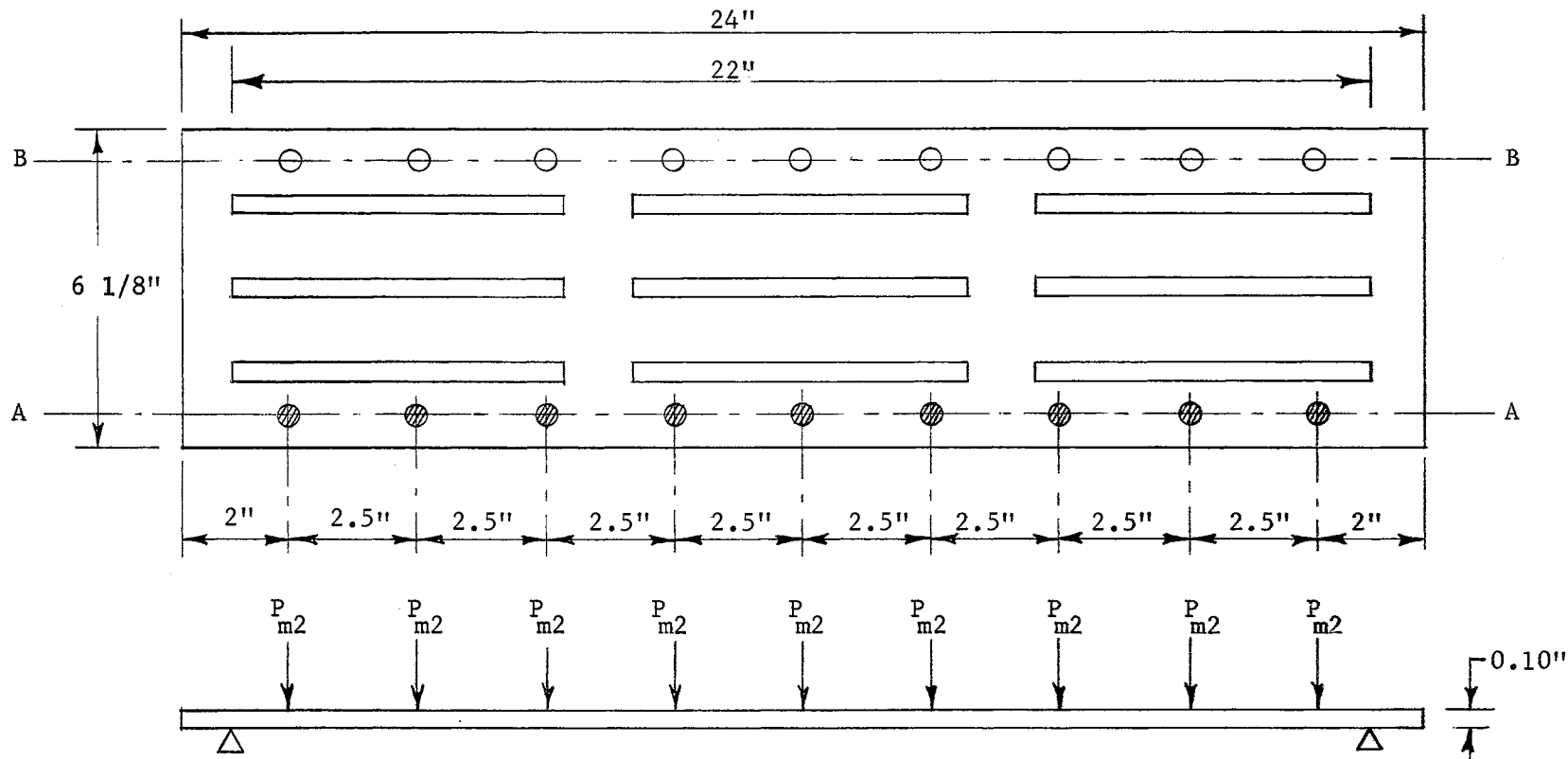
BENDING MOMENT IN PROTOTYPE IN LBF-IN.

LOAD NO. 1 APPLIED ON GRID NO. 3

REP.	LOAD APPLIED ON ZONE AA				LOAD APPLIED ON ZONE BB			
	1	2	3	4	1	2	3	4
1	5995.4285	4617.5061	4309.6723	4368.3073	4236.3785	4280.3549	4514.8948	5936.7935
2	5907.4760	4588.1885	4295.0135	4368.3073	4236.3785	4280.3549	4514.8948	6010.0873
3	5892.8173	4602.8474	4295.0135	4397.6249	4236.3785	4280.3549	4500.2361	5980.7698
4	5892.8173	4661.4823	4324.3311	4412.2836	4221.7198	4280.3549	4500.2361	5966.1111
5	5848.8409	4602.8474	4295.0135	4382.9660	4236.3785	4265.6960	4500.2361	5980.7698

⊗ Load Applied on Zone AA

○ Load Applied on Zone BB



$$P_{m2} = 0.0808 \text{ LBF}$$

$$\gamma = 10 \text{ In.}$$

$$\omega_3 = 20 \text{ In.}$$

Figure B-10. Model Grid Loading Diagram

TABLE B-XXVIII

STRAIN IN MICRO-INCHES PER INCH OF LENGTH

LOAD NO. 2 APPLIED ON GRID NO. 3

REP.	LOAD APPLIED ON ZONE AA				LOAD APPLIED ON ZONE BB			
	STATION				STATION			
	1	2	3	4	1	2	3	4
1	29.0000	23.2500	21.7500	21.9375	21.2500	21.7500	23.0000	29.5000
2	29.0625	23.3125	21.7500	21.9375	21.5625	21.8750	23.1250	30.1875
3	29.0625	23.1875	21.5000	21.7500	21.5000	21.6875	22.8125	29.5000
4	29.0000	23.2500	21.7500	21.8750	21.3125	21.8750	22.8750	29.6875
5	29.1250	23.2500	21.7500	21.9375	21.3125	21.9375	23.0625	30.0000

TABLE B-XXIX

BENDING MOMENT IN MODEL IN LBF-IN.

LOAD NO. 2 APPLIED ON GRID NO. 3

REP.	LOAD APPLIED ON ZONE AA				LOAD APPLIED ON ZONE BB			
	STATION 1	STATION 2	STATION 3	STATION 4	STATION 1	STATION 2	STATION 3	STATION 4
1	0.6176	0.4951	0.4632	0.4672	0.4526	0.4632	0.4898	0.6282
2	0.6189	0.4965	0.4632	0.4672	0.4592	0.4659	0.4925	0.6429
3	0.6189	0.4938	0.4579	0.4632	0.4579	0.4619	0.4858	0.6282
4	0.6176	0.4951	0.4632	0.4659	0.4539	0.4659	0.4872	0.6322
5	0.6203	0.4951	0.4632	0.4672	0.4539	0.4672	0.4912	0.6389

TABLE B-XXX

BENDING MOMENT IN PROTOTYPE IN LBF-IN.

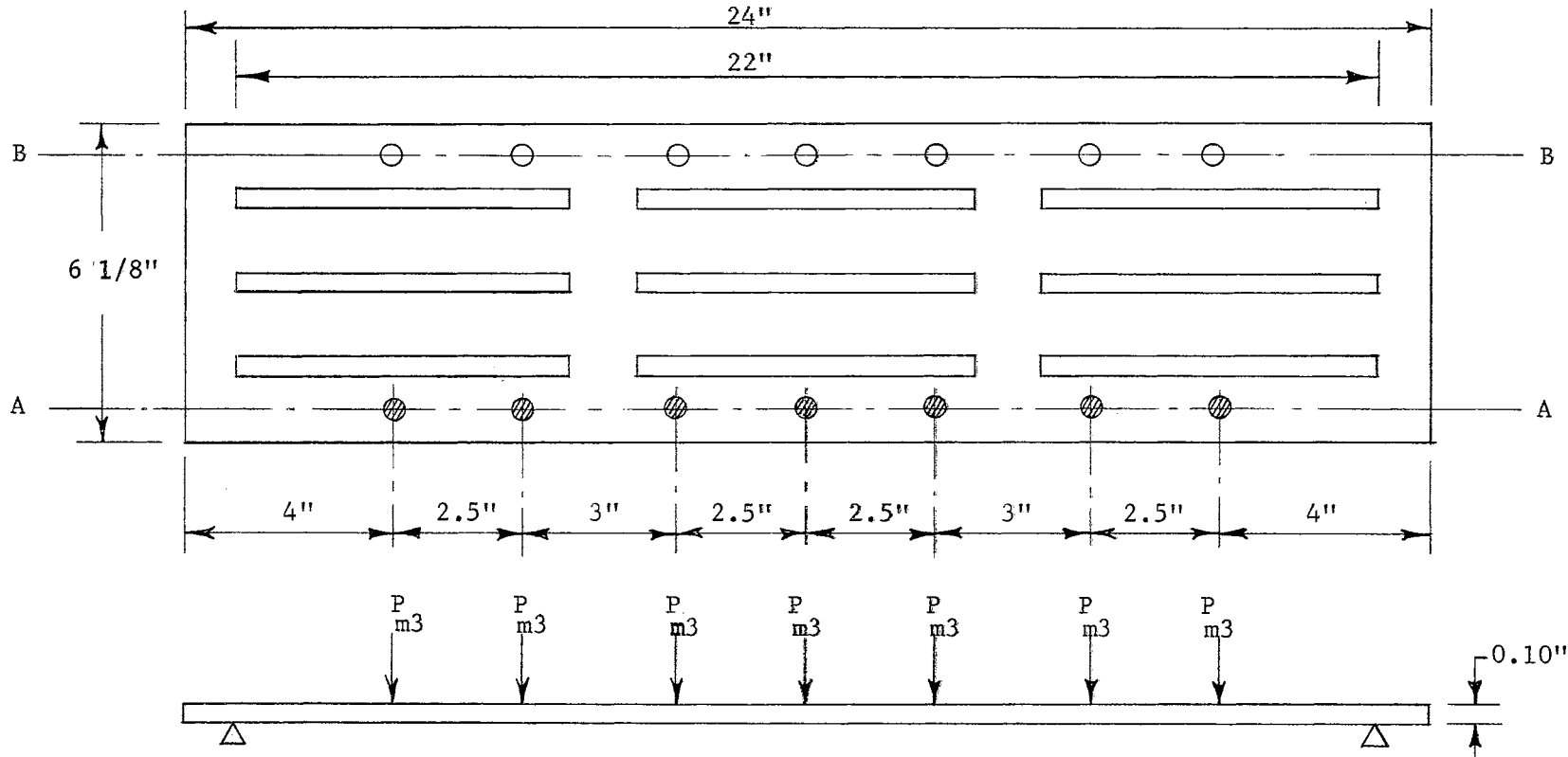
LOAD NO. 2 APPLIED ON GRID NO. 3

REP.	LOAD APPLIED ON ZONE AA				LOAD APPLIED ON ZONE BB			
	STATION				STATION			
	1	2	3	4	1	2	3	4
1	6801.6597	5453.0548	5101.2448	5145.2211	4983.9748	5101.2448	5394.4198	6918.9298
2	6816.3186	5467.7136	5101.2448	5145.2211	5057.2686	5130.5624	5423.7374	7080.1761
3	6816.3186	5438.3961	5042.6097	5101.2448	5042.6097	5086.5861	5350.4435	6918.9298
4	6801.6597	5453.0548	5101.2448	5130.5624	4998.6336	5130.5624	5365.1023	6962.9061
5	6830.9772	5453.0548	5101.2448	5145.2211	4998.6336	5145.2211	5409.0786	7036.1998



⊗ Load Applied on Zone AA

○ Load Applied on Zone BB



$$P_{m3} = 0.1010 \text{ LBF}$$

$$\gamma = 12 \text{ In.}$$

$$\omega_3 = 22 \text{ In.}$$

Figure B-11. Model Grid Loading Diagram

TABLE B-XXXI

STRAIN IN MICRO-INCHES PER INCH OF LENGTH

LOAD NO. 3 APPLIED ON GRID NO. 3

REP.	LOAD APPLIED ON ZONE AA				LOAD APPLIED ON ZONE BB			
	1	2	3	4	1	2	3	4
1	33.8125	27.0000	25.1250	25.0000	24.3125	25.1875	26.4375	34.3750
2	33.6875	27.0000	25.1250	24.9375	24.3750	25.2500	26.5625	34.6875
3	33.7500	26.9375	25.1250	25.0000	24.3125	25.1875	26.5000	34.6875
4	33.7500	27.0625	25.0625	24.9375	24.3750	25.1250	26.5625	34.6875
5	33.6875	26.8125	25.0000	24.9375	24.3750	25.3125	26.5625	34.6875

TABLE B-XXXII

BENDING MOMENT IN MODEL IN LBF-IN.

LOAD NO. 3 APPLIED ON GRID NO. 3

REP.	LOAD APPLIED ON ZONE AA				LOAD APPLIED ON ZONE BB			
	STATION 1	STATION 2	STATION 3	STATION 4	STATION 1	STATION 2	STATION 3	STATION 4
1	0.7201	0.5750	0.5351	0.5324	0.5178	0.5364	0.5630	0.7321
2	0.7174	0.5750	0.5351	0.5311	0.5191	0.5377	0.5657	0.7387
3	0.7188	0.5737	0.5351	0.5324	0.5178	0.5364	0.5644	0.7387
4	0.7188	0.5763	0.5337	0.5311	0.5191	0.5351	0.5657	0.7387
5	0.7174	0.5710	0.5324	0.5311	0.5191	0.5391	0.5657	0.7387

TABLE B-XXXIII

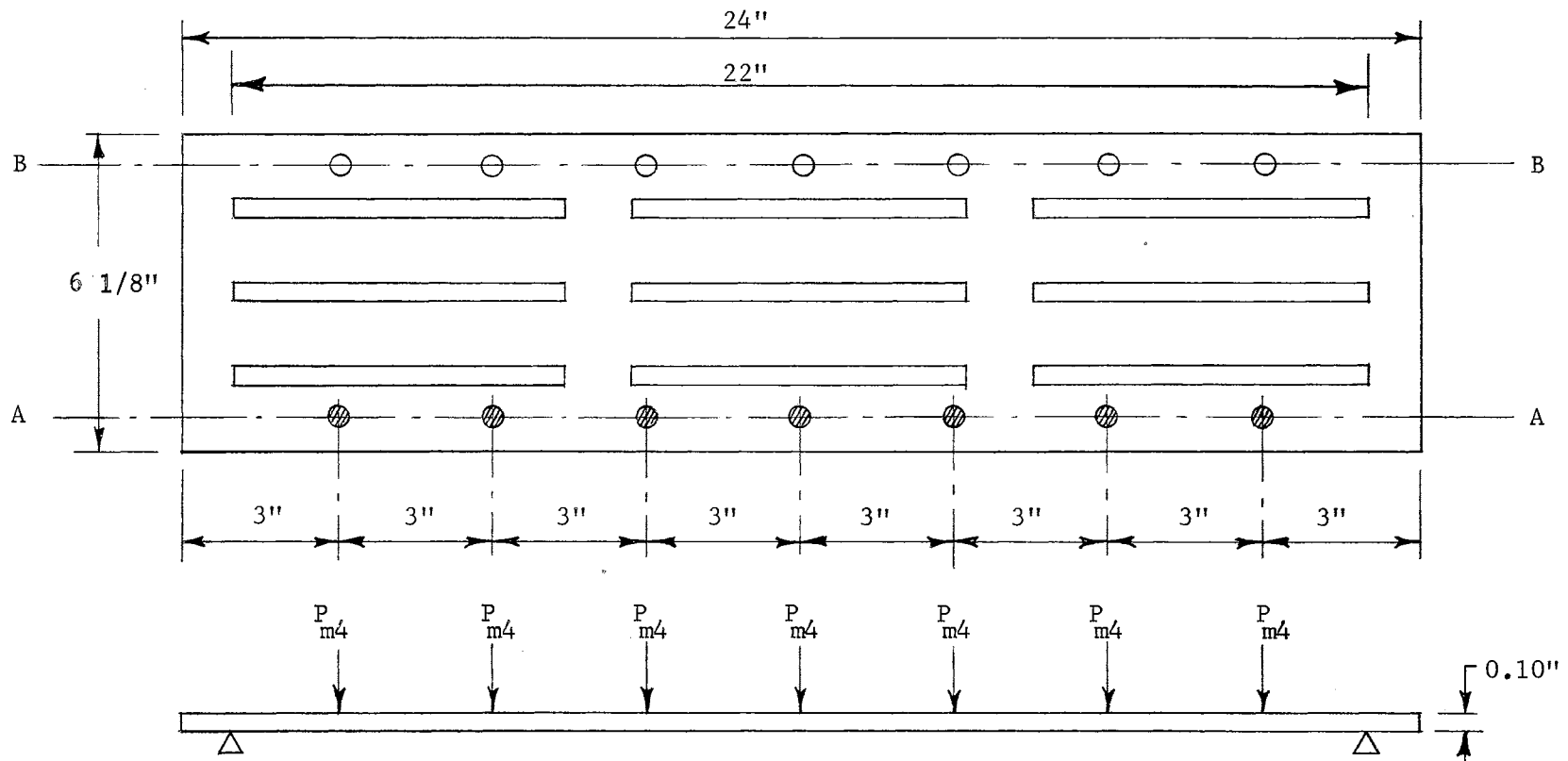
BENDING MOMENT IN PROTOTYPE IN LBF-IN.

LOAD NO. 3 APPLIED ON GRID NO. 3

REP.	LOAD APPLIED ON ZONE AA				LOAD APPLIED ON ZONE BB			
	STATION	STATION	STATION	STATION	STATION	STATION	STATION	STATION
	1	2	3	4	1	2	3	4
1	7930.3835	6332.5798	5892.8173	5863.4998	5702.2535	5907.4760	6200.6511	8062.3123
2	7901.0659	6332.5798	5892.8173	5848.8409	5716.9123	5922.1347	6229.9686	8135.6061
3	7915.7246	6317.9211	5892.8173	5863.4998	5702.2535	5907.4760	6215.3098	8135.6061
4	7915.7246	6347.2386	5878.1586	5848.8409	5716.9123	5892.8173	6229.9686	8135.6061
5	7901.0659	6288.6036	5863.4998	5848.8409	5716.9123	5936.7935	6229.9686	8135.6061

⊗ Load Applied on Zone AA

○ Load Applied on Zone BB



$$P_{m4} = 0.1212 \text{ LBF}$$

$$\gamma = 12 \text{ In.}$$

$$\omega_3 = 24 \text{ In.}$$

Figure B-12. Model Grid Loading Diagram

TABLE B-XXXIV

STRAIN IN MICRO-INCHES PER INCH OF LENGTH

LOAD NO. 4 APPLIED ON GRID NO. 3

REP.	LOAD APPLIED ON ZONE AA				LOAD APPLIED ON ZONE BB			
	STATION				STATION			
	1	2	3	4	1	2	3	4
1	36.5625	30.2500	27.8750	27.3125	26.5000	27.8125	29.0000	37.4375
2	37.1250	30.0625	28.1875	27.8125	26.5000	27.6250	28.8750	37.2500
3	36.3750	29.4375	27.5625	27.3125	27.1250	28.3125	29.7500	38.1250
4	36.4375	29.4375	27.5000	27.3750	26.9375	28.1250	29.5000	38.0625
5	36.5000	29.5625	27.5000	27.3125	26.6875	27.6250	29.3125	37.6250

TABLE B-XXXV

BENDING MOMENT IN MODEL IN LBF-IN.

LOAD NO. 4 APPLIED ON GRID NO. 3

REP.	LOAD APPLIED ON ZONE AA				LOAD APPLIED ON ZONE BB			
	STATION				STATION			
	1	2	3	4	1	2	3	4
1	0.7787	0.6442	0.5936	0.5817	0.5644	0.5923	0.6176	0.7973
2	0.7906	0.6402	0.6003	0.5923	0.5644	0.5883	0.6149	0.7933
3	0.7747	0.6269	0.5870	0.5817	0.5777	0.6030	0.6336	0.8119
4	0.7760	0.6269	0.5857	0.5830	0.5737	0.5990	0.6282	0.8106
5	0.7773	0.6296	0.5857	0.5817	0.5684	0.5883	0.6243	0.8013

TABLE B-XXXVI

BENDING MOMENT IN PROTOTYPE IN LBF-IN.

LOAD NO. 4 APPLIED ON GRID NO. 3

REP.	LOAD APPLIED ON ZONE AA				LOAD APPLIED ON ZONE BB			
	1	2	3	4	1	2	3	4
1	8575.3683	7094.8347	6537.8023	6405.8735	6215.3098	6523.1435	6801.6597	8780.5909
2	8707.2970	7050.8585	6611.0959	6523.1435	6215.3098	6479.1673	6772.3422	8736.6146
3	8531.3921	6904.2710	6464.5085	6405.8735	6361.8973	6640.4135	6977.5648	8941.8372
4	8546.0509	6904.2710	6449.8499	6420.5323	6317.9211	6596.4373	6918.9298	8927.1783
5	8560.7097	6933.5885	6449.8499	6405.8735	6259.2861	6479.1673	6874.9536	8824.5671



VITA

Berhane Berhe

Candidate for the Degree of

Master of Science

Thesis: AN EXPERIMENTAL ANALYSIS OF BENDING STRESSES INDUCED IN FLOOR  
GRIDS SUBJECTED TO LOADS FROM BEEF CATTLE

Major Field: Agricultural Engineering

Biographical:

Personal Data: Born in Adi Ghbai, Eritrea, Ethiopia, February 8,  
1938; the son of Berhe Abbay and Zaid Nemariam.

Education: Attended Elementary Schools in Asmara, Eritrea, Ethiopia;  
Graduated as Valedictorian of his class from Jimma Agricultural  
Technical School, Kaffa, Ethiopia, in June, 1958; Received  
"With Great Distinction" the degree of Bachelor of Science in  
Agriculture with a major in Agricultural Engineering Technology  
from Haile Selassie I University, College of Agriculture,  
Alemaya, Harar, Ethiopia, in July, 1962; completed the require-  
ments for the degree of Master of Science from Oklahoma State  
University in May, 1967.

Professional Experience: As a student worked for the Department of  
Agricultural Engineering Technology, the Department of Agricul-  
tural Economics and Business, and the Water Resources Department  
in an Agricultural Economics Survey of the Nile River Basin dur-  
ing Summer of 1961; after graduation served as a Graduate  
Assistant in teaching and research for one year at the College  
of Agriculture.